Biophysical Journal vol. 41, 1983

W-AM-MinA1 PROTEIN CRYSTALLOGRAPHY

Benno P. Schoenborn, Brookhaven National Laboratory, Upton, NY 11973

The main advantage of using neutrons instead of x-rays in the analysis of protein structure lies in the relatively large but significantly different scattering factors for hydrogen and deuterium.

In neutron diffraciton studies of single crystals of proteins, it is possible to determine hydrogen atom positions, atoms that play a dominant role in enzymatic function. Neutron diffraction not only permits the localization of hydrogen atoms, but also allows the differentiation of hydrogen from deuterium to study hydrogen exchange and water of hydration.

Structural investigations on three myoglobin derivatives (1) have now been completed allowing an accurate description of minor structural differences between the derivatives. Nearly complete replacement of hydrogen by deuterium is observed at amide hydrogen sites in crystals grown in D_2O with less exchange in crystals soaked in D_2O. Uncertainties in the observed atomic weights due to counting statistics, resolution and limitations in refinement techniques preclude, however, accurate determinations of partial H/D exchange ratios. From comparisons with exchange studies on ribonuclease (2), trypsin (3) and lysozyme (4) it seems that β sheet structures show less exchange than helical regions. It is, however, still too early to describe more definitive exchange patterns.

1) Raghavan N. and Schoenborn, B. P.; 2) Wlodawer A. A.; 3) Kossiakoff A.; 4) Mason S. A. in 1982 Brookhaven Symp. No. 32, Plenum Press, N. Y. 1983. (Supported by U.S. Department of Energy)

W-AM-MinA2 DEUTERIUM-HYDROGEN DIFFERENCE NEUTRON DIFFRACTION: AN APPROACH TO THE PHASE PROBLEM FOR SINGLE CRYSTALS OF ION-FREE GRAMICIDIN A. Roger E. Koeppe II, Department of Chemistry, University of Arkansas, Fayetteville, AR 72701.

The structure of gramicidin A crystallized from ethanol ($P2_12_12_1$: a = 24.6, b = 32.3, c = 32.5) has proven difficult due to a lack of isomorphous derivatives for x-ray phase determination. In such a case, neutron diffraction offers the possibility of approaching the phase problem by means of isomorphous deuterium-hydrogen substitution. The solvent (ethanol-water: 50-50) comprises about 15% of the mass of these crystals. Neutron diffraction data to 2 Å resolution have been recorded at Brookhaven's High Flux Beam Reactor for crystals of gramicidin A containing either H_2O/ethanol or D_2O/deuteroethanol. The average difference in $|\sqrt{I}|$ is 25% between these two data sets. Difference neutron Patterson maps show significant peaks which can be interpreted in terms of specific sites of deuterium replacement. The strongest difference peak refined to a centric R factor of 0.39 at 8 Å resolution (0.46 at 5 Å). This single site was then used to calculate difference Fourier projections to locate additional sites, which were then refined and used in further difference Fourier calculations. The procedure was stopped after the difference data had been fit using eight sites having occupancies ranging from 0.5 to four deuterons, the R factor of the fit being 0.28 for three centric projections at 3 Å resolution. SIR phases (mean figure of merit = 0.72 at 5 Å) were used to calculate projection and 3-dimensional Fourier maps at 5 Å resolution. The maps confirm previous indications concerning the cylindrical shape of gramicidin A in these crystals, and show possible positions for the indole side chains. The SIR phase ambiguity is being approached using crystals containing H_2O/deuteroethanol.

W-AM-MinA3 LOCALIZATION OF SMALL MOLECULES IN MODEL AND BIOLOGICAL MEMBRANES UTILIZING NEUTRON DIFFRACTION. L. Herbette. University of Connecticut Health Ctr., Cardiology Div., Farmington, CT 06032; Brookhaven National Laboratory, Upton, NY 11973.

Hydrated oriented multilayers of model membranes (dimyristoyllecithin and dipalmitoyllecithin) and the sarcoplasmic reticulum membrane (SR) were prepared to contain various small molecules in either protonated or deuterated form. Lamellar meridional neutron diffraction was recorded from these planar multilayers on an area detector at the Brookhaven National Laboratory High Flux Beam Reactor using the low angle diffractometer operating at 2.36 A. Neutron scattering density profiles were calculated from the background subtracted and appropriately corrected integrated intensity amplitudes which were phased by swelling (model membranes) or a disorder analysis (SR). Small molecule-membrane system pairs studied were: 1) specifically deuterated (vs. protonated) phospholipids reconstituted with the calcium pump protein (reconstituted SR); 2) perdueterated (vs. protonated) phospholipids exchanged into isolated SR; 3) deuterated (vs. protonated) propranolol, a β-adrenergic receptor blocking agent, in dimyristoyllecithin bilayers; 4) deuterated (vs. protonated) ethanol in isolated SR; and, 5) calcium isotopes (^{40}Ca vs. ^{44}Ca) in dipalmitoyllecithin bilayers. The difference profile corresponding to H_2O/D_2O of multilayer samples, the water profile structure, was used to scale different samples of each pair. Difference profiles for each molecule-membrane system were obtained providing the location of specific lipids, propranolol, ethanol and Ca in their respective membrane systems. We are extending the novel approach of determining the Ca profile structure in an attempt to locate the high affinity calcium binding sites of the SR. (Supported by NIH HL-21812, HL-26903, HL-27630, and a grant from the American Heart Association.)

W-AM-MinA4 Neutron Scattering Studies on Nucleosomes, G.Bunick, V.R. Ramakrishnan and E.C. Uberbacher, Univ. of Tennessee Oak Ridge - Graduate School of Biomedical Sciences, and Oak Ridge National Laboratory, Oak Ridge, TN 37830.

Neutron scattering is a powerful technique to study the solution conformation of nucleo-protein complexes, since by contrast variation techniques one can derive information about the conformation of the protein and nucleic acid components separately. Two kinds of experiments will be described: (i) HMG 14 and 17 are proteins which bind specifically to nucleosomes with a stoichiometry of 2 HMG's per nucleosome. They are believed to play a role in the activation of chromatin. Neutron scattering experiments have been done to study the conformation of nucleosomes as a function of HMG binding. The results indicate that there is very little overall change in the protein conformation, but the DNA is somewhat more extended. Possible models are proposed based on the data.
(ii) The conformation of 146 base pair and 175 base pair nucleosomes has been studied as a function of ionic strength. The observed data disagree significantly with previously proposed models for low ionic strength transitions, and models are proposed which are consistent with the observations. Our conclusion is that such transitions involve an unwinding of DNA from the histone core, rather than any extended superhelical forms of DNA.
Supported by N.I.H. grant GM 29818 to G.J.E.

W-AM-MinA5 **LIPOPROTEIN COMPLEXES**
D. Atkinson, Dept. of Biophysics, Boston University Medical School, Boston, MA

W-AM-MinA6 **INELASTIC SCATTERING: A NEW TOOL FOR ANALYSIS OF DYNAMICS**
D. Engelman, Dept. of Biochemistry and Molecular Biology, Yale Univ., New Haven, CT

W-AM-MinA7 HYDROGEN EXCHANGE STUDIES IN CRYSTALS OF MYOGLOBIN BY NEUTRON DIFFRACTION

Raghavan N. V. and Benno P. Schoenborn, Biology Department, Brookhaven National Laboratory, Upton, New York 11973

Neutron diffraction affords a valuable tool to probe hydrogen exchange in proteins. Single crystal structural studies on three myoglobin derivatives have been completed. These studies help illustrate the effects of different experimental conditions of crystal growth, soaking time in D_2O and pH have on the hydrogen exchange behavior of myoglobin crystals. It is observed that most amide hydrogens in myoglobin are exchangeable although at different rates depending on conditions.

In crystals grown from $(NH_4)_2SO_4$ at pH 5.6 and soaked in D_2O for two weeks there are 16 unexchanged amide hydrogens. In crystals that are soaked for six months there are 5 unexchanged hydrogens and in crystals grown from $(ND_4)_2SO_4$ at pH 5.6 and soaked for ten years there are 2 unexchanged hydrogens. The estimated error in these exchange ratios is about one-third of the scattering from a hydrogen atom. It is observed that the D helix exchanges very rapidly and the B and E helices exchange the slowest. (Supported by the United States Department of Energy.)

W-AM-MinB1 **cGMP AND ITS CONTROLLER ENZYMES IN ROD OUTER SEGMENTS AND ELSEWHERE**

Paul A. Liebman, Department of Anatomy, University of Pennsylvania, Philadelphia, PA.

Intracellular transmission events share the need for particulate signal carriers that diffuse through the aqueous cytoplasmic phase. Spatial propagation may incur dilutional attenuation, thus needing carrier particle amplification before and during propagation. cAMP and cGMP have been implicated as intracellular messengers in humoral activation of tissues throughout the body, in neurotransmission or modulation thereof, in the CNS and in visual receptors' response to light. In each case, transmission is gated on by a specific change in the configurational state of an integral membrane protein. After signal initiation, the gate must relax to terminate transmission. In all cases, the "on" state of the gate permits generation of a ramp of intracellular activity. A monomolecular gate thus yields a multimolecular product that integrates the gate action during its lifetime and thus amplifies. The cyclase or cyclic nucleotide phosphodiesterase (PDE) activation that causes the rise or fall of intracellular cyclic nucleotide level is always coupled to the gate by an additional protein. In rod disk membranes, this is [G-protein] that binds GTP to activate PDE, and it acts as more than a secondary gate. This intermediate step in activation produces a parabolic product integral of the secondary amplifier, PDE, to decrease cytoplasmic cGMP at about $10^6\ s^{-1}$ after a 1 s gate opened by a single photoisomerization. In vision, the gate protein is rhodopsin. The "on" state is Meta II and the "off" state is phosphorylated Meta II or any more slowly formed decay product.

The precise intracellular effect of the messenger is less certain. Evidence for modulation of Ca^{++}- dependent processes including protein phosphorylation, ionic conductance, and pumping in the CNS will be reviewed.

W-AM-MinB2 **REGULATION OF PHOTORECEPTOR CYTOSKELETON BY Ca^{++} AND CYCLIC NUCLEOTIDES**

Mary Beth Burnside, Dept. of Biology, University of California, Berkeley, CA 94720.

Teleost photoreceptors elongate and contract in response to changes in light conditions and to circadian signals. Retinal cultures and lysed-cell motile models have been used to characterize the mechanisms of force production and to identify messengers and agents responsible for regulating these movements. Teleost cones undergo actomyosin-dependent contraction in the light and microtubule-dependent elongation in the dark. Cone contraction is activated by elevating free Ca^{++} and inhibited by elevating cAMP. Conversely, cone elongation is activated by elevating cAMP and inhibited by elevating Ca^{++}. Thus Ca^{++} and cAMP regulate cone length in a mutually antagonistic manner.

W-AM-MinB3 VOLTAGE-GATED Ca^{2+} ENTRY AS INTRACELLULAR MESSENGER REGULATING MEMBRANE CONDUCTANCES.

Roger Eckert. Department of Biology and Ahmanson Laboratory of Neurobiology, UCLA, Los Angeles, CA 90024.

Intracellular Ca ions have been implicated in the regulation of numerous cell processes. Crucial for the role of Ca^{2+} as an intracellular messenger/regulator is the high specificity of Ca receptor molecules and the low ($<10^{-6}$M) background level of cytosolic free ionized Ca. High buffer affinity dampens perturbations in free Ca^{2+} and limits diffusion of Ca^{2+} entering the cell as a membrane current. Recently, Ca^{2+} entering excitable cells through voltage-gated channels has been found to modulate voltage-gated ion conductances of the cell membrane. This was first demonstrated in the Ca-dependent activation of K conductance (Meech and Standen, 1975, J. Physiol., 249:211). Voltage-gated Ca entry and accumulation can also act back on the Ca conductance itself (Brehm and Eckert, 1978, Science, 202:1203; Tillotson, 1979, PNAS, 76:1497). Ca ions accumulating during a depolarization feed back negatively on the Ca conductance, thus limiting the rate of Ca^{2+} entry during the depolarization. Contrary to classical voltage-dependent inactivation, this Ca-mediated inactivation of Ca conductance becomes weaker with increased membrane depolarization. The kinetics of Ca-mediated effects on Ca and K conductances are such in Aplysia neurons that Ca^{2+} left over from a prior depolarization leads to a depression of the Ca-dependent K current. This is due to the action of residual Ca^{2+} in reducing the rate of voltage-gated Ca^{2+} entry and accumulation, thereby reducing the extent of activation of the Ca-dependent K current. Thus, intracellular Ca^{2+}, by modulating the Ca current, can negatively regulate a Ca-dependent process.

W-AM-MinB4 COMPARISON OF ANTIPYRYLAZO III (Ap) AND ARSENAZO III (Az) SIGNALS FROM INTACT FROG SINGLE MUSCLE FIBERS. Emilia Quinta-Ferreira, S. M. Baylor and Chiu Shuen Hui. Depts of Physiology, Univ of Penn, and Biological Sciences, Purdue Univ.

Experiments have been carried out to examine further the various components of dye-related absorbance detectable following injection of Ap or Az (Baylor, Chandler & Marshall, JP, 1982). In response to a single action potential at 15-17 °C, the early isotropic (= calcium) signal from Ap has several favorable properties in comparison with that from Az: (1) its time course has an earlier peak, by several ms, and shorter half-width, by a factor of about 2 (cf Palade & Vergara, JGP, 1982); (2) its waveform, examined by taking ratios of $\Delta A(t)$ at spectral peaks for the Ca-dye response, is consistent with a single stoichiometry; (3) its spectrum, λ=450 to 800 nm, superimposes a scaled cuvette Ca-difference spectrum (pH=6.9, Mg=2 mM). These properties suggest that the Ap-Ca signal is a more faithful monitor of rapid changes in intracellular Ca and one that should be more easily calibrated. However, several features of the absorbance signals suggest that Ap has some complexity when used as a myoplasmic Ca indicator: (1) a readily detectable late isotropic signal likely due to a ΔMg or ΔpH; (2) an early dichroic signal with a time course and spectrum similar but not identical to that of the Ca signal itself; (3) a resting absorbance spectrum that for λ>630 nm is elevated in comparison with cuvette calibrations (Ca=0, pH=6.9, any Mg level) and which has a dichroic component also elevated at long λ. One possibility consistent with feature (3) is that a significant fraction of the injected Ap is bound at rest to oriented structures.

W-AM-MinB5 Ca^{++} REGULATION IN THE CYTOPLASM OF RETINAL RODS: AN EXAMPLE OF BIOLOGICAL FEEDBACK CONTROL.

W.A. Hagins and S. Yoshikami Lab. of Chemical Physics, NIADDK, N.I.H., Bethesda,Md. 20205

Retinal rod cells produce a steady current that circulates from outer to inner segments in darkness and involves such a large Na^+ and K^+ flux that most of the univalent cations are turned over in 1-5 m. The current is inhibited by increased internal Ca^{++}, which, in turn is controlled by Na:Ca exchange in the rod plasma membrane. This arrangement results in great stabilization of cytoplasmic Ca^{++} activity against changes in extracellular A_{Ca} and also shapes the kinetic form of rod responses to light flashes. These responses, which seem to result from release of Ca^{++} into rod cytoplasm from a light-sensitive internal store, provide a way to study the cytoplasmic control mechanism for A_{Ca}. Examples of ionic analyses, electrophysiological measurements and studies of net Ca^{++} movements are compared with the predictions of a simple model of ionic movements in rod cell membranes.

W-AM-A1 MODELLING TRANSMEMBRANE CALCIUM TRANSPORT WITH IONOPHOROUS PEPTIDES. C.M. Deber and D.A. Lannigan, *Research Institute, The Hospital for Sick Children, Toronto, Ontario, M5G 1X8.*

Experimental data remain sparse regarding the molecular events occurring between the binding of Ca^{2+} by membrane proteins and its subsequent release at the opposite membrane surface. One could hypothesize that such proteins -- from which dissociation of the cation must be efficient -- bind Ca^{2+} mainly via relatively weak electrostatic interactions in conformationally-mobile sites comprised of (neutral) peptide carbonyl groups. Binding to such sites, which would be unable to afford local neutralization of the divalent cation, could also result in separation of Ca^{2+} from directly accompanying ions, i.e., the Ca^{2+} ions would be translocated by a primary electrogenic mechanism. We have been examining the possibility that Ca^{2+} ions can traverse a membrane in this manner using a series of neutral carrier peptides of general structure cyclo(Glu(OBz)-(N-R_1)Gly-Gly-(N-R_2)Gly)$_2$ which we have designed and synthesized. These cyclic octapeptides, (i.e., R_1 = CH_3, R_2 = cyclohexyl, CYCLEX-2E; R_1 = R_2 = methylcyclohexyl, METHYLCYCLEX-4E) have been shown to bind Ca^{2+} selectively in a central cavity lined with peptide carbonyl oxygen atoms, and to discharge Ca^{2+} gradients across phosphatidylcholine (PC) bilayers. Recent experiments with METHYLCYCLEX-4E added to suspensions of $CaSO_4$-loaded PC vesicles have now shown (a) the vesicles retain SO_4^{2-} during peptide-mediated Ca^{2+} efflux; (b) the rate of Ca^{2+} efflux is stimulated by coupling to valinomycin/K^+ countertransport; and (c) the rate of Ca^{2+} efflux is diminished at pH 4 vs pH 6.8. These results are consistent with an electrogenic-type translocation of Ca^{2+} ions by the cyclic octapeptide, in conjunction with a (rate-determining) compensatory non-specific flux of hydroxide ions. The demonstration that a neutral ionophorous peptide can facilitate Ca^{2+} transport in PC bilayers suggests that this mode of peptide/Ca^{2+} interaction is a viable model for protein-mediated transfer of Ca^{2+} ions.

W-AM-A2 ROLE OF CONFORMATIONAL FLIP-FLOPPING OF IONOPHORES IN THEIR EFFECTIVENESS AS CATION CARRIERS. B.C. Pressman and G.R. Painter, Dept. Pharmacol., Univ. Miami, FL 33101.

We have utilized CD, NMR and computer modeling to study the conformational response of lasalocid A (L) to a solvent series encompassing the polarity range of biological membranes. Models suggest that L has two metastable conformations, an extended, low cation affinity form, at high polarity which complies with intrinsic bonding and steric factors, and a cyclic, high cation affinity form, at low polarity where intramolecular electrostatic forces are not attenuated by dipole interaction with the solvent. This correlates with a change in chirality of the L anion as shown by a graded increase in the CD band of the medial ketone in going from a solvent with a polarity index (Reichart) of E_T 39.1 (CH_3Cl) to E_T 51.9 (EtOH), probably reflecting alterations in the populations of the two conformers. An analogous shift is observed in several ^1H NMR bands of protonated L, occurring abruptly between E_T 39.1 (CH_3Cl) and E_T 42.2 (acetone). We interpret the shifts in H_{11} and H_{13} as conformer determining rotations about the "hinge" bonds on either side of the ketone. The shifts in terminal H_{41} and H_{21} presumably reflect head-to-tail cyclization of L at low polarity which exposes the tail of the molecule to ring currents of the aromatic head region. A similar polarity dependent conformational shift has been reported for salinomycin suggesting that an abrupt shift of favored conformation in different polarity regions of membranes promotes high cation transport turnovers of natural ionophores in general. This attribute has not been designed into the structure of synthetic ionophores or other cation ligands, e.g. prostaglandins, hence their poor transport effectiveness. (Supported by HL-23932).

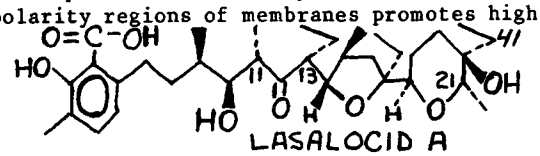

LASALOCID A

W-AM-A3 VOLTAGE-DEPENDENCY OF MONAZOMYCIN AND COLICIN K, A AND E1 CHANNELS IN LIPOSOMES. C. Kayalar and G. R. Erdheim. Department of Chemistry, University of California, Berkeley, CA 94720.

Monazomycin and certain colicins have been shown to act as voltage-dependent channels in planar bilayer membranes. In this study a qualitatively similar voltage-dependency is demonstrated in liposomal membranes. K+ diffusion potentials of opposite polarities were generated by valinomycin in large unilamellar vesicles (d = 0.1 μm). These potentials (approx. 100 mV) were monitored by ANS fluorescence. The channel activities of monazomycin and colicins K, A, and E1 were tested by their ability to dissipate these pre-formed membrane potentials. Phospholipid composition of the vesicles were either azolectin or PE:PG:CL (70:25:5). With azolectin vesicles and at low channel to vesicle ratios (< 10:1) monazomycin, colicin K and A showed channel activity only with trans-negative membrane potentials in the pH range studied (5.8-7.4). At higher ratios the dissipation of trans-positive potentials were also observed, rate of dissipation always being much slower than with trans-negative potentials. Using azolectin or PE:PG:CL vesicles in the pH range of 5.0 to 7.4, colicin E1 dissipated membrane potentials of both polarity with comparable rates even at low channel to vesicle ratios. In azolectin vesicles between pH. 5.0 to 6.0, colicin E1 dissipated a trans-negative potential at about a two to four times higher rate than trans-positive potential. (Supported by NIH Grant AI-18578-01)

W-AM-A4 TETANUS TOXIN FORMS CHANNELS IN PLANAR BILAYERS CONTAINING GANGLIOSIDES. H. Borochov-Neori, E. Yavin, U. Staerz and M. Montal. UCSD, La Jolla, CA 92093. Intr. by E. P. Geiduschek.

Tetanus toxin, a 150,000-molecular weight bacterial toxin, binds specifically to gangliosides[1]. The effects of the toxin-ganglioside interaction in membranes were investigated in asymmetric lipid bilayers containing gangliosides exclusively in one monolayer. Bilayers were formed by apposition of a monolayer of purified asolectin (AL-side) and a monolayer of AL supplemented with 5% disialosyl-N-tetraglycosylceramide (G_{D1b}, G-side), a putative toxin receptor. When toxin was added to the AL-side (25μg/ml), the membrane was unaffected and the conductance remained ≤ 4pS for ≥ 90min. In contrast, addition of toxin (2.5μg/ml) to the G-side of the membrane resulted in the appearance of channels after a lag time. The most frequent events had a single channel conductance, γ, of 14pS (0.1M NaCl, 0.01M Hepes, pH 7). The main occurrence was that of 2 channels acting simultaneously. Under these conditions, frequency histograms of channel open times followed a single exponential: the lifetime was 56±0.5ms at V=100mV (V positive in the compartment containing the toxin). Histogram of channel closed times were best fitted by a sum of 2 exponentials with the following amplitudes, A, and time constants, τ: A_1=1000, τ_1=2.3±0.7ms; A_2=100, τ_2=55±5ms. Similar results were obtained when G_{D1b} was substituted for mixed brain gangliosides. However, additional events with γ=2pS and $\tau_{open} \approx \tau_{closed} \approx 1.8$s were recorded. Furthermore, toxin produced channels in symmetric bilayers containing gangliosides but *not* in symmetric bilayers composed exclusively of AL. Therefore, gangliosides are required for channel formation. These results provide new insights into the mechanism by which tetanus toxin perturbs synaptic transmission.

1.Van Heyningen, W.E.(1963)J.Gen.Microbiol.31:275. Supported by NIH EY02084 and Guggenheim Fdn.

W-AM-A5 SINGLE CHANNEL FLASH PHOTOLYSIS STUDIES OF GRAMICIDIN-A. R.C. Waldbillig & D. Busath
Physiology Department. University of Texas Medical Branch, Galveston, TX 77550.

We have tested the hypothesis that peptide tryptophans may serve as ionic current control sites in transmembrane channels. Gramicidin-A is a tryptophan-rich (8/dimer) pentadecapeptide which forms cation conducting channels in lipid bilayers. We report here that gramicidin channels exhibit a multi-state conductance decrease when the tryptophan groups are photolyzed.

Lipid bilayers containing gramicidin-A were exposed to white xenon (80 mW/cm^2) or monochromatic UV light (14 mW/cm^2) and membrane and single channel conductance properties were measured. The results show that the bilayers containing many channels suffer an abrupt, irreversible conductance decrease when exposed to ultraviolet light. The action spectrum of the current decrease and the absorption spectrum of gramicidin-A are both sharply peaked near the 280 nm absorption band of tryptophan. The single channel conductance changes markedly after UV exposure. The distribution of the surviving population has a wide variety of low conductance channels without the usual 46 pS peak (1 M KCl). The channel lifetime (τ) is unchanged but the distribution departs from a single exponential due to an excess of short-lived events (< ½ τ).

Single channels were UV flash photolyzed shortly after opening. Light-struck channels suddenly switch to lower conductance states with a cascade of discrete steps leading to premature channel closure (τ < 5 sec vs. 45 sec). We suggest that the low conductance states arise from photo modification of individual tryptophans of the channel. It is concluded that peptide tryptophan groups are critical current control components of the gramicidin-A channels.

Supported by NIH grants GM-26980 & GM26897

W-AM-A6 A QUANTUM MECHANICAL APPROACH TO GATING OF CATIONIC SELECTIVE EXCITABLE CHANNELS

Jurgen F. Fohlmeister, Department of Physiology, University of Minnesota, Minneapolis, MN 55455

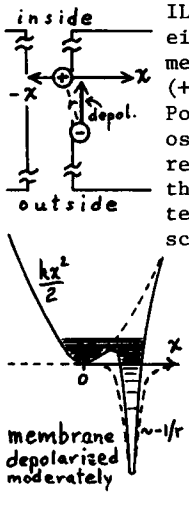

ILLUSTRATIVE MODEL: Gating involves the interaction of 2 charges (part of channel-protein, called(+)and(-)) with relative separation controlled by transmembrane field. Movement by(+)of x ≳ 0.4Å is sufficient to open or close the gate. (-)=gating voltage-sensor, (+)=electro-mechanical gate. Dynamics of(+)considered along axis x. Q.M.ASSUMPTIONS: 1) Potential energy term for vibrational states of(+)consist approximately of a harmonic oscillator ((+)bound), plus an ~-1/r potential due to(-)(strictly -1/r when(-)on x-axis) resulting in 2 minima separated by a voltage-dependent barrier. The ~-1/r component width increases with nearness of(-)and(+)(ie. with depolarization).2)Natural decay of states in the absence of thermal "stimulated emission" and excitation occurs on ms timescale.3)Mass of(+)and its restoring force imply closely spaced levels relative to kT, ⇒ much thermal excitation. By the "Adiabatic Theorem" this excitation is due to rapid ("sudden approx.") fluctuations in the Hamiltonian, containing frequency components ≳ 10^{13} Hz. 4)Mean value of the Hamiltonian changes with the voltage-step (~1 μs scale, therefore adiabatic).5)Probability of open/closed is given by $\int |\text{wavefunction}(x)|^2 dx$ with integration accross the -1/r well/harm. osc., respectively. MOTIVE: Electrostatic energy conversion during voltage transitions toward zero mV may be concentrated at aqueous channels due to their higher(vis-a-vie lipid)dielectric constant which can lead to a non-thermal population of states, leaving both the Arrhenius frequency, kT/h, and the Boltzmann factor, $\exp -\Delta G^*/RT$, of the absolute reaction rate theory undefined.

W-AM-A7 THE PARTIAL CLEARING OF GRAMICIDIN A' FROM Cd^{2+}-INDUCED GEL PHASE REGIONS OF PHOSPHATIDIC ACID/PHOSPHATIDYLCHOLINE MODEL MEMBRANES. Gerald W. Feigenson and Martin D. Caffrey, Section of Biochemistry, Molecular and Cell Biology, Clark Hall, Cornell University, Ithaca, NY 14853.

Using a simple model for a biological membrane we examine cation-induced gel phase formation and the depletion of polypeptide from the gel phase. The model system consists of vesicles of phosphatidic acid and phosphatidylcholine which contain gramicidin A'. Using x-ray diffraction and electron spin resonance to monitor lipid phase behavior, Cd^{2+} is found to induce gel and liquid crystal phase coexistence over a wide range of lipid composition. Quenching of gramicidin A' tryptophanyl fluorescence by spin-labeled phosphatidic acid or spin-labeled phosphatidylcholine is analyzed to obtain the partition coefficient, K_p, for gramicidin A' between gel and liquid crystal phases. The value of $K_p = 3$ favoring the liquid crystal phase indicates a partial clearing of the membrane-bound polypeptide from Cd^{2+}-induced gel phase regions of the membrane. (Supported by N.I.H. Grant HL-18255. G.W.F. is an Established Investigator of the American Heart Association.)

W-AM-A8 SINGLE-CHANNEL STUDIES ON MODIFIED GRAMICIDINS. J.-L. Mazet, R.E. Koeppe, II, and O.S. Andersen. Dept. Physiology and Biophysics, Cornell University Medical College, New York, NY 10021, Dept. Chemistry, University of Arkansas, Fayetteville, AR 72701.

Single-channel studies on gramicidin A (gramA) in NaCl solutions show that substitution of valine (Val) at position #1 by more polar amino acids decreases the channels maximal conductance (gmax) and increases their Na^+ affinity (estimated as the activity for half-maximal conductance, K-1/2). In contrast, replacement of polar amino acids at position #11 (tryptophane (Trp) in gramA, tyrosine (Tyr) in gramC) with the non-polar phenylalanine (Phe) in gramB reduces gmax and has little effect on K-1/2. To further study the differential effects of a given amino acid near the channel center (position #1) and near the aqueous phases (position #11) we have replaced the N-terminal Val of gramA and gramC by Trp, Tyr and Phe. Small-signal conductance jumps (g) in diphytanoylphosphatidylcholine/n-decane bilayers were measured in 0.1 and 1.0 M NaCl, to separate changes in g into changes in gmax and K-1/2. Comparison of the 1-Tyr- and 1-Phe-compounds (gramA and C) show that replacing Phe by the more polar Tyr decreases gmax and K-1/2 about 2-fold, in agreement with the results with aliphatic amino acids, but in sharp contrast with the findings at position #11, where the Phe-to-Tyr switch increases gmax 2-fold. In addition, the Phe-to-Tyr replacement at position #1 alters the monomer interactions in the channel, as we were unable to observe hybrid dimers between 1-Tyr-gramC and 1-Val-gramC. The 1-Trp-compounds seem incapable of forming stable transmembrane channels. The molecular characteristics of gramicidin channels depend critically on the identity and position of the amino acid side chains forming the channel exterior.
(Supported by the CNRS, France, the NSF and NIH grants #s GM-21342, NS-00648 and NS-16449.)

W-AM-A9 ANION EXCHANGE AT THE OXYNTIC CELL APICAL MEMBRANE AND THIOCYANATE INHIBITION OF HCl SECRETION. J.M. Wolosin and J.G. Forte. Dept. of Physiology-Anatomy, Univ. of Calif., Berkeley, CA 94720.

The effects of SCN^- on H^+-accumulation by vesicles derived from the apical membrane of secreting oxyntic cells are reported. SCN^- inhibited the formation of pH gradients in Cl^- and isethionate medium. In Cl^-, the concentration of SCN^- required to achieve a certain degree of inhibition of H^+-uptake (or dissipation of preformed gradients) was increased with the increase in Cl^- concentration indicating competitive phenomena between the anions. Comparison of the rates of dissipation of similar pH gradients achieved in Cl^- vs. isethionate suggested the existence of fast Cl^-:SCN^- exchange. Direct isotopic fluxes demonstrated the existence in the membrane of a cation-independent anion:anion exchange, along with the previously reported K-salt co-transport for both Cl^- and SCN^-. These mediated pathways in the apical membrane provide the means for rapid access of SCN^- to the acidic canalicular spaces of the oxyntic cell implicit in recent proposals to explain SCN^--inhibition of gastric HCl secretion. The rates of anion-exchange and K-salt transport were of similar magnitude, and the rates for SCN^- in either countertransport against Cl^- or co-transport with K^+ were twice as fast as the equivalent values for Cl^- suggesting that a single transport entity is responsible for both transport processes. To explain these quantitative relationships between co-transport and exchange, a model of two linked non-permeant positive (E^+) and negative (E^-) carriers is proposed. Each carrier is able to translocate the membrane only when loaded with ions of opposite charge or by pairing to form an electroneutral complex (EE). (Supported by USPHS Grant #AM10141)

W-AM-A10 A NON-EQUILIBRIUM THERMODYNAMIC MODEL OF THE PROXIMAL TUBULE EPITHELIUM OF THE RAT. Alan M. Weinstein, Cornell University Medical College, N. Y.

The rat proximal tubule epithelium is represented as well-stirred, compliant cellular and paracellular compartments bounded by mucosal and serosal bathing solutions. With a uniform PCO_2 throughout the epithelium, the model variables include the concentrations of Na,K,Cl,HCO_3,H_2PO_4, HPO_4,H, as well as hydrostatic pressure and electrical potential. Except for a metabolically driven Na-K exchanger at the basolateral cell membrane, all membrane transport within the epithelium is represented by the passive linear phenomenological equations of Kedem and Katchalsky. In particular, this includes the cotransport of Na-Cl and Na-H_2PO_4 and countertransport of Na-H at the apical cell membrane. Experimental constraints on the choice of ionic conductivities are satisfied by allowing K-Cl cotransport at the basolateral membrane. The model equations include those for mass balance of the non-reacting species, as well as chemical equilibrium for the acidification reactions. Time-dependent terms are retained to permit study of transient phenomena. In the steady state the energy dissipation is computed and verified equal to the sum of input from the Na-K exchanger plus the Gibbs free energy of mass addition to the system. The parameter dependence of coupled water transport is studied and shown to be consistent with the predictions of previous analytical models of the lateral intercellular space. Water transport in the presence of an end-proximal (HCO_3-depleted) luminal solution is investigated. Here the lower permeability and higher reflection coefficient of HCO_3 enhance net sodium and water transport. When there is significant tight junctional water permeability, this process may permit proximal tubule Na transport to proceed with diminished energy dissipation.

W-AM-A11 MONOCLONAL ANTIBODIES AGAINST THE lac CARRIER FROM ESCHERICHIA COLI. N. Carrasco, S. M. Tahara, D. Herzlinger, P. Viitanen, T. Goldkorn, D. L. Foster & H. R. Kaback, Roche Institute of Molecular Biology, Nutley, NJ 07110.

Monoclonal antibodies directed against the lac carrier protein purified from the membrane of E. coli were prepared by somatic cell fusion of mouse myeloma cells with splenocytes from an immunized mouse. Several clones produce antibodies that react with the purified protein as demonstrated by solid phase radioimmunoassay and by immunoblotting experiments. Antibody from hybridoma 4B1, an IgG_{2a} immunoglobulin, inhibits membrane potential-driven lactose transport and carrier-mediated efflux down a concentration gradient in proteoliposomes reconstituted with the purified lac carrier and in right-side-out membrane vesicles. In contrast, the antibody has no effect on the generation of the proton electrochemical gradient by membrane vesicles, it does not alter the ability of vesicles containing the lac carrier to bind p-nitrophenyl-α-D-galactopyranoside nor does it inhibit transmembrane exchange of lactose. It is apparent therefore that the antibody causes uncoupling of proton and lactose movements at the level of the carrier. The concentration of antibody required for a given degree of inhibition is proportional to the amount of lac carrier protein in the membrane. Antibody-induced inhibition occurs within seconds, indicating that the epitope is accessible on the surface of the membrane, a contention supported by binding studies with iodinated 4B1 which binds to right-side-out but not to inverted vesicles. Absence of immunocompetition between antibodies 4A10R, 4B1 and 5F7 suggests that the antibodies are directed against different epitopes. The epitopes are currently being characterized by cyanogen bromide fragmentation and proteolysis of the antigen followed by monoclonal antibody affinity chromatography.

W-AM-A12 A GENERAL EQUATION FOR MICROELECTRODE IONOPHORESIS. Herbert Drouin, (Intr. by M.C.Cornwall), Boston University School of Medicine, Department of Phyisiology, 80 East Concord Street, Boston, Ma. 02118.

Recently (R.D.Purves, J.Physiol. 300, (1980) 72P), attempts have been made to give ionophoretic studies with microelectrodes a more quantitative basis. Although a detailed discussion of the relation between the electric current and ionophoretic drug release has been presented, restrictive assumptions have been made in the derivation of the theoretical relation between electric current I and drug efflux q. Therefore, an equation is presented for the general case of a completely dissociated electrolyte: $K_{\nu_1}A_{\nu_2} = \nu_1 K^{z_1} + \nu_2 A^{z_2}$ (ν_1, ν_2 = mole number of cations or anions; z_1, z_2 = valency of cations or anions). The ions are considered to have different valencies and different electrical mobilities. The general equation is:

$$q_i = -(-t_i I/z_i F + \nu_i q_D^*(1-w))/(1 - \exp(-(1-t_i I/z_i F \nu_i q_D^*(1-w))\ln w))$$

t_i = transport number of ion i; F = Faraday's constant. q_D^* is the diffusional leak of the microelectrode if the concentration C_o of the filling solution were the same as that C_o^* of the external bathing solution, that is $w = C_o/C_o^* = 1$. In the case of ion ejection, I/z_i takes positive values and in the limit towards positive infinity the result is $q_i = t_i I/z_i F$. This equation has been widely used in the ionophoretic literature. Supported by NIH Grant NS11429-09

W-AM-B1 RESTING POTENTIAL IN SQUID AXONS: COMPARISON BETWEEN FITTINGS OF THE GHK EQUATION AND A MODIFIED CONSTANT FIELD EQUATION. D. C. Chang, Department of Physiology, Baylor College of Medicine, Houston, TX 77030

The resting potential in the squid axon has been measured at various concentrations of Cl, K, Na, and Ca ions. The results of these measurements are compared with the Goldman-Hodgkin-Katz (GHK) equation and a modified constant field equation that was derived by including currents carried by divalent ions and effects of the unstirred layer and the periaxonal space. This modified constant field equation is in the form

$$V = \frac{RT}{F} \ln \left\{ \frac{[K]_o + b[Na]_o}{[K]_i + b[Na]_i} + c \right\}$$

where $b = P_{Na}/P_K$ and c is a constant not sensitive to $[K]_o$ or $[Na]_o$. It is shown that, although the original GHK equation can fit the V versus $[K]_o$ data well, it has difficulty explaining the observed dependence of V on $[Na]_o$ when the axon is bathed in K-free artificial sea water. The use of the modified constant field equation removes this difficulty. (Work supported by ONR contract N0004-76-C-0100.)

W-AM-B2 TRANSIENT EXCITABILITY INCREASE IN AN INTEGRATIVE AXON AT HYPERBARIC PRESSURE. Yoram Grossman and Joan J. Kendig, Unit of Physiology, Faculty of Health Sciences, Ben Gurion Univ. of the Negev, Beersheva, Israel, and Dept. of Anesthesia, Stanford Univ. Med. School, Stanford, CA.

Vertebrate peripheral nerve and squid giant axons show no excitability increase at hyperbaric pressure. The bifurcating motor neuron to deep abdominal extensor muscles of the spiny lobster Panulirus sp. has frequency dependent integrative properties and relative sensitivity to anesthetics. We explored the responses of this interesting axon to hyperbaric (He) pressure at 13°-21°C. At 50, 100, and 150 atm, there were transient (5-15 min) increases in extracellularly recorded action potential amplitude, conduction velocity, and ability to conduct 2-5 high-frequency impulses. These variables then declined to levels below control, occasionally to the point of conduction block through the branch point. On decompression, there was a much larger transient increase in all three variables, followed by a decline to approximately control levels. To establish the basis for these effects, vaseline gap voltage clamp studies of this axon were carried out. At 6 °-10 °C, there was reasonable control of membrane voltage at the artificial node. Depolarizing test pulses evoked a fast transient inward current followed by an outward current which partially inactivated. At 50 atm, the inward current transiently increased over 5-10 min, then declined to below control levels. Compression to 100 atm evoked a transient increase in inward current again, followed by further decline. Over this time period, there was little transient change in the outward current, which declined together with the inward current. The behavior of the inward current at hyperbaric pressure is consistent with the extracellular findings and represents a pressure induced increase in axon excitability.

W-AM-B3 DETERMINING THE OPTIMUM DESIGN OF A MYELINATED AXON BY ANALYSIS OF ITS EQUIVALENT UNIFORM AXON F.A. Dodge, IBM Research, T.J.Watson Research Center, Yorktown Heights, NY 10598.

The conduction velocity (θ) of an axon is maximum when the ionic channels are distributed uniformly; but for a nonuniform distribution, there is little slowing of θ until the separation between excitable patches becomes much larger than the space constant of the foot of the propagating impulse. Thus, with practical accuracy, we can estimate θ by applying the uniform wave assumption to a model in which the ionic conductance and extra capacitance of a node of Ranvier is spread uniformly over the internodal cable. (This estimate can then be improved by a correction for nonuniformity that depends on the ratio of the internodal length to the space constant of the foot.) The uniform axon approximation immediately explains that θ is proportional to diameter (D) simply because the thickness of the myelin is proportional to D. Moreover, variation of cable and membrane parameters can be explored over a wide range using Huxley's 1959 dimensional analysis of the uniform axon. For example, we can draw curves for varying the thickness of myelin (d/D) and for varying the internodal length (L), and we find that the optimum values of d/D and L should depend weakly on the temperature: for frog myelinated axons the optimum d/D is .65 at 10°C, shifting to .61 at 30°C, and the L is 140D at 10°C, shortening to 77D at 30° C. It also predicts how θ should vary with temperature, which is in excellent agreement with experiment. However, in order to match experimental values of θ/D, the membrane models derived from voltage-clamp data on nodes had to be adjusted to give a lower threshold, say, by reducing the leakage conductance of the nodal membrane. The equivalent uniform axon approximation is also useful for fitting a nonuniform partial differential equation to experimental data.

W-AM-B4 LASER SCANNED IMAGES OF ELECTRICAL ACTIVATION: 4096 ACTION POTENTIALS. S. Dillon and M. Morad, Univ. of Penna. Dept. of Physiol. and Regional Laser Lab., Phila., PA 19104

We have previously described a laser scanning technique for recording optical action potentials from 128 arbitrarily disposed sites on the heart (Science 214:453, 1981). The laser spot was positioned in a random-access manner by a pair of acousto-optic deflectors. The new technique exploits the same property of the dye (WW781) to transduce electrical activity into fluorescence but uses a different mode for acousto-optic laser deflection. The laser beam (Kr laser, 647 nm, 20 mW incident power) is continuously swept out in lines across the preparation, incrementally stepping from top to bottom, giving a raster of 64 lines. Sixty four samples of fluorescence are digitized during each line sweep so that an image of 4096 "pixels" are recorded every 12 msec. At present there is memory sufficient for 24 frames (288 msec of continuous recording). The insets show 4 consecutive images of a frog heart (Rana pipiens) during impulse propagation away from a stimulus site at the upper right corner of the ventricle. Action potential upstrokes recorded from individual spots on the image also shown for reference.

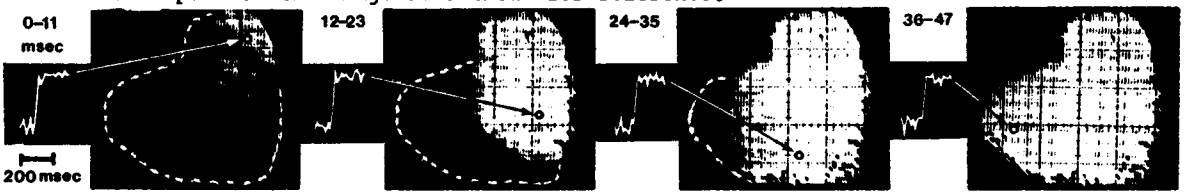

W-AM-B5 MULTIPLE SITE OPTICAL RECORDING OF MEMBRANE POTENTIAL IN GLANDULAR TISSUE: INTERACTION OF SYNAPTIC AND ELECTROTONIC SOURCES OF EXCITATION IN A SALIVARY GLAND. B.M. Salzberg, D.M. Senseman, H. Shimizu, and I.S. Horwitz. U. of Pennsylvania, Philadelphia, PA. 19104.

The interaction between synaptic and electrotonic excitation of cells from the salivary gland of the snail Helisoma was studied using the linear potentiometric probe NK 2367. Silicon photodiode arrays were used to record simultaneously the electrical response to neuronal stimulation of as many as 124 separate regions of the gland. Laterally opposed acini exhibited highly synchronous electrical activity, suggesting a high degree of electrical coupling. In the longitudinal direction, coupling appeared weaker. The onset of depolarization following neuronal stimulation was progressively retarded along the length of the gland, in agreement with the measured conduction velocity of the presynaptic nerve spike. In most instances, neuronal stimulation directly activated a regenerative response at the junction between the anterior and central duct. Excitation of distal gland regions was usually mediated by electrotonic spread from active, more proximal sites. Multiple site optical recording of membrane potential changes can be a powerful tool for studying the spatial and temporal patterning of electrical activity in complex electrical syncitia. Other exocrine, as well as endocrine and neurosecretory systems should be susceptible to this approach.

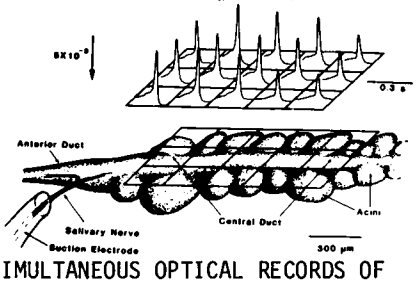

SIMULTANEOUS OPTICAL RECORDS OF ACTION POTENTIALS FROM 15 SITES IN A SALIVARY GLAND. SINGLE SWEEP.

Supported by USPHS grants NS 16824 and DE 05271.

W-AM-B6 FAR FIELD EVOKED RESPONSES FROM NERVE TRUNK VOLLEYS. Leonard Zablow, Department of Neurology, College of Physicians and Surgeons, Columbia University, New York, N.Y. 10032

The diagnostic use of cerebral evoked responses to specific stimuli has triggered much research into the anatomical locations of the generators of these waves. In the case of somatosensory responses to stimulation of nerve trunks in the upper limb, there is difficulty in interpreting certain features of the scalp-recorded pattern which have latencies too short to be reasonably assigned to phenomena in brain stem or higher centers. However, the far fields from volleys in peripheral nerve trunks can be enhanced either by their own geometrical peculiarities, or the passive effects of tissues near them, and can contribute to the scalp potentials.

The equivalent generator of a volley in a straight nerve consists of a pair of back to back dipoles whose negative charges are superimposed. This symmetry is that of a linear quadrupole whose voltage, recorded between a nearby and a distant electrode, falls off as the inverse cube of the distance to the closer electrode. Three possible ways in which the quadrupolar symmetry could be broken are 1) a sharp bend in the nerve trunk, 2) an abrupt change in the conductivity of, and 3) a change in the cross section of the medium surrounding the nerve. As the volley moves past one of these transitions, if the length of the transition region were short compared to the length of the active region in the trunk, a dipole-like field would be generated. Its voltage is attenuated only as the inverse square of the distance to the nearby electrode. Therefore, this could contribute significant voltages at more distant electrodes and be responsible for the short latency features of the somatosensory response on the scalp elicited by stimulating nerves in the arm.

W-AM-B7 TETRODOTOXIN SENSITIVE DEPOLARIZATIONS INDUCED BY VERATRIDINE AND α-SCORPION TOXIN IN PRIMARY ASTROCYTES IN CULTURE. Charles L. Bowman, Charles Edwards, and Harold K. Kimelberg. Neurobiology Research Center SUNY - Albany and Albany Medical College, Albany, N.Y.

The combination of veratridine and α-scorpion toxin induces a measurable uptake of labelled Na in mouse CNS glial cells in culture. Veratridine alone has no effect (Y. Berwald-Netter et al., submitted for publication). The effects of these agents on the membrane potential of astrocytes in primary culture derived from neonatal rat brains (see Kimelberg et. al. Brain Res. 177:533 (1979)) have been measured. The resting potential of these cells is predominately a K^+ diffusion potential with a value of -65 to -75mV, and the cells appear to be electrically silent since their IV curves are approximately linear (Kimelberg et al., Soc. Neurosci. Abst. 8:238 (1982)). Addition of veratridine (0.11 mM) usually caused a large transient depolarization (14 cells) that disappeared upon washout (9 cells). Addition of veratridine (0.11 mM) and α-scorpion toxin (0.25 μM) caused a more sustained transient or a longer lasting depolarization (9 cells) compared to the effect of veratridine alone. Tetrodotoxin (1.6 μM) prevented the depolarization induced by either veratridine alone (5 cells) or veratridine plus α-scorpion toxin (4 cells). If this concentration of tetrodotoxin is specific for Na channels in this system, the results would appear to suggest the existence of latent Na channels in these glial cells. Supported by NIH grant NS07681 to CE.

W-AM-B8 EFFECTS OF EXTERNAL pH ON INTRAMEMBRANE CHARGE MOVEMENTS IN VOLTAGE-CLAMPED MYXICOLA GIANT AXONS: NEGATIVE GATING CHARGES? C. L. Schauf. Department of Physiology, Rush University, Chicago, Illinois 60612.

Experiments investigating the effects of external Zn++ in squid axons have been interpreted as indicating that negative gating charge may move inward during activation of the Na+ conductance (Gilly and Armstrong, J. Gen. Physiol. 79: 935, 1982). This is in conflict with experiments in which the dependence of the asymmetry currents in frog myelinated nerve on external pH was examined (Neumcke et al., Biophys J. 31: 325, 1981). We have investigated this issue using voltage-clamped Myxicola giant axons. Decreasing the extracellular pH from 7.3 to 5.5 decreases total intramembrane charge movement by 23 ± 6%. In addition, the time constant for ON charge movement is increased by 33 ± 7%. The rate of OFF charge movement is, however, quite unchanged. In the same axons acidic pH decreases the maximum Na+ conductance by 22 ± 10% and slows Na+ activation by 24 ± 6%. However, Na+ tail currents are unaffected. These data cannot be explained by a simple surface charge effect, but could be taken as supporting a model in which a portion of the initial outward gating current consisted of negative charges moving inward. In contrast to acidic external pH, an internal pH of 5.5 does not alter either the magnitude or time course of intramembrane charge movement (although the Na+ conductance is reduced), suggesting that the gating charges may not move entirely across the membrane. Like external acidic pH, external Zn++ in Myxicola slows both ON gating current and the activation of the Na+ conductance (but not OFF gating currents or Na+ tails), but although the Na+ conductance is decreased, total charge movement is unaffected. (Supported by USPHS grant NS15741 and NMSS grant 1313A2).

W-AM-B9 A VOLTAGE SENSITIVE CHANNEL IN THE SURFACE COMPARTMENT MODEL OF AN EXCITABLE MEMBRANE. Martin Blank, Physiology Dept., Columbia Univ., New York, NY 10032

The Surface Compartment Model (SCM) includes the effects on transport of ionic processes (e.g. binding, concentration changes) in the surface regions of membranes. Using the SCM, it has been shown that a sodium ion influx can occur in an excitable membrane as a result of a non-specific increase in the permeability to cations (Bioelectrochemistry and Bioenergetics 9:427, 439, 1982). In addition, the physical properties of a channel protein compatible with this mechanism have been described. A molecular model for a voltage activated channel, in line with the results of the SCM studies, has been developed based on subunit dissociation equilibria of oligomeric proteins. The dissociation of hemoglobin tetramers into dimers occurs when the surface charge is approximately the same as on the inner face of the squid axon membrane (Colloids and Surfaces 1:139, 1980). The small shifts of charge across excitable membranes that precede the ion permeability changes of the action potential can lead to the opening of a molecular pore by the same mechanism.

A model for the gating of an ionic channel has been developed assuming that the channel is an oligomeric protein with the same dissociation constant as hemoglobin. Combining the relation between the hemoglobin dissociation constant and charge, together with the estimated number of (tetrodotoxin binding) channels in the axon membrane, one obtains a relation between the fraction of channels open and the surface charge density. This latter relation has been incorporated into the SCM, so that the gating currents give rise to voltage dependent changes in ion permeability, and the imposition of a voltage clamp causes a sodium ion influx as in excitable membranes. Supported by Research Contract N00014-80-C-0027 from the Office of Naval Research.

W-AM-B10 THE IONIC BASIS FOR ELONGATED ACTION POTENTIALS IN CRAYFISH GIANT AXONS INDUCED BY PLATINIZED-TUNGSTEN METAL. Liston A. Orr and E.M. Lieberman, Dept. of Biology and Dept. of Physiology, Sch. Med. East Carolina U., Greenville, NC 27834

Crayfish giant axons were studied using axial wire, space and current clamp techniques. Following cannulation of an axon with a platinized-tungsten wire electrode both propagated and space-clamped action potentials (AP) elongated. AP duration was typically 200-300 mSec (maximum to 4 secs.) A slight slowing of the AP rise was noted. The process was reversible upon removal of the electrode from the axon. The effect was not dependent on the passing of current through the platinized-tungsten metal nor on any component of the platinizing solution. Neither pure tungsten or platinum nor platinized-platinum electrodes were effective. Membrane resistance (Rm) during the AP plateau was 20-50% higher than Rm at rest. The steady state I-V plot of the altered axon exhibited anomalous rectification for both depolarizing and hyperpolarizing steps. In the absence of an inward sodium current (TTX or low external Na^+), anomalous rectification was abolished, while an inhibition of normal rectification remained. Ca^{2+} channel blockers verapamil and La^{3+} as well as Low Ca^{++} and K^+ were antagonistic to plateau formation. In 3xN[Ca^{++}], Rm during the plateau was 200-300% higher than at rest. Comparisons of IV plots of altered axons bathed in 4xN[K^+] and in normal [K^+] exhibited minimal differences in steady-state Rm at comparable potentials. It is concluded that a product of the platinum-tungsten:axoplasm interaction produced elongated AP's by altering the membrane by: 1)block of normal K^+ outward rectifying current; 2) decrease of steady-state outward K^+ current; and 3) accentuation of an inward Ca^{++} current during AP generation.
Supported in part by a grant from Sigma Xi to L.A.O.

W-AM-B11 CHARACTERIZATION OF SCHWANN CELL RECEPTORS FOR GLUTAMATE IN SQUID NERVE. J. Villegas*, D.W. Herzfeld and V. Reale. Centro de Biofísica y Bioquímica, I.V.I.C., Apartado 1827, Caracas 1010A Venezuela.

The sensitivity of the Schwann cell membrane and axon electrical potentials to L-glutamate, D-glutamate, L-aspartate, L-glutamine, and γ-aminobutyric acid (GABA), was investigated in the giant nerve fiber of the tropical squid *Sepioteuthis sepioidea*. It was found that none of these compounds at concentrations of 10^{-7}M in the external seawater medium, has any appreciable effect on the axon resting membrane potential; whereas L-glutamate, but not the other compounds, produces large variations in the resting membrane potential of the Schwann cells in the same giant nerve fibers. It was also found that following a brief (3 min) exposure to L-glutamate, which produces a 10 mV transient hyperpolarization in the Schwann cells, the responses of these cells to the propagation of nerve impulse trains by the axon and to similar subsequent applications of the aminoacid, remain apparently unchanged. However, following a more prolonged (10 min) exposure to L-glutamate, which is accompanied by a delayed but sustained 20 mV depolarization of the Schwann cells, the hyperpolarizing responses of these cells to the aminoacid and to repetitive axonal excitation are reversibly suppressed for a period of 10-30 min. However, during such a recovery period the Schwann cells are still sensitive to the external application of 10^{-6}M carbamylcholine. The chemical specificity of the Schwann cell response to L-glutamate found in these experiments, shows the presence of specific receptors for the aminoacid in the plasma membrane of this cell. The suppressive effect of glutamate application on the hyperpolarizing phase of the Schwann cell responses to the aminoacid and to axonal excitation, suggests that such membrane sites may be involved in the modulation of the Schwann cell cholinergic responses to nerve impulse train conduction by the axon.

W-AM-B12 DETERMINATION OF Ca CONCENTRATIONS IN SQUID AXONS WITH Ca SELECTIVE ELECTRODES. DiPolo, R., Rojas, H., Vergara*, J., López, R. and Caputo, C. C.B.B., IVIC, Apdo. 1827, Caracas 1010A, Venezuela. *Dept. Physiology, UCLA, Los Angeles, CA 90024, USA.

Measurements of free Ca^{2+} in squid axons from D. plei, under different experimental conditions have been carried out using Ca selective electrodes prepared with glass cannulae (20μm diameter) plugged with a PVC gelled ETH 1001 sensor (kindly supplied by Prof. Simon). These electrodes showed good selectivity for Ca^{2+} over Mg^{2+}, H^+, K^+ and Na^+, a Nernstian behaviour down to pCa 6 and subNernstian, but still useful responses down to pCa 8. Each electrode was calibrated with solutions prepared with different Ca buffers (EGTA, HEEDTA, NTA) using apparent Ca association constants measured under conditions of pH and ionic strength closely resembling the axoplasmic environment. In freshly dissected axons, incubated in artificial sea water containing 4 mM Ca^{2+}, the mean resting free Ca^{2+} was 0.106 μM (n=15). This value could be significantly altered by changes in the external $|Ca|$, its increase in high $|Ca|_o$ could be blocked by TTX. Intact axons, whose internal Ca was slightly increased (about 0.20 μM) were able to recover their original low resting $|Ca^{2+}|_i$ value, in the absence of external sodium. On the other hand, poisoned axons loaded with Ca (about 10 to 20 μM) could decrease their $|Ca^{2+}|_i$, by a sodium dependent process, but only to values near 1 μM. These results are consistent with the idea that the Na-Ca exchange mechanism operates more effectively in a high range of $|Ca^{2+}|_i$ while the $|Na|_o$ independent, metabolically driven Ca pump, regulates the $|Ca^{2+}|_i$ in the physiological range.
(CONICIT S1-1144, S1-1148)

W-AM-B13 SINGLE GLYCINE-ACTIVATED CHLORIDE CHANNELS IN SPINAL CORD NEURONS DISPLAY ANOMOLOUS SELECTIVITY FOR ANIONS

O.P.Hamill, J.Bormann and B.Sakmann. Max-Planck Institut für biophysikalische Chemie, Göttingen, F.R.G.

Compared with the extensive knowledge of the ion selective mechanisms of various cation channels in nerve membrane there is relatively little detail regarding anion selective channels. One of the main reasons for this deficiency has been the inability to accurately manipulate and maintain constant, internal anion concentrations while studying their effects on anion conductance changes. In the present study we overcome this difficulty by measuring, in isolated membrane patches of cultured spinal cord neurons, single channel currents activated by glycine, a putative inhibitory transmitter known to increase the anion conductance of the soma membrane of spinal motor neurons. We find that for anions of the halide series the pemeability sequence(Br>I>Cl>F)differs from the conductance sequence(Cl>Br>F>I). This behaviour is inconsistent with previously invoked electrodiffusion pore models of ion permeation in anion channels in which ions are selected according to their hydrated size. It indicates that permeant anions interact with the channel.

W-AM-B14 DYNAMICS OF NEURAL NETS CONSTRUCTED OF CELLS WITH CHEMICAL AFFINITY

P.Anninos and M.Kokkinidis. Dept. of Physics, University of Crete, Iraklion Crete, Greece

Previous studies with neural nets constructed of discrete populations of formal neurons have assumed that all neurons have the same probability of connection with any other neuron in the net. (Anninos et al,1970).Although this approach has been fruitful in inspiring and shaping whole line of research in neural modeling,it does not incorporate the behavior of the neural systems in which the nerve connections can be set up by means of chemical markers carried by the individual cells. The examination of this important constraint gives rise to ordered patterns of nerve connections. With this new approach we studied again the dynamics of isolated neural nets as well as the dynamics of neural nets with sustained imputs.One of the main important finding so far is that the class A nets (Anninos et al,1970) which give all the time sustained activity for any initial activity less than one($a_0 < 1$)(without the new constraint) do not give sustained activity when we incorporate the chemical markers under certain choice of parameters.With more studies in this direction we hope to understand better the relationship between structure and function of neural systems.

W-AM-C1 PROTEIN CRYSTALLIZATION IN TWO DIMENSIONS by E.E.Uzgiris,General Electric Research & Development Center, Schenectady, New York 12301

Two dimensional crystallization has been shown to occur for antibodies bound to hapten conjugated phospholipid monolayers.[1] It could be said that we can now establish the generality of this phenomenon and that orientation of bound molecules (through specific ligand interactions) and their freedom to rearrange on the surface (through lipid mobility) are the principal conditions for ordering in two dimensions. This technique could then be employed with different types of molecules for structure determination. In addition to the antibody crystallization, I report on the two dimensional ordering of lectins when bound to glycolipids dispersed in a phospholipid monolayer.

[1]E.E.Uzgiris and R.D.Kornberg, Nature(in press)

W-AM-C2 STRUCTURE-FUNCTION RELATIONSHIPS IN THE CORE HISTONE OCTAMER AND THE NUCLEOSOME. E. N. Moudrianakis, C. L. Hatch, R. Burlingame, W. E. Love, Departments of Biology and Biophysics, The Johns Hopkins University, Baltimore, MD. 21218

We have recently grown x-ray quality crystals of the undegraded core histone octamer. The space group is $P3_121$ or its enantiomorph, and the crystals diffract to better than 3.5A resolution.[1] Data have been collected from two putative heavy metal derivatives and are being analyzed.

The organization of the histones within the purified octamer or octamer-DNA complexes was also probed by proteolytic enzymes. We have determined the conditions which regulate the accessibility of the "unstructured" histone termini and produced a number of modified histone octamers. Additionally, we were able to determine the order of cleavage of the amino- and carboxy-termini of a specific histone. The modified forms of octamer have been reconstituted with DNA and the various reconstitutes have been characterized with respect to their stability and degree of compaction. Furthermore, the role of the various structures of these reconstituted complexes in the in vitro transcription assay has been analyzed.

W-AM-C3 KINETIC AND EQUILIBRIUM FOLDING MUTANTS IN THE α SUBUNIT OF TRYPTOPHAN SYNTHASE. C. R. Matthews, M. M. Crisanti, J. Manz, Department of Chemistry, Penn State University, University Park, PA 16802.

Equilibrium and kinetic difference UV studies on the reversible unfolding of the wild type α subunit of tryptophan synthase from E. coli and two missense mutants have shown that mutations can elicite two different types of responses. One type, exemplified by the substitution Glu 49 ⟶ Met 49, is most easily explained by an increase in the free energy of an intermediate form while the energies of the transition state and the native form are unchanged. This type can be described as an "equilibrium" mutant. The second type, exemplified by the substitution Gly 211 ⟶ Glu 211, is explained by an increase in the energy of the transition state while the energies of the native and intermediate forms are nearly unchanged. This behavior is that expected of a "kinetic" mutant. Although the behavior of both mutants clarify the model for folding of the α subunit, the "kinetic" mutant focuses attention on the nature of the rate limiting step linking a partially folded intermediate and the native conformation. Since the amino acid at position 211 has been inferred to be at the interface between domains in this two domain protein, this and other data suggests that the transition from the intermediate to the native form may be limited by the association of the two prefolded domains. Supported by PHS grant GM 23303.

W-AM-C4 RIBONUCLEASE T_1 BINDS WITH AN ISOSTERIC NON-ACTIVE PHOSPHONATE ANALOGUE OF GpU
Robert J. Kreitman, Ohio State Univ. College of Medicine, Pharmacology Dept., Columbus, OH 43210
Frederick G. Walz Jr., Kent State Univ., Biochemistry Dept., Kent, OH 44242
Introduced by Dr. Philip B. Hollander

We have prepared guanylyl(3'-6')6'-deoxyhomouridine (GpcU), which is a substrate analogue of RNase T_1. This analogue has all of the known groups which are involved in the interaction of the substrate GpU with RNase T_1: These include the guanine base, the guanosine 2' hydroxyl and 3' phosphate groups, and the leaving nucleoside (Osterman, H.L. and Walz, F.G. (1978) Biochemistry 17, 4124). GpcU is not subject to RNase T1 catalysis because the scissile phosphorus-oxygen bond in GpU is replaced by a stable phosphorus-carbon bond. GpcU was synthesized by condensing pyridinium 2',3'-O-isopropylidene-6'-deoxyhomouridine-6'-phosphonate (1.2 mMol) with N^2-benzoyl-5'-O-di-p-methoxytritylguanosine (1.5 mMol) in the presence of DCC and pyridine. After deblocking, GpcU was separated from its 2'-6' isomer using chromatography on DEAE Sephadex A-25. The isolated GpcU (0.13 mMol) appeared to be pure, as evidenced by TLC in 3 different solvent systems. TLC and UV-spectroscopy revealed that the product is nearly identical to GpU. The binding of RNase T_1 has been studied using UV difference spectroscopy at pH 5.5, 0.2 M ionic strength, and 25°C. A 1 : 1 enzyme:GpcU binding stoichiometry was observed with a dissociation constant of $5.42 \pm .16 \times 10^{-5}$ M, which is very close to the K_M value observed for GpU of 2.8×10^{-5} M (ibid). These results suggest that the guanine base and guanosine 2' hydroxyl and 3' phosphate groups of GpcU are interacting with the enzyme. Therefore, GpcU will be useful for equilibrium relaxation kinetic and X-ray crystallographic studies aimed at elucidating the mechanism of RNase T_1 catalysis.

W-AM-C5 CD STUDIES OF FIBRONECTIN STRUCTURE
N.M. Tooney#*, D.L. Amrani*, G.A. Homandberg* and M.W. Mosesson* Department of Chemistry, Polytechnic Institute of New York, Brooklyn, NY (#) and the Department of Medicine, Mt. Sinai Medical Center, Milwaukee, WI (*).

Human plasma fibronectin has an unusual far uv circular dichroism (CD) spectrum with relatively weak ellipticity bands at 227, 212 and 199nm. The latter two bands have the sign but not the typical magnitude representative of β sheet structures. The presence of a positive ellipticity band at 227nm for proteins has been ascribed to β turns or to specific orientations of aromatic chromophores. We have examined the near uv CD spectrum of intact fibronectin, proteolytic fragments of fibronectin, chemically modified fibronectin, and fibronectin from another species (rat) to determine the origins of the far uv CD spectrum.

We find that three major proteolytic fragments of human fibronectin (25,60 and 140 Kd) have quite different spectral characteristics, with the 25 Kd and 60 Kd fragments having a pronounced band at 227nm and negative bands in the 275-285nm and 290-300nm regions. There are two prominent negative bands due to tryptophan at 292 and 299nm. Only the 25 and 60 Kd fragments have a band at 299nm. Brief treatment of intact fibronectin with N-Bromosuccinimide affects primarily the 299nm and the 227nm bands. Rat fibronectin, in contrast to human, has weak ellipticity bands at 227 and 299nm. These data suggest that the 227nm band is related to the 299nm band of tryptophan and that these spectral characteristics are primarily associated with the 25 and 60 Kd regions of the fibronectin molecule.
Supported by NIH grant HL 28444.

W-AM-C6 ACTIVATION AND INACTIVATION OF PURIFIED BOVINE BRAIN ACETYLCHOLINESTERASE (AChE) BY MULTIVALENT CATIONS.
By J. K. Marquis & E. E. Black, Department of Pharmacology and Experimental Therapeutics, Boston University School of Medicine, Boston, MA 02118.

Kinetic analysis of the interaction of trivalent cations with AChE revealed at least three distinct populations of anionic binding sites. AChE was purified from bovine caudate nucleus by affinity chromatography to a specific activity of 1.1mmoles ACh/hr/mg protein. The cations studied included the chloride salts of Y^{3+}, La^{3+}, Tb^{3+} and Sc^{3+} in low and high ionic strength buffers (2mM Pipes ± 0.1M NaCl) and a chlorohydrate compound of Al^{3+} in 2mM Tris ± 0.1M NaCl. In all cases, a high-affinity noncompetitive or allosteric activation was observed at very low concentrations (1-10μM); at higher concentrations (50-200μM) these cations were purely noncompetitive inhibitors; and at 300-500μM they exerted a mixed competitive-noncompetitive inhibition. Inhibition by 100μM of all the cations was fully reversed by addition of 1mM EDTA, while inhibition by 500μM Y^{3+}, La^{3+} or Tb^{3+} was unaffected by EDTA, suggesting a nonspecific action of these cations at higher concentrations. As shown by Roufogalis and Wickson (J. Biol. Chem. 248: 2254, 1973) for bovine erythrocyte AChE, the water-soluble carboxyl group affinity reagent, 1-ethyl-3-(3-dimethylaminopropyl) carbodiimide, specifically blocked the activating effect of the multivalent cations on purified brain enzyme, supporting the suggestion that the β- or "activator" peripheral anionic site (P_1) involves a carboxyl group outside the enzyme active site. The relationship of these binding sites to peripheral anionic sites described by others is analyzed; and the effects of trivalent and divalent cations on the interaction of organophosphate inhibitors with the catalytic site of mammalian brain AChE is under investigation. (Supported by U.S.Army ARO #DAAG29-82-K-0042, and the Center for Brain Sciences and Metabolism, Cambridge, MA).

W-AM-C7 STRUCTURAL AND ELECTROSTATIC IMPLICATIONS FOR ENZYME-SUBSTRATE RECOGNITION AND CATALYSIS IN COPPER, ZINC SUPEROXIDE DISMUTASE. Elizabeth D. Getzoff and John A. Tainer, Dept of Immunopathology, Research Institute of Scripps Clinic, 10666 N. Torrey Pines Road, La Jolla, CA 92037.

Cu, Zn superoxide dismutase (SOD) catalyzes the very rapid two-step dismutation of the toxic superoxide radical ($O_2 \cdot^-$) to molecular oxygen and hydrogen peroxide through the alternate reduction and oxidation of the active site Cu ion. Computer graphic analysis of the refined 2 Å model and its molecular surface defined the topography of the active channel in atomic detail; and in combination with biochemical information suggested a specific model for the enzyme mechanism. The molecular surface of the channel shows a single, highly complementary position for $O_2 \cdot^-$ to bind both the Cu(II) and the essential Arg 141 with the correct geometry; two water molecules form a ghost of the $O_2 \cdot^-$ in this position.

Calculation and color computer graphics display of the electrostatic potential and the electrostatic field vectors in the active channel of SOD defined the electrostatic contributions to the enzyme-substrate recognition process. Sequence-invarient active channel residues participate in a unique electrostatic environment appropriate for the binding of the negatively charged substrate. Furthermore, the electrostatic field around the enzyme codes for substrate recognition and guidance to the catalytic site prior to actual collision. Dissection of the electrostatic potential gradient indicated the relative contributions of individual charged residues and suggested an important role for Lys 134 and Glu 131 in directing the approach of the $O_2 \cdot^-$. This technique may be of general use for the elucidation of long-range electrostatic recognition processes important in controlling the specificity of macromolecular interactions and assembly. (Supported by Sigma Xi)

W-AM-C8 STRUCTURE AND FUNCTION OF THE ENZYMES OF β-OXIDATION. Jack Schmidt, Camilo Rojas, and James T. McFarland, Department of Chemistry, University of Wisconsin-Milwaukee, Milwaukee, Wisconsin 53201.

Resonance Raman (RR) studies on fatty acyl CoA dehydrogenase and oxidase indicate differences in the spectra of the two enzymes which are similar to spectral differences between aqueous and nonaqueous solutions of FMN. The RR spectrum of the oxidase is similar to that of an acetonitrile solution of flavin while the spectrum of the dehydrogenase is similar to that of an aqueous solution of flavin. Since flavin is known to be strongly hydrogen bonded to water but not to acetonitrile these data suggest that FAD is hydrogen bonded to the protein of the dehydrogenase but not to the oxidase. Functional studies using FPCoA (a pseudo substrate producing a chromophoric product) indicate that the chemically important step of hydrogen transfer is rate limiting for both enzymes and that the data for each enzyme are consistent with a mechanism in which reaction takes place through acid catalyzed labilization of the C-2 proton through C=O protonation followed by base catalyzed removal of that proton with formation of a charge transfer complex between substrate anion and enzyme bound flavin. The functional difference between the oxidase and dehydrogenase depends on the difference in stability of the charge transfer complexes. The oxidase does not form stable product complex. For those product complexes of dehydrogenase which are kinetically labile, dissociation of the complex leads to oxidase activity. The structural basis of this functional difference will be discussed.

W-AM-C9 RELAXATION OF ADENYLATE CYCLASE FROM ACTIVATED AND INHIBITED STATES by P.M. Lad, D.M. Reisinger, and P.A. Smiley, Kaiser Regional Research Laboratory, 4953 Sunset Boulevard, Los Angeles, CA 90027.

The turkey erythrocyte adenylate cyclase system shows the unique property of binding tightly the guanine nucleotides GDP, GDPβS, Gpp(NH)p. This unique feature allows for the analysis of ligand requirements and rates of transition from nucleotide occupied states. With GDP as the resident nucleotide two reaction steps are observed: rapid release of nucleotide with time of completion (Tc= 1 min) and a slower restoration of activation (Tc=20 min). Isoproterenol (iso) and GMP are re-required for the slow step. Modification of the cyclase system with cholera toxin abolishes the requirement for GMP with a ten fold increase in the rate of the slow step ($Tc < 1$ min). With Gpp(NH)p as the resident nucleotide two relaxation conditions are observed, these include (i) a spontaneous ligand independent process (ii) an iso induced process which does not require GMP ($Tc < 4$ min). Regardless of the relaxation mode Gpp(NH)p retains only partial access to the system upon dissociation. EDTA, which is without effect with GDP as the occupying nucleotide, markedly potentiates Gpp(NH)p associated relaxation. When a hybrid GDP/GDPβS complex is formed GDPβS is release by iso alone ($Tc \sim 10$ min) while the further release of GDP requires the simultaneous presence of iso and GMP ($Tc \sim 6$ min). The data indicates that the type of nucleotide and the state of membrane (native or modified) are key determinants of relaxation of the cyclase system. In addition, the results will allow for the formulation of a kinetic assay for site closure within the regulatory complex.

W-AM-C10 ALUMINUM-INDUCED CHANGES IN CALMODULIN. Neal Siegel and Alfred Haug (Intr. by E. J. McGroarty). Department of Botany and Plant Pathology and Pesticide Research Center, Michigan State University, East Lansing, MI 48824.

The interaction of aluminum ions with bovine brain calmodulin has been examined by fluorescence spectroscopy, circular dichroism spectrophotometry, and by the calmodulin-dependent activation of 3':5'-cyclic nucleotide phosphodiesterase. Spectroscopic studies indicate that aluminum binds to calmodulin stoichiometrically and in a positively cooperative manner. There appear to be four specific aluminum binding sites on calmodulin. Binding of two aluminum ions per protein suffices to produce a major structural change. Estimates indicate that the binding affinity for the first mol of Al^{3+} bound to the protein is approximately one order of magnitude stronger than that of Ca^{2+} to its specific sites. As monitored by a hydrophobic fluorescent probe, ANS, aluminum ions also induce changes in the hydrophobic surface domains of calmodulin, which are considerably more pronounced than those observed in the presence of calcium ions only. Interactions of aluminum ions with calmodulin lead to a helix-coil transition, whereby the helix content decreases by about 30% relative to that of the native structure. Four mol of Al^{3+} per mol of calmodulin completely block the activity of 3':5'-cyclic nucleotide phosphodiesterase. The aluminum-induced inhibition of the enzymatic activity probably results from an improper interface between the enzymatic protein and the aluminum-calmodulin complex. Highly hydrated aluminum ions apparently promote disordered polypeptide regions in calmodulin which, in turn, profoundly influence the protein's flexibility. The aluminum-calmodulin complex may be a crucial lesion in aluminum toxicity. This work was supported by DOE contract No. DE-AC02-76ER01338.

W-AM-C11 INTRAMOLECULAR ELECTRON TRANSFER IN XANTHINE OXIDASE. A. Bhattacharyya and G. Tollin, Department of Biochemistry, University of Arizona, Tucson, Arizona 85721, M. Davis and D.E. Edmondson, Department of Biochemistry, Emory University, Atlanta, Georgia 30322.

Laser flash photolysis studies on the transfer of electrons from 5-deazariboflavin radical to xanthine oxidase under anaerobic conditions has shown that the protein-bound FAD and both Fe/S centers are readily reduced. Kinetic traces obtained at 467 and 483nm indicate that the reduction is biphasic, with Fe/S_I being reduced more rapidly ($t_{1/2}\simeq$10ms) than Fe/S_{II} ($t_{1/2}\simeq$60ms). The reduction kinetics of the two Fe/S centers does not change appreciably with protein concentration, nor by treatment with CN^- or alloxanthine. In the alloxanthine-treated deflavo enzyme however, Fe/S_{II} reduction is completely absent, and Fe/S_I is reduced at a rate twice that observed in the native enzyme ($t_{1/2}\simeq$5ms). The decay of the 5-deazaflavin radical is dependent on protein concentration in both native and deflavo enzymes. This dependence is abolished by treatment with alloxanthine, indicating that molybdenum provides an entry point for electrons.

The formation of FADH·, observed at 590nm, occurs within 1ms ($t_{1/2}\simeq$120μs), and is independent of protein concentration, while the decay occurs more slowly and is essentially complete by 100ms. In the alloxanthine-complexed enzyme, FADH· kinetics are appreciably altered and the signal contribution due to FAD reduction at 467nm is diminished, indicating that two different pathways leading to FAD and Fe/S reduction are operative in the native enzyme.

From an analysis of kinetic traces and reported redox potentials, we have been able to assign rate constants to each of the inter- and intramolecular processes representing equilibration of electrons between the different redox centers of the native enzyme. (Supported in part by NIH Grant #AM15057).

W-AM-C12 AN ELECTROSTATIC MODEL APPLIED TO ELECTRON TRANSFER PROTEINS. J. A. Watkins and Michael Cusanovich. University of Arizona, Biochemistry Department, Tucson, AZ 85730.

A model for the electrostatic potential energy of a protein is developed that provides an analytic representation of the effect of ionic strength on a bimolecular rate constant. According to the model, an electron transfer protein is considered as a low dielectric sphere with a surface of finite thickness, an interior, and an active site located within a region of the surface. Proteins approaching with relative orientations leading to collisions at the regions containing the active sites form bimolecular complexes that will react. The bimolecular rate constant at finite ionic strength is largely dependent on the electrostatic fields in the regions around the active sites of the proteins. The electrostatic potential energy of complex formation is approximately proportional to the interactions between charge configurations and effective dipole moments in the region of intermolecular contact around the active site. The model is applied to a bimolecular reaction between cytochrome c and either flavodoxin or cytochrome b_5. Analysis of kinetic data available in the literature (1,2) using the model gives areas of intermolecular contact in good agreement with structural models of the bimolecular complexes (3,4). The effective net charges and dipole moments in the region of contact are consistent with the structural models when the average effective dielectric constant in the active site region of the bimolecular complex is 15±5.

Supported by NIH grant #2 R01 GM 21227-07A1.

1) Stonehurner, et. al. (1979) Biochemistry 18: 5422-5427.
2) Simondsen, et. al. (1982) Biochemistry, in press.
3) Salemme (1976) J. Mol. Biol. 102, 563-568.
4) Matthew, et. al. 1982, in press.

W-AM-C13 CONFORMATIONAL STUDIES ON THE CORTICOTROPIN-RELEASING FACTOR. K. Bode, M. Mabilia, P. Pallai and Murray Goodman, Department of Chemistry, University of California, San Diego, La Jolla, CA 92093 and J. Rivier, The Salk Institute, San Diego, CA 92138

Corticotropin-releasing factor (CRF) is a 41-residue peptide stimulating the secretion of corticotropin and β-endorphin-like immunoactivities. A theoretical study of its secondary structure by the prediction method of Chou and Fasman suggested a largely α-helical secondary structure. Spectroscopic investigations by means of circular dichroism in trifluoroethanol confirmed the theoretical results revealing the existence of a high α-helical structure (ca. 80%). In aqueous solutions, the helicity was shown to be much lower (ca. 20%) than in trifluoroethanol. The high resolution ^{1}H-NMR spectra in TFE-d_3, D_2O and H_2O confirm these findings. Broad signals in the aliphatic region of the NMR spectra in TFE indicate a high percentage of ordered structure. The three aromatic residues present in CRF (Phe^{12}, His^{13}, His^{32}) were used as markers to obtain more information about the distribution of the helical regions in the peptide.

W-AM-D1 BARIUM EFFECTS ON POTASSIUM EFFLUX FROM DEPOLARIZED FROG SKELETAL MUSCLE. B.C. Spalding, J.G. Swift and P. Horowicz. Dept. of Physiology, Univ. of Rochester, Rochester, N.Y. 14642.

In frog twitch fibers, the K^+ delayed rectifier inactivates for steady internal potentials more positive than -20 mV, so that at these potentials, K^+ moves through the inward rectifier system. At a constant internal potential in the range of -20 to 0 mV, K^+ efflux through the inward rectifier increases from a low value when $[K^+]_o$ = 0 mM to a high value when $[K^+]_o \geq 200$ mM. The K^+ efflux increment is a sigmoidal function of $[K^+]_o$ which at low $[K^+]_o$ is proportional to $[K^+]_o^2$. For low $[K^+]_o$'s, K^+ unidirectional fluxes through the inward rectifier channel conform to the independence principle. However, as the channels get converted to the high flux state by increasing $[K^+]_o$, n' in the flux ratio equation, influx/efflux = $\exp[-n'(V-V_K)F/RT]$, increases in value from 1 to 2. To better understand the differences between the low and high flux states of the inward rectifier channels we have studied their sensitivity to $[Ba^{++}]_o$ by measuring K^+ efflux when $[K^+]_o$ = 0 mM and when $[K^+]_o$ = 225 mM. In order to keep the fibers depolarized during the measurement, sartorius muscles were pre-equilibrated in a high $[K^+]_o$ and $[Cl^-]_o$ solution where $[K^+]_o$ = 305 mM and $[Cl^-]_o$ = 120 mM, and $V_i \neq 0$ mV. When $[K^+]_o$ = 0 mM and the inward rectifier is in the low flux state, the $[Ba^{++}]_o$ which produces a 50% reduction in K^+ efflux is about 3.8 mM. When $[K^+]_o$ = 225 mM and the inward rectifier is in the high flux state, the $[Ba^{++}]_o$ which produces a 50% reduction in K^+ efflux is about 1.6 mM. This result suggests that when the inward rectifier channels become converted from the low to the high flux state they become more sensitive to blockade by external Ba^{++}.

(Supported by grants from the USPHS and the MDA).

W-AM-D2 CONTRACTILE ACTIVATION IN SMOOTH MUSCLE OF THE TUNICATE, Ciona intestinalis. G.A.D. Nevitt and Wm. F. Gilly. Hopkins Marine Station of Stanford University, Pacific Grove, CA.

Smooth muscle comprising the somatic musculature of this primitive chordate was characterized morphologically and physiologically. Each longitudinal muscle band contains many parallel bundles of muscle fibers. A bundle is composed of 4-8 fibers, each about 10 μm in diameter and separated from one another by about 20 nm. A basement membrane that does not penetrate the clefts surrounds the bundle; evidence for gap junctions or electrical coupling between fibers in a bundle is as yet equivocal. Myofilaments are located peripherally; mitochondria and other organelles are in the central core of the rosette-like arrangement. A subsarcolemmal network of vesicles and/or invaginating tubules exists but does not penetrate the myofibrillar space. Individual fibers are at least several mm long; they may run the entire muscle band's length.

Muscle fibers make a brief (10-20 ms at 20°C), all-or-nothing action potential and twitch when a bundle is locally stimulated with a bipolar electrode. Twitches rise to a peak in a few hundred ms and relax over several seconds. Action potentials appear to be Ca spikes: 1) Twitches are abolished in Ca-free media; 2) Total Na replacement does not inhibit twitches; 3) Sr and Ba substitute for Ca in twitch generation; 4) 1-2 mM La or 4-5 mM Cd block twitches in the presence of 60 mM Ca. The rates at which Ca-removal abolishes tetani vs. KCl contractures are not markedly different. These observations suggest the intracellular release of Ca may not be very important, and that most activator Ca enters during the action potential. This relatively simple preparation seems promising for certain physiological studies of smooth muscle, e.g. mechanics. Preliminary results indicate that the length-tension relation may not have a descending limb out to twice resting length.

W-AM-D3 INWARD RECTIFICATION IN THE T-SYSTEM OF FROG SKELETAL MUSCLE J.A. Heiny, F. M. Ashcroft[a] and J. Vergara. Dept. of Physiology, UCLA School of Medicine, Los Angeles, CA; [a]Univ. Laboratory of Physiology, Oxford, UK.

Inward rectifier currents were recorded from frog single fibers voltage-clamped with a three-vaseline gap method. The potential change across the T-system membranes was simultaneously monitored optically using the absorbance change from the non-penetrating potentiometric dye NK2367 at 670 nm (Heiny & Vergara, 1982). The effects of the inward rectifier conductance on the time course and magnitude of the tubular membrane potential were studied in response to voltage clamp steps from -140 to +80 mV, both in a 100 mM K Ringer's and in the presence of blocking ions. For hyperpolarizing steps, large inward currents were recorded, and the peak amplitude of the tubular optical signals was attenuated. This attenuation (A neg./ A pos.) approached a maximum value of 55% at -140 mV. In addition, the inward currents were associated with a decrease in the time constant of the hyperpolarizing optical signal. Both effects were reversibly blocked by the addition of 10 mM Cs and 50 mM TEA. At lower Cs concentrations, the voltage-dependence of the Cs block (Gay & Stanfield, 1977) was readily observed in the tubular optical signals. These findings provide independent evidence for the presence of an inward rectifier conductance in the T-system,and suggest that activation of this conductance results in a significant decrement of potential in the T-system. They are well predicted by a radial cable model for the T-system which includes a voltage-dependent inward conductance.

Supported by USPHS grant AM-25201, MDA grant JLNRC #6, MDA postdoctoral fellowships to JAH & FMA, and NIH training grant NS-07101 to JAH.

W-AM-D4 SPECTRAL DEPENDENCE OF ABSORBANCE SIGNALS FROM SKELETAL MUSCLE FIBERS STAINED WITH MEROCYANINE DYES AND ILLUMINATED WITH LINEARLY POLARIZED LIGHT

J.A. Heiny and J. Vergara, Dept. of Physiology, UCLA School of Medicine, Los Angeles, CA.

The absorbance signals recorded from voltage-clamped skeletal muscle fibers stained with the potentiometric dye NK2367 and illuminated with unpolarized light consist of both tubular and surface membrane components, with the relative proportion of these components being strongly wavelength dependent (Heiny & Vergara, JGP:80,203-230,1982). To further investigate these wavelength-dependent phenomena, we have performed experiments in fibers illuminated with linearly polarized light and stained with dye NK2367, or the closely related analogue WW375. Our results indicate that the signals recorded with both dyes are highly dichroic. The spectral dependence of both the surface and T-system signals changes when the plane of polarization is varied from 0° to 90° with respect to the fiber axis. When the 0° and 90° spectra are subtracted, the resulting spectra of the dichroism for the two membrane compartments is of opposite sign. This suggests that the different absorbance signals arise from membrane compartments having orthogonal net orientations.

Supported by USPHS grant AM25201, MDA grant JLNRC #6, MDA postdoctoral fellowship and NIH training grant NS07101 to JAH.

W-AM-D5 CORRELATION BETWEEN SLOW INWARD CALCIUM CURRENTS AND EXCITATION-CONTRACTION COUPLING. Gonzalez-Serratos, H. and R. Valle-Aguilera. Dept. of Biophysics, University of Maryland, Baltimore, Md. and Dept. of Pharmacol. Univ. de San Luis Potosi, San Luis Potosi, Mexico.

In a previous report, preliminiary experiments indicated that slow inward calcium currents (I_{Ca}) play no obvious role in excitation-contraction coupling mechanisms in phasic skeletal muscle cells from the frog. The present experiments were designed to further investigate the above problem. In a group of experiments intracellular recorded action potentials were elicited in the presence of the I_{Ca} blocker Diltiazem. Concentrations between $1x10^{-7}$ to $1x10^{-5}$ M have no effect on the action potential, $1x10^{-4}$ M increased its duration in approximately 30% without affecting the after potential. In another group of experiments single muscle fibers were mounted in a vaseline gap voltage clamp system and the optimal depolarization to produce I_{Ca} with 1.8 or 8 mM Ca^{2+} test solutions was determined. The following results were found: a) the 100% recovery time of I_{Ca} after a first depolarization pulse is of 1.5 to 2 minutes; b) between 2 and 6 seconds after the first pulse, I_{Ca} is still completely inactivated; c) different frequencies of depolarization (1 to 0.3 per minute) produce a larger and continuous decline of I_{Ca} magnitude during each pulse; d) no correlation was found between the appearance of I_{Ca} and mechanical activation; e) I_{Ca} is very dependent on temperature, the lower the temperature, the smaller the magnitude of I_{Ca}; f) preliminary results indicate that Diltiazem acts on the external surface of the muscle membrane; and g) removing the I_{Ca} inhibition produced with Diltiazem inside the cell increases the number of Ca channels that open during the following depolarization. Supported by a grant from the NIH: NS17048-02S1.

W-AM-D6 KINETICS OF CHARGE MOVEMENT IN RAT MUSCLE ARE WELL-DESCRIBED BY A FIRST ORDER REACTION IN A DISTRIBUTED T-SYSTEM. B.J. Simon & K.G. Beam, Dept. of Physiol. & Biophysics, Univ. of Iowa.

The measured kinetics of slow asymmetric charge movement in skeletal muscle are complicated by the delayed propagation of voltage in the t-system. Previous models of charge movement have either ignored this delay or treated the t-system as a simple lumped RC. Such a lumped model fails to describe charge movement in rat muscle (see Figure). Thus, we adopted a "distributed model" in which: (i) the t-system is approximated as 12 concentric annuli of equal areas (ii) charge moves according to a first order process in which the rate constants follow constant field voltage-dependence, and (iii) charged groups are uniformly distributed throughout the t-system. The passive properties of the t-system were adjusted to fit the linear capacity transient. A Boltzmann two-state relationship was fit to the steady-state Q vs. V data thereby constraining the voltage-dependence of the rate constants but not their absolute magnitude. This remaining free parameter was determined by fitting the theory to an experimental charge movement at a single potential, which in turn determines the fits at all other potentials. The theory was compared with charge movements for upward steps in potential from -90 mV to test potentials ranging from -60 to +10 mV and for downward steps from 0 mV to -30 to -90 mV. At all potentials, and for temperatures from 3 to 25° C, the theoretical curves agreed well with measured charge movements (see Figure, T=3°). Supported by MDA and NIH (NS14901).

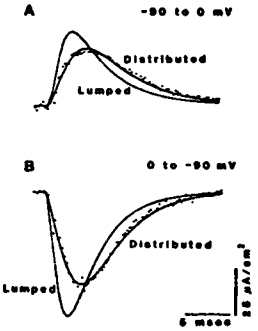

W-AM-D7 RATE OF CALCIUM RELEASE IN FROG SKELETAL MUSCLE. W. Melzer, E. Rios and M.F. Schneider. Department of Physiology, University of Rochester, Rochester, NY 14642.

The rate dR/dt of calcium release during voltage clamp depolarization of cut frog skeletal muscle fibers containing the Ca-indicator dye antipyrylazo III (Kovacs et al, Nature 279: 391, 1979) was determined as the sum of the instantaneous "uptake" rate dU/dt plus the rates of change of the myoplasmic concentrations of calcium-dye complex [CaD_2], free calcium [Ca], and calcium bound to rapidly-equilibrating intrinsic binding sites [CaB(fast)]:

$$dR/dt = dU/dt + d[CaD_2]/dt + d[Ca]/dt + d[CaB(fast)]/dt.$$

[CaD_2] was obtained directly from the light absorbance change ΔA at 700 nm. [Ca] + [CaB(fast)] was calculated from ΔA using a scale factor obtained from analysis of the effects of varying dye concentration on the rate constant for the decline of [Ca] after pulses of various durations. Since this rate constant depended on events during the pulse (Kovacs et al, 1979 and present results), dU/dt was monitored as the rate of decline of [CaD_2] + [Ca] + [CaB(fast)] after pulses of various durations and its time course during a pulse was estimated by interpolation between these values. Calculated dR/dt time courses exhibited early peaks and much lower steady values during depolarizing pulses, both for intermediate depolarizations where [Ca] also peaked and declined and for larger depolarizations where [Ca] did not decline during the pulse.

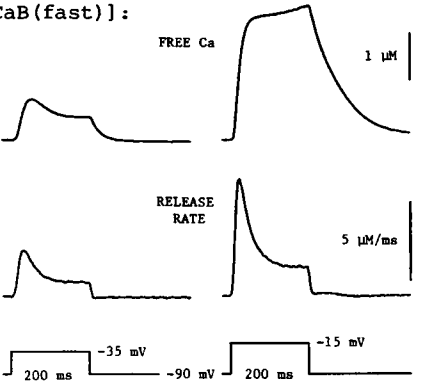

W-AM-D8 AN INTRINSIC OPTICAL SIGNAL IS RELATED TO THE CALCIUM TRANSIENT OF FROG SKELETAL MUSCLE. E. Rios, W. Melzer and M. F. Schneider. Department of Physiology, University of Rochester, Rochester, N.Y. 14642.

Intrinsic light transmission changes Y(t) and changes in myoplasmic free calcium concentration ("Ca transients", [Ca](t)) associated with depolarizing voltage clamp pulses were measured in cut skeletal fibers containing the dye Antipyrylazo III. The Ca transients were derived from the changes in transmission of light of 700 nm wavelength due to the formation of the Ca:dye complex (Kovacs et al., Nature 279:391, 1979). The intrinsic transmission changes were measured at 850 nm, a wavelength at which neither free dye nor its metal complexes absorb light. Typical records are shown. The time derivative of the intrinsic transmission (third trace) was seen to follow approximately the time course of [Ca] so that Y(t) had approximately the time course of the integral of [Ca]. A cellular structure binding Ca at a rate proportional to [Ca] would change its contents proportionally to the integral of the Ca transient. The intrinsic transmission change thus has the right kinetic properties to be monitoring the Ca contents of a compartment or structure that binds myoplasmic calcium.

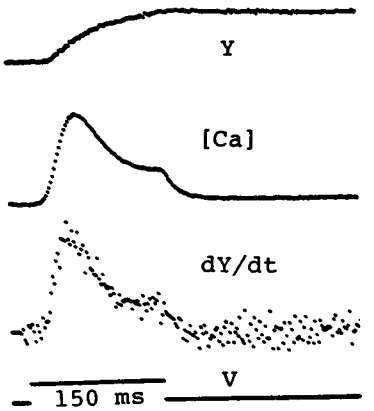

W-AM-D9 CAFFEINE POTENTIATION OF CALCIUM RELEASE IN SKELETAL MUSCLE OBSERVED USING CALCIUM- AND VOLTAGE-SENSITIVE DYES. M. Delay, B. Ribalet and J. Vergara, Dept. of Physiology, UCLA, Los Angeles, CA 90024.

The effects of caffeine, a potentiator of muscle tension, were studied in single cut skeletal muscle fibers. The fibers were stimulated either under voltage clamp or by action potential. The calcium-sensitive dye Antipyrylazo III was diffused internally to monitor calcium release, and caffeine was applied externally in the range 0 to 2.5 mM. In some experiments, the fiber was stained with the nonpenetrating potentiometric dye NK2367, which can be used at 670 nm to monitor the tubular membrane potential. A marked potentiation of calcium release occurred following action potential, increasing with caffeine concentration, and ranging from 30% at 0.5 mM to a 2-3 fold increase at 2 mM. Despite these increases, the time course of the rising phase of the scaled calcium transients was unchanged by caffeine, though the falling phase was prolonged. The voltage dependence of the calcium release under voltage clamp conditions was likewise unchanged by caffeine. Measurements using NK2367 showed no clear effect of caffeine at 0 and 0.5 mM caffeine on the tubular membrane potentials, nor was any effect noticed on surface membrane action potentials. Recent studies using calcium microelectrodes in skeletal muscle fibers have shown that the ambient cytosolic calcium level is unchanged at 0.5 mM caffeine, but is increased at 2 mM (Lopez *et al.*, 1982). Therefore, though high levels of caffeine may enhance developed tension by increasing ambient calcium levels, caffeine at any concentration acts at the level of the E-C coupling to directly potentiate calcium release.

Supported by USPHS (AM 25201), MDA (Project 6 of JLNRC), AHA-GLAA, and Crump Foundation.

W-AM-Pos1 VACUUM ULTRAVIOLET CIRCULAR DICHROISM STUDIES OF PEPTIDES, SACCHARIDES AND GLYCOPEPTIDES. E.S. Stevens, Department of Chemistry, State University of New York, Binghamton, New York 13901

Previous applications of vacuum ultraviolet circular dichroism (VUCD) spectroscopy have included distinguishing parallel and antiparallel beta-pleated sheets (e.g., D.J. Paskowski, E.S. Stevens, G.M. Bonora and C. Toniolo (1978) Biochim. Biophys. Acta 535, 188). Recent semiempirical energy calculations on alanine and valine beta-sheets (H. Scheraga, communcation) are in accord with our original interpretation.

We have now extended our VUCD applications to the conformational analysis of L-α-amino-*n*-butyric acid homo-oligopeptides (C. Toniolo, G.M. Bonora, M. Crisma, F. Bertanzon, and E.S. Stevens (1982) Makromol. Chem., in press), N-methyl polypeptides (R.T. Coffey, E.S. Stevens, A. Cosani and E. Peggion, submitted for publication), polysaccharides (e.g., J.N. Liang and E.S. Stevens (1982) Int. J. Biolog. Macromol. 4, 316), and the galactofuranosyl-containing glycopeptide of *Penicillium charlesii* (D. Herschlag, E.S. Stevens and J.E. Gander (1982) Inter. J. Peptide Prot. Res., in press). In all of these applications the spectroscopic data obtained by including the vacuum ultraviolet region allow important new conclusions concerning molecular conformation. In particular, saccharide transitions are being characterized, which will provide an additional method of conformational analysis for complex glycopeptides.

Supported by NIH Grant GM 24862 and NSF Grant PCM 79-04293.

W-AM-Pos2 A NEW PROPOSED COIL DESIGN FOR TOPICAL MAGNETIC RESONANCE

Alan Rath*, S.B.W. Roeder*, and E. Fukushima**

The application of nuclear magnetic resonance to the study of living systems (TMR, and NMR Tomography) is limited by several factors. One of these factors is the difficulty of creating a substantial field throughout a large volume. Another is the poor sensitivity/selectivity of conventional surface coils in current use.

We are proposing a coil configuration with promising application to each of these areas: two nested coils (e.g. a solenoid of small radius inside one of larger radius) with currents flowing in opposite directions. Computer modelling shows that the magnetic field generated by this system has the unique property of being small near the coil, while increasing to a maximum value at a remote point in space, along the axis of symmetry.

Two possible applications of this configuration are: 1) as the source of a unipolar static field. This would facilitate the use of NMR in studying large objects (such as a human torso) without the need for an exceptionally large bore magnet. 2) As an RF irradiating/receiver coil with improved selectivity at remote distances.

Variations in the relative geometries and field strengths of the two opposed coils allow for a wide range of positions and amplitudes of the remote maximum, for both the static and RF cases.

* Department of Chemistry, San Diego State University, San Diego, CA 92182
** Group INC-4, The Los Alamos National Laboratory, Los Alamos, NM 87545

W-AM-Pos3 MEASUREMENT OF INTRACELLULAR OXYGEN BY ELECTRON SPIN RESONANCE. Philip D. Morse II, Harold Bennett, and Harold M. Swartz. College of Medicine, University of Illinois, Urbana, IL 61801.

The measurement of intracellular oxygen is an important parameter in studying cellular physiology but so far has been limited to cells in which electrodes can be inserted or to systems in which the production of respiratory chain products can be measured.

We have developed a non-invasive method generally applicable for measuring intracellular oxygen using EPR. The spin label TEMPOL (2,2,6,6-tetramethypiperidine-N-oxyl-4-ol) has superhyperfine structure which is very sensitive to oxygen broadening. Our results show that this broadening is linear over a range of 1 to 6 ppm oxygen which covers the important physiological range of oxygen concentration. Viscosity, TEMPOL concentration, and instrument modulation also affect superhyperfine structure. The intracellular signal is isolated by addition of impermeable transition metal ions, like potassium ferricyanide, which broaden away the intracellular TEMPOL signal. Because TEMPOL equilibrates rapidly across cell membranes, the TEMPOL signal in the presence of cells and ∿50-100mM ferricyanide arises from the intracellular environment. Control studies with liposomes and red blood cells show that extracellular oxygen measured by an oxygen probe corresponds to oxygen measured by superhyperfine broadening. Our results with a cell-culture line (Mouse Thymus-Bone Marrow) shows that these cells maintain an intracellular oxygen concentration lower than the extracellular oxygen concentration. We will also present data using the effect of oxygen on the power saturation of melanin to verify our results with pigmented cells.

We gratefully acknowledge support by the National Foundation for Cancer Research, Washington D.C.

W-AM-Pos4 RAPID MEASUREMENT OF LIPOSOME PERMEABILTITY USING SPIN LABELS AND TRANSITION METAL IONS. Philip D. Morse II, and Richard Magin. College of Medicine and Department of Electrical Engineering, University of Illinois, Urbana, IL 61801.

Liposome permeability can be measured rapidly by trapping the spin label CAT_1 (2,2,6,6-tetramethylpiperidine-N-oxyl-4- trimethylamine) and observing loss of signal in the presence of transition metal ions. We studied large unilamellar vesicles made from 20% dipalmitoyl phosphatidylglycerol and 80% dipalmitoyl phosphatidylcholine by reverse phase evaporation and trapped CAT_1 or Ara-C ([^{3}H]1-β-D-arabino furanoside) in the aqueous volume.

EPR studies were performed by adding isotonic potassium trioxalatochromiate (CrOX) or potassium ferricyanide (FeCN) to the liposomes and measuring the height of the CAT_1 signal. Control experiments showed that neither CrOX or FeCN had any effect on the phase transition tempurature (Tm) of the liposomes. Dialyzed liposomes gave identical signal heights. When the liposomes were warmed through Tm, (41°C) the signal dropped to a few percent of its original height. The temperature dependence of the signal was quite sharp (±1°C). Liposomes heated quickly through Tm by placing in a boiling water bath, then cooled slowly through Tm gave essentially equivalent results. All results were confirmed by incubating the vesicles in a water bath and measuring ^{3}H Ara-C in the supernatant as a function of temperature. EPR experiments carried out by continuously varying the temperature (1°C/min) also showed a sharp drop in CAT_1 signal at Tm. We conclude that the transition metal EPR technique gives a distinct advantage over other methods of measuring release of liposomal contents.

Supported by the National Foundation for Cancer Research and NIH grant CA29010.

W-AM-Pos5 SATURATION TRANSFER EPR SPECTROSCOPY ON SPIN-LABELED MUSCLE FIBERS USING A LOOP-GAP RESONATOR. David D. Thomas, Christine H. Wendt, *W. Froncisz, *James S. Hyde, Dept. of Biochem., Univ. of MN, Mpls, MN, *Nat'l Biomedical ESR Center, Medical College of WI, Milwaukee, WI.

Previousiy, saturation transfer (ST-EPR) studies of biomolecular dynamics have involved the use of a resonant cavity and the V_2' display (absorption, second harmonic, out-of-phase). In the present study, we replaced the resonant cavity with a loop-gap resonator and used the U_1' display (dispersion, first harmonic, out-of-phase) to study spin-labeled muscle fibers. The new resonator produced virtually noiseless U_1' spectra on a 0.4 μl sample using a 4 minute scan; whereas previous U_1' experiments using a conventional rectangular cavity resulted in an unacceptably low signal-to-noise ratio. The high filling factor of the new resonator facilitated the study of these extremely small fiber bundles and permitted high microwave field intensities to be achieved at much lower incident microwave power levels, thus greatly enhancing the signal-to-noise ratio. This made it possible to benefit from the other advantages of U_1' over V_2', such as stronger signals, simpler lineshapes, and simpler data analysis. For these muscle fiber samples, the resulting sensitivity (signal/noise/sample volume) of the U_1' signals was more than 100 times that of V_2' signals obtained in a conventional cavity. Another advantage of the U_1' display is that signals from weakly immobilized probes (nsec motion relative to the labeled protein) are greatly suppressed relative to strongly immobilized probes. This reduces the ambiguity of spectral analysis, and eliminates the need for chemical treatments (e.g. using $K_3Fe(CN)_6$) that were previously required in muscle fibers and other systems. Further suppression was achieved by increasing the microwave power and decreasing the field modulation frequency.

W-AM-Pos6 NEW SPECTRAL PARAMETERS FOR ANALYZING ST-EPR:INCREASED SENSITIVITY TO MOLECULAR DYNAMICS. Thomas C. Squier and David D. Thomas. Dept. Biochem., Univ. of Minn. Med. School, Mpls.,MN. 55455.

Saturation transfer electron paramagnetic resonance (ST-EPR), used to measure rotational correlation times (τ_c) of nitroxide spin labels in the microsecond range, has been studied in the past primarily using spectral parameters introduced by Thomas, Dalton, and Hyde (1976, J. Chem. Phys. 65:3006). These parameters are ratios of peaks in the V_2' spectrum. However, in addition to changes in spectral shape, indicated by peak ratios, motion also causes a decrease in the overall absolute amplitude of the V_2' spectrum. Therefore, we have studied parameters that are sensitive to changes in both shape and absolute amplitude, thus increasing the sensitivity to motion.

As in earlier studies, we used spin-labeled hemoglobin to generate reference spectra, varying the glycerol concentration and temperature to obtain τ_c values from 10^{-8} to 10^{-3} sec. (calculated from $\tau_c = V\eta/kT$). The appropriate microwave power for H_1 = 0.25 G was measured using PADS saturation characteristics, and changes in Q were offset by changes in incident power to keep H_1 constant. The most commonly used parameter in the past has been L"/L. Since both of these parameters decrease with motion, we found greater sensitivity to τ_c when we plotted the absolute value of L", normalized by a motion-independent parameter (either the in-phase spectral amplitude at low power or the double integral of V_1). This display increased sensitivity by a factor of 2 or 3. The other parameter we investigated was the integral of V_2'. A plot of this parameter vs. τ_c shows increased sensitivity over both L"/L and L", particularly in the range of 10^{-7} to 10^{-5} sec. Although this integration obscures possible information about complex motion, it has the advantage of suppressing signals from weakly immobilized probes (Evans, 1981; J. Mag. Res. 44:109).

W-AM-Pos7 CIRCULAR INTENSITY DIFFERENTIAL SCATTERING OF ORIENTED LIQUID CRYSTALS (K. B. Hall, B. Samori, D. Keller, M. F. Maestre, C. J. Bustamante and I. Tinoco, Jr., Department of Chemistry and Donner Laboratory, University of California, Berkeley, CA 94720.)

We have applied the recently developed technique of circular intensity differential scattering (CIDS) to the study of oriented cholesteric liquid crystals. The chirality of the liquid crystals and the ease of manipulation of their helical parameters make them an ideal system for investigating the dependence of the CIDS pattern on handedness and pitch. We have studied both right- and left-handed liquid crystals of pitch from 200nm to 4μ, with the helix axis oriented either parallel or perpendicular to the incident beam. Our results showed that in the perpendicular orientation (focal conic), the right-handed liquid crystals scattered more right-circularly polarized light in the back and side directions, and more left-circularly polarized light in the forward direction. The left-handed liquid crystals gave the opposite pattern; more left-circularly polarized light was scattered to the back and side, and more right-circularly polarized light to the front. For the focal conic orientation, the position of the first zero [CIDS = $(I_L - I_R)/(I_L + I_R) = 0$] is determined by the pitch of the liquid crystal; with increasing pitch, the first zero moves closer to the forward direction (0°). For the liquid crystals oriented with the helix axis parallel to the incident laser beam (planar orientation), the scattering patterns show a zero value at 0°. We are making a detailed comparison of these experimental results to the patterns predicted by the theory (1). We hope that the CIDS of the liquid crystals can provide insight into the interpretation of the CIDS from more complex biological systems. 1. Bustamante et al., J. Chem. Phys. 1980: 73, 4273; 73, 6046; 1981: 74(9), 4839; 1982: 76, 3440.

W-AM-Pos8 ANALYSIS OF SEVERAL CURRENT FEEDBACK METHODS FOR COMPENSATION OF MEMBRANE SERIES RESISTANCE (R_S) AND CYTOPLASMIC ACCESS RESISTANCE (R_{DE}) IN GAP VOLTAGE CLAMPS. Gunter N. Franz and David G. Frazer. Dept. of Physiology, West Virginia University Medical Center and Lab. Investig. Branch, Div. of Respir. Dis. Studies, NIOHS/CDS/PHS Dept. of Human Health Services, Morgantown, WV 26506.

We investigated the effect of current feedback for series resistance compensation in several voltage clamp arrangements employing sucrose gaps or vaseline seals. The clamps studied were single- or dual-amplifier clamps of the inverting ("I"), non-inverting ("N"), and bootstrap ("B") type (Franz and Frazer, Bioph. J. 37: 73a, 1982). Compensation criteria were developed for "incomplete" (R_S) and "complete" (R_S, R_{DE}) compensation; the former compensating only for the membrane series resistance (R_S), the latter compensating for both R_S and R_{DE}, the cytoplasmic access resistance. "Complete" compensation significantly enhances clamp fidelity. The form of the compensation transfer function, $G_S(s)$, depends on (1) the location of the equivalent compensation voltage source, $V_S = G_S(s)I(s)$, (2) the clamp topology, (3) the method of obtaining the current signal (ideal current measurement, current-to-voltage converter, pool voltage, e.g. V_E), and (4) the parasitic properties of the gaps. We present a listing of $G_S(s)$ for various clamp topologies and compensation schemes.

W-AM-Pos9 AN AUTOMATED LANGMUIR BALANCE FOR MEASURING SURFACE PRESSURES OF MONOLAYERS AT AN AIR/WATER INTERFACE, Michael W. Kendall-Tobias (Intr. by Michael Seibert), Solar Energy Research Institute, 1617 Cole Boulevard, Golden, CO 80401.

An automated null-point detection surface pressure measuring device has been constructed based upon the design of the original Langmuir differential surface tension balance (1). The apparatus consists of a galvonometer with its moving arm attached to a teflon ribbon (the Langmuir barrier). A photodiode and bicell photodetector sense movement of the arm and produce a corresponding differential voltage. Feedback circuitry is used to generate a current through the galvonometer coils in order to keep the moving arm at a null point. This current is linearly proportional to the surface pressure. Instrumental accuracy is about ±0.1% of reading, with a maximum sensitivity of 10^{-3} dynes/cm and linearity up to 90 dynes/cm. Repeatability was about 10^{-3} dynes/cm under ideal conditions. This instrument was constructed for the measurement of surface pressures exerted by lipid and protein monolayers at an air/water interface. The apparatus will be compared to previous designs.

(1) I. Langmuir, J. Amer. Chem. Soc. 39, 1848 (1917).

W-AM-Pos10 USING DUAL JFETS FOR LOW NOISE AND LOW FREQUENCY MEASUREMENTS IN EPITHELIA.
D.D.F. Loo. Dept. of Physiology, U.C.L.A. Medical School, Los Angeles, California 90024.

The measurement of current and voltage fluctuations across epithelial cell membranes has given us valuable information on the nature of the epithelial sodium and potassium channels. As revealed by fluctuation analysis, relaxation processes in epithelial cell membranes are long with corresponding spectral frequencies in the range .01-100 hz. Measurement and analysis of such signals require the use of low noise (input voltage noise approx. 5 nV/hz) and low frequency amplifiers. Van Driessche and Lindemann (Rev. Sci. Instrum. 49, 52-57, 1978) have proposed a design for a differential amplifier based on the selection of carefully matched high gain (forward transconductance) n-channel JFETS (2N6451, Texas Instruments). Optimal noise performance was obtained when the drain-source current was large (close to the saturation drain current). We have investigated alternate designs which are simpler to implement, based on the use of low noise pre-matched dual n-channel JFETS with low gain (for example, 2N5521, Silonix). These JFETS are found to operate with optimal low frequency noise when the drain-source current was small. This is opposite to the situation of the high gain JFETS. A discussion of the low frequency performance of different types of JFETS and their application to noise analysis in epithelia will be presented.

Supported by grants GM 14772 and AM 17328 (UCLA Center for Ulcer Research and Education).

W-AM-Pos11 USE OF ALTERNATE CURRENT METHODS IN STUDIES OF PESTICIDE-INDUCED CHANGES IN MEMBRANES
J. Hobbs and P. Smejtek, Env. Sci. and Resources Program, Dept. of Physics, Portland State University, Portland, Oregon.

Membrane relaxation reflects changes in transport kinetics and membrane structure. Interpretation of membrane relaxation spectra in terms of equivalent circuits is not unique and it is not possible to assign, in general, a particular combination of resistors and capacitors to reflect properties of distinct structural regions. Equivalent circuits constructed on an intuitive basis ignore interplay of several physical processes [1]. We illustrate, using a typical case, how membrane current relaxation in the time domain $I(t)=I_\infty(1+\alpha_1\exp(-1/\tau_1)+\alpha_2\exp(-t/\tau_2))$ and the corresponding spectra in frequency domain can be interpreted in terms of 4 different circuits containing a minimum number of elements, 3 resistors and 2 capacitors. The equivalent circuits can be validated only on a basis of physical models but cannot be justified by the fit of the model parameters to experimental results. We have compared several graphic methods: (1) impedance, $\mathrm{Im}\,Z(\omega)$ vs. $\mathrm{Re}\,Z(\omega)$, (2) admittance, $\mathrm{Im}\,Y(\omega)$ vs. $\mathrm{Re}\,Y(\omega)$, (3) $|Z(\omega)|$ and $|Y(\omega)|$, and phase angle vs. ω, and (4) Loss tangent vs. ω from the point of view of the resolution and characterization of individual relaxations.

Pesticide-induced changes of membrane structure can be in some cases separated from contributions of membrane transport kinetics. Such an effect has been found for pentachlorophenol, a pesticide which changes membrane relaxation spectrum due to hydrogen transport kinetics [2] as well as due to the change of membrane capacitance. The results suggest the presence of structural changes of membrane/water interface region. Supported by NIH Grant 5R01 ES00937-08.

[1] H.-W. Trissl. Bioph. J. 33:233. 1981. [2] A. Pickar, J. Hobbs. BBA. 1982. To be published.

W-AM-Pos12 THE MECHANICS OF HUMAN VISUAL ACCOMMODATION
Jane F. Koretz* and George H. Handelman#, Depts. of *Biology and #Mathematics, Rensselaer Polytechnic Institute, Troy, NY 12181

The crystalline lens of the human eye is that part of the visual system providing the variable refraction necessary for focusing on near objects. This contribution results from the systematic deformation of the lens, such that both surface curvature and overall thickness are altered. When the lens supplies its minimum contribution to the visual system, it is under maximum stress. Accommodation, the process by which focusing occurs, is thus the result of a controlled elastic recovery. We have formulated a mathematical representation of the accommodative mechanism in the young eye using a few very simple assumptions: anterior lens curvature is spherical; for a very small accommodation, the arc length distance of a point from the lens pole remains unchanged; and elastic anisotropy is directed along the r and z axes. We also used the a priori criteria that, for the age 11 eye, the visual range is 14 diopters, and that zonular tension decreases with increasing accommodation. On the basis of our calculations, we determined that: the lens capsule acts as a force distributor, spreading the discretely applied force of the zonular apparatus fairly evenly over the lens fiber surface; on the anterior surface, the zonules contribute to the process both by a relaxation of applied force and by a change in the angle of force application; on the posterior surface, the vitreous acts primarily as a passive reactive support; and the posterior zonules cannot, geometrically, supply all the balancing forces necessary to achieve equilibrium at the new accommodative state.

Research supported by NIH grant EY02195.

W-AM-Pos13 STRIATED MUSCLE CELL DIGITAL IMAGE ANALYSIS. P. Paolini, J. Swanson and W. Williams, Dept. of Biology and Molecular Biology Institute, San Diego State University, San Diego, CA 92182.

We have developed two image processing systems which can be used to monitor the positions of individual sarcomeres within striated muscle cells. The first system employs a TV camera mounted on an inverted microscope; camera output is processed by a Z80-based microcomputer with 80 KBytes of memory and a real-time video frame grabber of medium resolution (240x256 pixels x 16 gray levels). The second system utilizes a Zeiss Universal microscope with 0.5 um step automatic stage, photometer, 35 mm camera, 1100 line resolution video camera and 1728 element linear photodiode array; light sources include DC, strobe and HeNe laser. The microscope is equipped with differential interference (DIC) and phase contrast optics, and is controlled by a dedicated (Zonax) microcomputer. Light detector outputs are sent to a UNIX operating system computer with 68000 and 8086 processors, 768 KBytes RAM and 21 MBytes of disk storage, with video processing hardware of 480x512 pixels x 256 gray level resolution. We have studied two muscle preparations: enzymatically dissociated Ca^{2+}-sensitive rabbit cardiac myocytes, and chemically skinned frog semitendinosus fibers. Either analyser can track contracting sarcomeres by processing sequential videotaped images to give length vs time data and derived values for shortening velocity, % shortening and relaxation time. Numerous algorithms for shading correction, contrast enhancement, edge detection, filtering and line shrinking have been applied to produce optimized images of striation patterns. Serial DIC optical sections (1.2NA, 63x immersion objective) have been used to produce pseudocolor reconstructions of these cells. (Supported in part by NSF grant PCM-8101984 and by NIH grant BRSG S07 RR 07004-06.)

W-AM-Pos14 DYPHYLLINE SUBSTRATE-LABELED FLUORESCENT IMMUNOASSAY. G.A. Bush, T.M. Li, D.M. Manzuk, J.L. Benovic, R.P. Hatch and J.F. Burd, Ames Division, Miles Laboratories, Inc., Elkhart, IN 46515.

Dyphylline, 7-(2,3-dihydroxypropyl)theophylline, is a theophylline derivative indicated for relief of acute bronchial asthma and reversible bronchospasm of chronic bronchitis or emphysema. Careful administration should include therapeutic drug monitoring to prevent toxic side effects. A non-isotopic homogeneous substrate-labeled fluorescent immunoassay (SLFIA) has been developed for monitoring dyphylline serum concentrations. The SLFIA utilizes the principles of competitive protein binding with a limiting amount of antibody to dyphylline, a constant amount of fluorogenic drug reagent (FDR), a β-galactosidase enzyme and the clinical sample containing dyphylline. The FDR is β-galactosylumbelliferone attached to 1-(6-aminohexyl)3-methyl-7(2,3-dihydroxypropyl)xanthene. The 1-(6-aminohexyl)3-methyl-7-(2,3-dihydroxypropyl)xanthene hapten was also attached to bovine serum albumin for use as an immunogen to produce rabbit anti-dyphylline antiserum. Antibody-bound FDR is non-fluorescent and not a substrate for β-galactosidase. Dyphylline in the clinical sample competes for antiserum binding, giving a higher level of free FDR. Free FDR is hydrolyzed by the enzyme, producing strong fluorescence in direct proportion to the amount of dyphylline in the clinical sample. A standard curve is set up and the fluorescence intensity of unknown samples can be directly related to dyphylline concentration. Typical intra-assay % CV's for mid-range dyphylline controls are $\leq$4%. Cross-reactivity necessary to produce a 20% increase in the 15 μg/mL dyphylline control required $\geq$25 μg/mL caffeine and $\geq$100 μg/mL theophylline. The assay format is identical to all current SLFIA procedures, with high specificity, accuracy, precision and convenience.

W-AM-Pos15 A LINEAR MODELS APPROACH TO THE ESTIMATION OF MICHAELIS-MENTEN PARAMETERS FROM IN VIVO RADIOPHARMACEUTICAL DATA. Marcia A. Testa, Richard P. Spencer, Depts. of Research In Health Education (Biostatistics) & Nuclear Medicine, Univ. Connecticut Health Center, Farmington, CT 06032.

Nutrients and analogues, which emit gamma rays or positrons, are opening the way toward studies in which the effects of substrate concentrations (on reaction rates) can be determined by external monitoring of blood/tissue. We have carried out an analysis of the necessary conditions and developed analytic methodology for estimation of the parameters V (maximum velocity) and K (Michaelis constant) when Michaelis-Menten kinetics apply after intravenous administration of a labeled substrate. Assumptions were: 1) Radiolabeled material is extracted by peripheral tissue(s) after intravenous administration. 2) During the study, reentry of activity into the blood is neglibible. 3) Transport or metabolic events which are competing are either small or can be included in an "effective" rate constant. 4) Changes in radiotracer levels are assumed to monitor substrate changes. Use of several substrate concentrations in succession is time consuming and might overload the biological system. Parameter estimation for V and K can be obtained by using the observed time-activity curve data for substrate concentration (S). The change in substrate concentration with time ($dS/dt = V.S/(K + S)$)is inverted (Counotte & Prins) and integrated to yield the expression: $V.t = S - So + K.\ln(S/So)$, where So is the substrate concentration at time zero. Parameter estimates and corresponding standard errors are obtained directly from regression procedures, enabling the inclusion of covariates if applicable. (Supported by USPHS CA 17802 National Cancer Institute).

W-AM-Pos16 ELECTROIMMUNOASSAY: A COMPETITIVE, PROTEIN-BINDING ASSAY USING AN ANTIBODY-SENSITIVE ELECTRODE. G.R. Connell and K.M. Sanders, Department of Physiology, University of Nevada, School of Medicine, Reno, NV 89557.

A novel assay technique was developed in which antibody sensitive membranes containing conjugates of prostaglandin E_2 (PGE_2) and the ionophore, dibenzo-18-crown-6, were used in a competitive, protein binding reaction. Ionophore-hapten (PGE_2) conjugates were synthesized and dissolved along with polyvinyl chloride in tetrahydrofuran. Plastic membranes were cast in air. Transmembrane potential was measured in potassium gradients at constant pH and ionic strength. The membranes were selective to monovalent cations. Transmembrane potential was affected in a concentration-dependent manner by adding anti-PGE_2, antisera to the external buffer solution. Non-specific sera had little or no effect on membrane potential. These data indicate that the membrane response to anti-PGE_2 antibodies was a specific interaction with the PGE_2 molecules fixed in the membrane. Electroimmunoassays were performed by establishing competition between "fixed" PGE_2 molecules in the membrane with "free" PGE_2 added to the antibody solution. Antisera and PGE_2 (0-860 nM) were added to a series of tubes. PGE_2 reduced the antibody response in a concentration dependent manner. The voltage response (V_o) vs. PGE_2 concentration was plotted to obtain standard curves. The specificity of the antibody-hapten interactions was tested by substituting PGD_2 or PGF_{2a} as the "free" prostaglandin. These structurally similar compounds had insignificant effects on the antibody response. Electroimmunoassay is potentially an important technique in the study of endogenous, biologically active substances and industrial monitoring if "on-line" measurements become feasible. (Supported by NIH grant AM 32176.)

W-AM-Pos17 THE DYNAMIC RESPONSE OF A HEAT FLOW DIFFERENTIAL SCANNING CALORIMETER, Donald B. Mountcastle, Departments of Physics and Biochemistry, Bennett Hall, University of Maine, Orono, Maine 04469.

The dynamic response of a differential scanning microcalorimeter of the heat conduction type has been analyzed, using both time response and frequency response techniques.[1] The parameters characterizing the instrument include a cell volume of 1 ml, a static calibration constant of 0.33 watt/C°, which with a Seebeck coefficient of 50 mv/C°, yields 6.5 watt/volt. By physically modeling the instrument geometry and thermal properties, at least two time responses are predicted, a first order response of ca. 25 seconds due to the cell and thermopile characteristics, and a second order response due to the sample itself (approximately 15 seconds if the sample is in liquid water). The dynamic response characteristics do show more than one response time. By measuring the response of the cell to an electrical input signal which is physically located first inside, and then outside the sample liquid, the response clearly shows the existence of thermal gradients occuring within the aqueous sample, an effect which is commonly ignored. The possible application of these techniques to measure the kinetics of thermal events in the sample are under current investigation.

This work is supported by NIH Grant # GM 28338.

1. S.L. Randzio and J. Suurkuusk, "Interpretation of Calorimetric Thermograms and their Dynamic Corrections", in Biological Microcalorimetry, A.E. Beezer, ed., Academic Press, 1980.

W-AM-Pos18 MICROCALORIMETERS FOR 2-100 MG SAMPLES OF CELLS AND TISSUE.
Rex Lovrien, Biochemistry Department, University of Minnesota, St. Paul, Minnesota 55108

Calorimeters for monitoring heat from cells and tissue are becoming easy to use. The heat of metabolism is much influenced by O_2, the carbon source, cofactors and regulating compounds. There is much advantage in use of small (2-100 mg) samples. Often the limitation is not supply of sample. Rather, the rate limit of indiffusion of metabolites, O_2, hormones, drugs, etc., and rates of outconduction of heat, set the overall time resolution. Reaction chambers not more than 7 mm thick, 2 to 4 ml volume are optimum. In this case, velocities of heat generation can be gotten without much deconvolution of the raw data. Sample responses of only a few seconds can be clearly seen. A number of such instruments were described recently [Biotech. Bioeng. 22, 1249 (1980) (purged batch); Analyt. Biochem. 100, 77 (1979) (liquid flow); J. Biochem. Biophys. Meth. 5, 307 (1981) (gas flow)]. If regulating compounds (hormones), O_2 and carbon source are adequate, the rate limitations tend to become dependent on how close the carbon source happens to fit the existing metabolic paths, and the intrinsic velocities of cell metabolism. Microcalorimeter initial response times are 2-4 seconds, full rise time 8-10 seconds, relaxation time 40-60 seconds. The entire course of combusting metabolites to completion can easily be followed if the sample is small enough so indiffusion isn't limiting, and if completion occurs in 50-300 seconds. The figure of merit (Seebeck coefficient) is 2 to 7 μWatt input/μVolt output. Amplifier instability and input noise values are less than 1 μVolt. Thus, if a signal of 10-200 μV is to be generated for 200 seconds, ca. 11-220 nanomoles hexose (aerobic metabolism) are required. Many tissue and cell systems use a few dozen nanomoles of carbon, in a few dozen seconds.

W-AM-Pos19 PULSED INERTIAL STOPPED OR QUENCHED FLOW APPARATUS WITH THERMAL DETECTION. R.L. Berger, Laboratory of Technical Development, NHLBI, Bethesda, C.A. Wanman, and G.H. Pekar, Commonwealth Technology, Incorporated, Alexandria, Virginia

A new syringe drive flow system has been built which utilizes a closely controlled variable-speed D.C. motor, a flywheel energy reservoir, and a spring-wrapped, solenoid-released half-revolution clutch driving a cam cut in the form of an Archimedes spiral. A unique syringe advance mechanism is incorporated which permits multiple shots before reloading. Depending on cam cut, the velocity profile may be tailored for virtually instant (2 ms) rise from zero to constant velocity with flow times to 50 ms, a constant acceleration followed by constant velocity, or any desired profile that is a continuous function. Various syringe sizes from 10 ml down can be accommodated. .10 ml from each syringe is used per shot. Larger amounts can be used up to the entire syringe. Up to 6 driving syringes with 5 succesive mixers can be used for quenched flow. The configuration to be described uses two 2.5 ml driving syringes and two 2.5 ml receiving syringes. This permits a zero pressure drop accross the mixer, or if desired, any static pressure up to several thousand pounds per sqin. Flow velocities in a 3 mm diameter observation tube using either water or 92% glycerol in the driving syringes of 5 m/s were achieved at two thirds operating speed of the flywheel. Less than 2 millidegrees heating occurred across the mixer. Total dead time is 2 milliseconds at present at this velocity. Velocities of 7.5,5, and 2.5 m/s, or anything in between, are quickly attainable. A pulsed flow mode with automatic timing is provided so that aging times from zero to 2000 milliseconds, or longer, can readily be achieved.

W-AM-Pos20 A BETTER UNDERSTANDING OF THE SUCROSE GAP TECHNIQUE AND AN IMPROVEMENT IN ITS PERFORMANCE. J. P. Pooler, Dept of Physiology, Emory University, Atlanta, GA 30322

In the original theory for the double sucrose gap technique the membrane under sucrose was considered to play no role because it was isolated by the high resistance sucrose solution. Subsequent work suggested that membrane under sucrose actually plays a significant role. Because the normal sucrose solution has a very low ionic strength it is hypothesized that a large negative surface potential on the membrane under sucrose shifts the K g-V curve in the hyperpolarizing direction and leads to a much lower membrane resistance than in the node. This hypothesis was tested on lobster axons by doping the sucrose with ions which should be effective in reducing the surface potential in the order Na<Ca<La. The concentrations were set to yield equivalent gap resistances. Measured leakage properties in voltage clamp were compared with theoretical predictions of the conventional sucrose gap theory and the leakage model of McGuigan and Tsien. Resting potential behavior was compared with conventional gap theory and a simplified cable model. The results confirm that membrane resistance under sucrose is low and that it is raised by doping the sucrose with multivalent cations. The behavior is not consistent with conventional sucrose gap theory but is accounted for by modeling the system as a high resistance node flanked by cables with low resistance membrane and an extracellular resistance determined by the sucrose resistance. Both the resting potential and leakage in voltage clamp are dominated by the membrane under sucrose rather than the node. With appropriate doping conditions the leakage is actually lower in doped sucrose than normal sucrose even though this partially shunts the gaps. A practical consequence of this work is a dramatic improvement in preparation stability and longevity by doping the sucrose with La.

W-AM-Pos21 METHODOLOGY FOR ANALYSIS AND QUANTITATION OF LOW MOLECULAR WT. PROTEINS OF MUSCLE USING ONE-DIMENSIONAL SILVER STAINED SLAB GELS. G. Giulian*, R. Moss* and M. Greaser+, Dept. of Physiology* and The Muscle Biology Lab.+, Univ. of Wis., Madison 53706 (Intr. by R. Haworth).

Quantitation of the relative amounts of the light chain subunits of myosin within segments of single muscle fibers (see, Moss, et al., JBC, 257:8588, 1982) and small samples of heart muscle required the development of procedures for processing and analyzing very small amounts (< 0.1 μg) of protein. The system that we have developed for these purposes has high sensitivity (down to 0.1 ng for some proteins) and general applicability to quantitation of small samples of protein. Vertical slab gels (0.75 mm thick) were cast using Thomas' (Tech. Prot. Enz. Biochem., B106:1, 1978) modification of the Laemmli system. The concentration of acrylamide was 9% in the stacking gel and 15% in the running gel, with acrylamide:bis ratios of 20:1 and 200:1, respectively. This procedure together with our methodology for sample preparation provided high resolution band patterns for the low molecular wt. (<60K daltons) subunits of the contractile and thin-filament linked regulatory proteins of heart muscle and fast- and slow-twitch skeletal muscles of the rabbit. We have modified the silver staining procedure of Oakley, et al. (Anal. Biochem. 105:361, 1980) for accurate quantitation of low molecular wt. proteins from short fiber segments (<1.5 cm long). The linearity of the stain response for the myosin light chains and Tn subunits was excellent for skeletal muscle fibers between about 1 and 5 mm in length and for LC_1, LC_2 and TnI extended to at least 10 mm. Linearity of stain response was observed for several non-muscle protein standards in the range between 2 and 70 ng/band. A dry-down procedure for subsequent scanning, photography and storing of the gels will be described. (Supported by grants from NIH, the MDA and the American Heart Assoc.).

W-AM-Pos22 SINGLE CARDIAC PURKINJE CELLS FOR INTERNAL PERFUSION AND VOLTAGE CLAMP J. C. Makielski, C. T. January, M.F. Sheets, and A.I. Undrovinas. (Introd. by E. Page) Dept. of Pharmacological and Physiological Sciences, The University of Chicago, Chicago, Il 60637.

Single canine cardiac Purkinje cells were isolated using collagenase by the method of Sheets et al (Circ.66:II-14,1982). The cells had resting potentials around -73 mV at room temperature, and stimulated action potentials showed upstroke and repolarization characteristics similar to intact cells at that temperature. We were able to obtain seals with the flow-through suction pipette (Kostyuk et al, Nature 257:691-693,1975) adequate for internal perfusion and voltage control. The external solution was HEPES-buffered Tyrodes solution with 150 mM Na^+ and 0.3 mM Ca^{2+}. The internal perfusate contained 1mM EGTA and Tris glutamate, with various amounts of Na glutamate at pH 7.3. The effectiveness of internal perfusion was shown by absence of outward currents and by the appropriate shift in E_{rev} for Na^+ current when the internal solution was changed from 10 mM Na_i to 100 mM Na_i, and the failure to obtain reversal when the internal perfusate Na^+ was zero. The decay of the capacity current could be fit with a single exponential, with time constants between 200 and 700 μsec. Threshold for Na^+ currents was near that found for action potentials in intact strands, so there was little shift in the voltage range of Na^+ current activation. The advantages of this method for the study of cardiac membrane currents is that the Purkinje cells have no T tubules, so accumulation or depletion should be minimized, and the flow-through perfusion pipette permits rapid change of the intracellular solution. (Dr. Undrovinas is from the All-Union Cardiology Research Center, Academy of Medical Sciences of the USSR, Moscow, 101 837, USSR).

W-AM-Pos23 TIME-RESOLVED EXAFS APPLICABLE TO PROTEIN DYNAMICS. H. W. Huang and W. H. Liu, Physics Dept., Rice University, Houston, TX 77251

We have developed a method of measuring time-resolved EXAFS with a time-resolution variable from nanoseconds to 1000 μs (H.W. Huang, W.H. Liu and J. A. Buchanan, NIM, Dec. 1982). With a synchrotron radiation beam of 10^{12} photon/s·ev, a realistic time resolution is 100 μs. An example of such applications is the structural study of the heme dynamics in myoglobin (Mb) and hemoglobin (Hb) at about 100°K, where e.g., the MbCO recombination time (after photodissociation) is about 1s. The samples need to be transparent to light for photoexcitation and thick for a sufficient x-ray absorption. We achieve that by making PVA film samples. As a result Fe atoms account for 2% of the total absorption at the Fe-edge. The Fe-EXAFS with S/N ∿5 can be measured in the transmission mode without repetition. However, this requires a high-speed, high-bit ADC which may become available soon. A similar precision can be achieved in the fluorescence mode by repeating 100 times per data point. Some data will be presented.

W-AM-Pos24 MEMBRANE SURFACES SEEN AFTER SCANNING ELECTRON MICROSCOPE AUTORADIOGRAPHY. Weiss, R. L., (Intr. by R. Sabbadini), Botany Department & Molecular Biology Institute, San Diego State University, San Diego, CA 92182.

A new technique, scanning electron microscope (SEM) autoradiography, has been successfully applied to visualize isotopes in SEM samples (Weiss, R.L., SEM/1980/IV:123). Several cell types have been examined: a single-cell alga, Chlamydomonas reinhardi, cultured chick embryo fibroblasts and an established rat hepatoma cell line. A general scheme on how to successfully apply this approach to membranes on particulate (single-cell or isolated membranes) or attached (cultured cells) samples is offered. This scheme includes quantitation of a new polylysine-detergent binding method used with particulate samples. Information on technical difficulties encountered and how to surmount these difficulties in particular applications is presented. The use of isotopes of various energy levels is also considered and evaluated for its application in SEM autoradiography. Supported by NIH R01 GM 25636-02.

W-AM-Pos25 SCANNING OPTICAL SPECTRAL MICROSCOPY WITH 500Å SPATIAL RESOLUTION. Aaron Lewis, Michael Isaacson, Andrew Muray and Alec Harootunian, School of Applied and Engineering Physics, Cornell U., Ithaca, NY 14853

Over the last two years we have been developing a scanning nanometer optical spectral microscope (SNOS) which obtains with visible 5000Å radiation a spatial resolution of 500Å. The system we have devised is composed of 6 elements. First, we have developed a method using a scanning transmission electron microscope to make apertures of $\leq$500Å in a regular array. Second, we have demonstrated that in a variety of materials light of 5000Å is readily transmitted through these apertures. Third, we have used the theoretical and experimental results of electrodynamics demonstrating that light in near field is directed rather than diffracted. Fourth, we have employed a technique of internal reflectance to limit the information in all three directions to ~500Å. Fifth, we have developed a scanning stage that can be translated in 100Å steps. Sixth, we use the developments of low light level multichannel detection laser spectroscopy. The integration of these components and concepts into a workable scanning nanometer optical spectral microscope will be discussed and resolution tests and detection limits for the instrument will be presented.
[This work has been supported by the U.S. Army and the National Science Foundation through the National Research and Resource Facility for Submicron Structures.]

W-AM-Pos26 REFRACTIVE INDEX PROFILE IN A GOLDFISH EYE LENS. Douglas Lerner and Daniel Axelrod, Biophysics Research Division and Dept. of Physics, Univ. of Michigan, Ann Arbor, MI 48109

Certain geometric optical properties of the spherical lens from a goldfish eye, such as the short focal length and the relatively low spherical aberration, have led to the conclusion that the lens' index of refraction decreases with radial distance from the center. We have employed a non-invasive method to determine the index of refraction profile. A thin laser beam is incident upon the lens in an equatorial plane at some distance y_1 from the center line. The position of the point y_2 at which the beam emerges from the lens is recorded photographically. The dependence of y_2 upon y_1 is then recorded onto a computer by digitizing the positions y_1 and y_2 with a bubble chamber photograph scanner. A numerical fit to the y_2 vs. y_1 data derived from a theoretical expression for the path of a ray through the lens allows determination of the actual index of refraction profile.

A computer graphical simulation, using a ray tracing method, shows the appearance of rays through a spherical lens of heterogeneous refractive index, and corresponds to photographs of laser rays actually traversing the lens as seen from the outside.

Supported by USPHS NS 14565.

W-AM-Pos27 CHARACTERIZATION OF NONMUSCLE CREATINE KINASE. S.J. Koons and R. Cooke, Department of Biochemistry/Biophysics and the CVRI, University of California, San Francisco, CA 94143.

We have developed an especially sensitive creatine kinase (CK) assay to measure CK activities in extracts from a variety of nonmuscle cells. Measurement of the rate of ATP production in the presence of ADP and phosphocreatine (PCr) constitutes an assay for CK. With a modified fluorimeter to measure ATP sensitive luciferin-luciferase luminescence, we can assay the CK activity of less than one pg of purified muscle CK. This method has been used to detect significant CK activities in extracts from Dictyostelium discoideum amoebae, PtK1 cultured cells and frog eggs (Xenopus). The high sensitivity of the assay allows us to characterize some of the CK kinetic parameters from cell extracts. Lysate from frog egg, an unusually rich source of CK, was diluted by a factor of 10^6 and assayed at different concentrations of ADP and PCr. Although other enzymes are present, substrates from the extract have been diluted far below their natural levels. Adenylate kinase activity was inhibited with diadenosine pentaphosphate. No increase in ATP level was observed in the absence of either PCr or ADP, confirming the lack of interfering enzyme activities. Apparent Michaelis constants (K_a, PCr; K_b, ADP) under the reaction conditions at pH 7.6 may be estimated from double reciprocal plots. The values for frog egg of K_a=3 mM, K_b=70 µM are not very different from those for rabbit muscle CK of K_a=5 mM, K_b=30 µM. Thus the frog egg CK is kinetically similar to muscle CK. Together with the relative abundance of CK in the extract (approx. 1% of soluble protein) and the previously demonstrated role of CK in energy supply for mitosis, these data suggest a role for CK in frog egg development possibly as significant as that in muscle contraction. Supported by USPHS grants HL16683 and HL07192.

W-AM-Pos28 EFFECT OF LIDOCAINE ON THE PHYSICO-CHEMICAL CHARACTERISTICS OF CYTOCHROME c. H. James Harmon, Departments of Zoology and Physics, Oklahoma State University, Stillwater, OK 74078.

Addition of lidocaine, a commonly used local anesthetic, causes a decrease in the midpotential of soluble cytochrome c from +275 mV to +248 mV. Lidocaine also causes an increase in the absorbance of the Soret band (407 nm) of ferricytochrome c. The g_z tensor of ferricytochrome c increases in value from g=3.06 to g=3.09 while g_y values decrease from g=2.24 to g=2.16 in the presence of lidocaine. Contact shifted NMR resonances of the heme in ferricytochrome c are altered by addition of 2 mM lidocaine but not procaine. Shifts in resonances at 6.9 ppm and 7.57 ppm due to the phe-36 and trp-57 residues are also observed. Phe-36 and trp-57 are located near the heme. This data suggests that the aromatic non-polar ring of lidocaine is capable of interacting with soluble cytochrome c in the hydrophobic heme pocket. Procaine interacts with (hydrophilic) surface-oriented portions of the protein. This may provide insight into a mechanism of interaction of anesthetics with proteins associated with ion movements.

This research was supported by a Grant-in-Aid from the American Heart Association with funds contributed in part by the Oklahoma Affiliate.

W-AM-Pos29 MULTIPLE ACID PHOSPHATASES IN AVIAN PECTORALIS MUSCLE, Jeffrey H. Baxter and Clarence H. Suelter (Intr. by David G. Mc Connell)

Phosphatases are involved in the regulation of many cellular processes, including activation and inactivation of enzyme activities, modulation of membrane fluidity and regulation of various transport systems. Acid phosphatases (APase), originally thought to be lysosomal in nature, have been demonstrated to have multiple locations in liver, kidney and histochemically in muscle, as well as in yeast. We report three forms of APase activity in avian pectoralis muscle. These enzymes differ in subcellular location, apparent molecular weight, isoelectric points, substrate specificity and sensitivity to a variety of known phosphatase inhibitors. The microsomal APase (apparent MW = 365,000, pI = 7.9 & 8.4) is inhibited by F^-, tartrate, Hg^{++}, $MoO_4^=$ and $HPO_4^=$. The lysosomal form (apparent MW = 198,000, pI = 8.1 & 8.4) shows similar inhibition whereas the cytosolic form (apparent MW = 68,000, pI = 6.5, 6.6 & 7.6) is only inhibited by Hg^{++}. Extracts from muscle, containing >98% of the total APase activity, have been used to quantitate the enzymes in muscle. In 15 day ex ovo birds, 47% of the total APase activity is microsomal, 13% is lysosomal and 40% is cytosolic. Quantitation of the enzymes from dystrophic muscle shows that the previously reported increase in APase activity results from increased levels of the microsomal form, (the other forms are not significantly different). The significance of these data in the eitiology of muscular dystrophy, and the physiological role of multiple acid phosphatases in muscle is not yet clear.
This work was supported by NIH grant GM20716.

W-AM-Pos30 INTERACTION OF MONOVALENT CATIONS WITH A PYRIDOXAL MODEL COMPOUND. K. Ismail and M. Ashraf El-Bayoumi. Department of Chemistry, Michigan State University, E. Lansing, MI and Chemistry Department, Alexandria University, Alexandria, Egypt.

Interaction of monovalent cations with a pyridoxal model compound, salicyaldehyde is studied in media that favor ion-pair formation. Interaction of monovalent cations with salicylaldehyde resulted in the formation of tight ion-pairs. In these ion-pairs salicylaldehyde is very likely to act as a bidentate anion through its phenolate and carbonyl oxygen atoms. Para-substituted phenols form less tight ion-pairs with monovalent cations. The resulting red-shifts in their electronic spectra increases with the ionic radius of the metal ion. Excited-state dissociation of the solvent-separated ion-pairs is reported. This study provides interesting results relevant for the study of the role of monovalent cations in the activation of several enzymes.

W-AM-Pos31 AN IRON PROTEIN IN CYTOPLASMIC OXYGEN TRANSPORT. J.B. Wittenberg and B.C. Antanaitis, Department of Physiology and Biophysics, Albert Einstein College of Medicine, Bronx, N.Y. 10461

We discern 5 independently evolved cytoplasmic oxygen supply systems, each consisting of a cytoplasmic hemoglobin (myoglobin or leghemoglobin) and an equimolar amount of an iron-bearing protein. These systems, which differ in the organelle targeted for oxygen transport, include: vertebrate red muscle, target organelle is mitochondria; molluscan and annelid muscle and nerve, target organelle unknown; Gastrophilus (an insect) tracheal organ, target organelle unknown; nitrogen-fixing legume root nodules, target organelle Rhizobium bacteroids; modified gills of certain clams (living in hydrogen sulfide-rich environments), target organelle is sulfide-oxidizing symbiotic bacteria (C. Cavanaugh, private communication).

We report the isolation from pigeon breast muscle of an iron protein, present in equimolar concentration with myoglobin. Isolation was achieved solely by exclusion chromatography and electrophoresis in dextran media. Iron recoveries were approximately 90% at each chromatographic step, strong evidence that the product isolated corresponds to that equimolar with myoglobin in the tissue extract. Although the protein presumably bears 1 iron atom per molecule, it is colorless. As isolated the protein (0.3 mM in iron) exhibits no X-band EPR resonances between 10° and 77° K (other than a minor g' = 4.3 signal). Furthermore, no EPR signal attributable to the protein was detected at any stage of the purification, including intact tissue.

[Supported by NSF grant PCM 80-04472 (to JBW) and USPHS grant AM-15056 (to P. Aisen). JBW is a Career Awardee 5K06 HL00733 of the USPHS, NHLB Institute.]

W-AM-Pos32 CHARGE CHARACTERISTICS OF TYPE II COLLAGEN CYANOGEN BROMIDE PEPTIDES. Jess C. Rajan and LeRoy Klein, Department of Orthopaedics, Case Western Reserve University School of Medicine, Cleveland, Ohio 44106

The macromolecular organization of the type II collagen fibrils in cartilage is different from that of type I collagen in tendon, bone, or skin. Electrostatic forces due to polar amino acids have been suggested as dominant factors in controlling aggregation of collagen molecules into fibrils. These polar residues appear to occur in clusters along the peptide chains and are capable of binding metal salts, and interaction with other macromolecules such as glycoproteins and proteoglycans.

We investigated the charge and/or size characteristics of CNBr-derived peptides of types I and II collagens from 18-day-old chicks by electrophoresis on polyacrylamide gels. Homologous peptides α1(I)-CB3 and α1(II)-CB8 (M_r=13,000) were found to be acidic. However, the major acidic peptide unique to type II collagen was α1(II)-CB10 (M_r=30,000). This peptide which is relatively rich in the acidic amino acids, aspartic and glutamic acids may contain sequences that are functionally significant for cartilage structure. (Supported in part by National Institutes of Health Grants AG 00361 and AG 00258).

W-AM-Pos33 PHOTOAFFINITY LABELLING OF THE PROGESTERONE BINDING SITE IN HUMAN OROSOMUCOID. J. A. Wallace and H. B. Halsall. Intro. by E. D. Sprague. Department of Chemistry, University of Cincinnati, Cincinnati, OH 45221.

Serum orosomucoid contains a single binding site for progesterone with an association constant of ~10^6 M^{-1}. Current evidence suggests that parts of the progesterone binding domain are shared with that of basic drugs, a group of ligands also sequestered by orosomucoid. A simplified two-step procedure was used to prepare diazoacetate analogues of progesterone. Photoactivation was followed by CNBr and chymotryptic digestion. Separation of peptides by HPLC, amino acid analysis and sequencing permitted the identification of modified amino acids by comparison with the published sequence. Residues lys 162 and glu (136, 140, or 143) were modified. An additional lys was found at position 163, previously unreported, which is also found in the largely homologous rat orosomucoid. Insertion of lys at 163 increases the rat-human homology at the carboxy terminal. The existence of cys-cys at 72-165 and modification of lys 162 are in concordance with the extreme sensitivity of progesterone binding to disulphide bridge perturbants. Comparison of the competitive binding efficiency of a variety of diazoacetate progesterone analogs suggests that the modified residues lie at the periphery of a binding domain whose central region is hydrophobic.

Supported by NIH grant HD 13207.

W-AM-Pos34 ISOLATION AND CHARACTERIZATION OF MONOCLONAL ANTIBODIES TO NA^+,K^+-ATPase. William J. Ball, Jr. Department of Pharmacology and Cell Biophysics, University of Cincinnati, College of Medicine, Cincinnati, Ohio 45267.

Several hybridoma cell lines secreting antibodies specific to the membrane Na^+,K^+-dependent ATPase (NKA) from lamb kidney medulla have been isolated. These antibodies are IgG_1 immunoglobulins directed against the catalytic subunit of NKA. They show no reactivity against the glycoprotein subunit of the lamb enzyme nor any cross-reactivity with the NKA from rat kidney. Cotitration and competition binding studies have shown three of these cell lines produce antibodies directed against distinctly different sites of the catalytic subunit. One of these epitopes is a functionally important site. Antibody M7-PB-E9 acts as a competitive inhibitor with respect to the ATP dependence of the ATPase reaction. In contrast, this antibody acts as an uncompetitive or mixed inhibitor relative to the Na^+ and K^+ dependence of the ATPase activity and does not alter the cooperativity of the Na^+ and K^+ binding sites. This antibody has also been found to stimulate ouabain binding in the presence of Mg^{2+}. It does not inhibit the K^+-dependent dephosphorylation step of the catalysis reaction, nor does it effect the K^+-dependent p-nitrophenyl phosphatase activity. These studies may demonstrate the existance of antigenically distinct portions of the catalytic site, and they illustrate the specific nature of the effects that this monoclonal antibody has on NKA function (Supported by NIH grants HL24941 and HL22619 and an American Heart Association grant-in-aid).

W-AM-Pos36 SEPARATION OF PHENOXYBENZAMINE MODIFIED CALMODULINS BY HIGH PERFORMANCE LIQUID CHROMATOGRAPHY T. J. Lukas and D. M. Watterson, Howard Hughes Medical Institute and Department of Pharmacology, Vanderbilt University, Nashville, Tennessee 37232

Calmodulin, a relatively ubiquitous calcium modulated protein, has been shown to bind to phenothiazine drugs in calcium dependent manner. These drugs, the α-adrenergic inhibitor, phenoxybenzamine, and the beta antagonist, propanolol, also inhibit the calmodulin activation of phosphodiesterase in a dose dependent fashion (Watterson, et. al., Adv. Cyclic. Nucl. Res., in press). Since phenoxybenzamine is capable of covalent modification through its nitrogen mustard functionality, we decided to label calmodulin with tritiated drug and isolate the products. An HPLC method was developed to separate the labeled proteins and follow the reaction kinetics. Native and three drug-modified calmodulins were readily separated on a reversed phase column using a phosphate buffer-acetonitrile mobile phase. Two of the initially formed products had one equivalent of bound drug, while a later product had 2 equivalents of bound drug. Thus, individual adducts were isolated and tested for phosphodiesterase activation. Previous studies of chemically modified calmodulin rarely addressed the number of adducts present or their difference in activity. Preincubation of calmodulin with chlorpromazine or W7 (N-(6-aminohexyl)-5-chloro-1-napthalene sulfonamide) blocked the reaction with phenoxybenzamine in a concentration dependent manner. This indicated an overlap of binding regions and provides a comparison of the relative affinities of various drugs for the protein. Experiments testing the ability of phenoxybenzamine-modified calmodulin to activate phosphodiesterase are in progress. Preliminary results indicate that one of the adducts retained full activity. (Supported by NIH grant GM 30953)

W-AM-Pos37 EFFECT OF FATTY ACIDS UPON THE CLEAVAGE OF SYNTHETIC TETRADECAPEPTIDE RENIN SUBSTRATE BY MOUSE SUBMAXILLARY GLAND RENIN. Martin Poe, Department of Biophysics, Merck Institute for Therapeutic Research, Merck Sharp & Dohme Research Laboratories, P.O. Box 2000, Rahway, New Jersey 07065

When 0.32 μg of pure renin A from the submaxillary gland of male mice was incubated for 0.5 hr at 37°C in 1 ml buffer (50 mM sodium acetate, pH 5.38) with 5.7 nmoles synthetic tetradecapeptide renin substrate (STRS), it had an activity of 4.4 μMoles STRS cleaved/hr/mg renin. Inclusion of palmitic acid in the buffer led to a dose-dependent, saturable increase in the activity to 33 μMoles/hr/mg at extrapolated infinite palmitic acid concentration with half-maximal stimulation at 14 μM palmitic acid. Stearic and myristic acidsalso increased the activity in a dose-dependent, saturable manner, with half-maximal stimulation at 22 μM and 46 μM, respectively, and with extrapolated maximal rates of 39 and 37 μMoles STRS cleaved/hr/mg renin. Linoleic acid was much less potent at increasing the rate of STRS cleavage by mouse renin, with half-maximal stimulation at 270 μM for an extrapolated maximal rate of 33 μMoles/hr/mg. The dose-dependent, saturable increase in mouse submaxillary renin activity due to the fatty acids was not seen when incubations were carried out near pH 7. The above data provide a direct mechanism whereby the mouse could protect itself against the high renin activity in its saliva; the salivary gland renin if swallowed would be inactivated by the acid pH of the stomach through loss of its constituent fatty acids.

W-AM-Pos38 DEPHOSPHORYLATION OF cAMP-DEPENDENT PROTEIN KINASE REGULATORY SUBUNIT (TYPE II) BY CALCINEURIN (PROTEIN PHOSPHATASE 2B). D.K. Blumenthal and E.G. Krebs, Howard Hughes Medical Institute, SJ-30, University of Washington, Seattle, WA 98195.

It has recently been shown that calcineurin ($CaM\text{-}BP_{80}$) is identical to the highly specific, calmodulin-dependent protein phosphatase termed protein phosphatase 2B (Stewart et al., FEBS Letters, 137, 80). We report here that the autophosphorylation site on the regulatory subunit (R_{II}) of the type II cAMP-dependent protein kinase (cAK) is readily dephosphorylated by protein phosphatase 2B. In the presence of 2mM $MnCl_2$, 1μM calmodulin, pH 7.0 at 30°, the Km and Vmax were 5μM and 1μmol/min/mg, respectively, with R_{II} and protein phosphatase 2B from bovine heart. The reaction was inhibited more than 90% by 150μM trifluoperazine, 50mM phosphate, or cAK catalytic subunit at a concentration equal to that of R_{II}. Half-maximal activation was observed at 3nM calmodulin. A synthetic heptapeptide corresponding to the sequence (residues 91-97) around the autophosphorylation site (Ser 95) was not readily dephosphorylated, nor was the major tryptic fragment (residues 93-400) of R_{II}. A chymotryptic fragment (residues 91-400) was dephosphorylated at 8% the rate of native R_{II}, whereas Staph. protease generated a fragment (residues 1-100) which was dephosphorylated as rapidly as native R_{II}, thus indicating the relative importance of the N-terminus of R_{II} for recognition by protein phosphatase 2B. We are currently attempting to determine more precisely which elements of structure in the N-terminus of R_{II} are recognized by protein phosphatase 2B in order to better understand the properties and function of this enzyme.

W-AM-Pos39 DIFFERENCES IN STRUCTURE AND REACTIVITY OF DIFFERENT CYTOCHROME OXIDASE PREPARATIONS. Kumar, C., Naqui, A., Chance, B., Johnson Res. Fdn., Univ. of Penna., Phila., PA, Ching, Y., Powers, L., Bell Labs., Murray Hill, NJ and Hartzell, C.R., A.I. DuPont Inst., Wilmington, DE

The differences in peroxide binding capacity of different cytochrome oxidase preparations reported by Bickar et al [1] and the differences in F^-+NO reactivities reported by Brudvig et al [2] are extended and traced to the presence of different proportions of a "pulsed like" conformation in the resting cytochrome oxidase prepared by different methods.

Cytochrome oxidase prepared according to the Yonetani method shows low reactivity towards both cyanide and peroxide in the resting state. On reduction and reoxidation, the cyanide and peroxide binding as well as the catalatic activity of the cytochrome oxidase preparations increases many fold. This enhanced reactivity persists for many hours, long after the spectral changes identified with the presence of "oxygenated" enzyme have decayed [3].

Cytochrome oxidase prepared according to the Hartzell-Beinert or Caughey methods, however, show significantly higher reactivity towards peroxide and cyanide in the resting state. A structural basis for these differences are presented by L. Powers, et al (this volume).

Preliminary results from experiments directed towards identifying the dominant conformation of cytochrome oxidase in intact mitochondrial membranes will also be presented. Supported by NIH GM 28308 & SSRL Project 623B(DOE,BES,NSF,DMR & NIH,BRP,DDR).

[1] Bickar, D., Bonaventura, J. & Bonaventura, C. (1982) Biochem. 21:2661-2666.
[2] Brudvig,G.W., et al. (1981) Biochem. 20:3912-3921.
[3] Orii, Y. & King, T.E. (1976) J. Biol. Chem. 251:7487-7493.

W-AM-Pos40 NON-ENZYMIC ACETYLATION OF PROTEINS BY ASPIRIN.
Cyra Hun-Opfer and Julio F. Mata-Segreda. Department of Biochemistry and School of Chemistry, University of Costa Rica. San José 2060, COSTA RICA.

The acetylation of proteins by aspirin is a well-documented process:

$$\text{Protein-NH}_3^+ + \text{Aspirin} = \text{Protein-NH-Ac} + \text{Salicylate}$$

The secondary complications of diabetes (retinopathy, microangiopathy) are mainly generated by a slow glucosilating reaction on the terminal amino groups and lysine residues which leads to an irreversible biochemical lesion of the proteins.

Since the acetylation of such groups has been considered as a possible competitive reversible process, which could be useful to slow the advance of the secondary problems of diabetes, we have determined the kinetics of the above process at pH = 7,2 and 37°C.

The results are:

$$d(\text{Salicylate})/dt = k\ (\text{Protein})\ (\text{Aspirin})$$

where k is $0{,}117 \pm 0{,}004\ s^{-1}\ M^{-1}$ for seroalbumin and $0{,}040 \pm 0{,}001\ s^{-1}\ M^{-1}$ for ovoalbumin.

The results to be presented also include data on the kinetics of hydrolysis of model R-NH-Ac's and the pharmacological considerations derived from this study.

W-AM-Pos41 EFFECT OF HYDROGEN PEROXIDE ON SULFHYDRYL OXIDATION OF BRAIN ATPase. L. L. Morriss, C. A. Colton, and J. S. Colton. Univ. of Nevada, Sch. of Med., Reno, NV 89557.

The sodium-potassium activated ATPase (Na-K ATPase) has been shown to contain 34 sulfhydryl groups on the 98,000 dalton catalytic subunit (Schoot, et al., 1978, 1980) which are susceptible to thiol oxidation or alkylation. Such treatment results in a decrease in enzyme activity. As part of our investigations on oxygen-induced seizures it became of interest to observe the effects of H_2O_2 on sulfhydryl oxidation of the Na-K ATPase. Xanthine 1×10^{-4} M/Xanthine oxidase (1 unit) was used to generate H_2O_2. Incubation for 15 min produced a 26% decrease in activity. When the enzyme was exposed to 6×10^{-6} M H_2O_2 only, a 72% decrease in activity was observed. H_2O_2-pretreated enzyme washed with the thiol-reducing agent dithiothreitol (DTT) at 1×10^{-2} M restored activity to 53% of control. When the enzyme was preincubated with 6×10^{-6} M H_2O_2 in Mg^{++}-K^+ free or 12 mM Mg^{++}-24 mM K^+ containing media (which causes a conformational change from the E_1 to the E_2 configuration of the enzyme), it was found that activity in the Mg^{++}-K^+ free media was 34% higher compared to the ion containing media. These observations suggest that H_2O_2 is an inhibitor of Na-K ATPase through thiol oxidation. The effects of H_2O_2 can be partially reversed by thiol reduction with DTT or protected against by changing enzyme conformation which presumably shields SH containing active sites. An additional decrease in enzyme activity through lipid peroxidation is also possible.

W-AM-Pos43 RESONANCE RAMAN SPECTRA OF THE HEME IN LEGHEMOGLOBIN: EVIDENCE FOR THE ABSENCE OF RUFFLING AND THE INFLUENCE OF THE VINYL GROUPS. M. R. Ondrias, Department of Chemistry, The University of New Mexico, Albuquerque, NM 87131; D. L. Rousseau, Bell Labs, Murray Hill, NJ 07974; G. N. LaMar, S. B. Kong and K. M. Smith, Department of Chemistry, University of California, Davis, CA 95616.

Resonance Raman spectra of deoxy and carbonmonoxy leghemoblogin (Lb) are compared to the corresponding forms of human adult hemoglobin (HbA). It is found that the heme "core size" indicator line has nearly the same frequency for the two deoxyhemoglobins and the π-electron density sensitive line also falls at the same frequency. However, several other modes occur at very different frequencies in the spectra of the two proteins. From an examination of the spectrum of an HbA derivative in which the β-carbon atoms of the heme vinyl groups were deuterated, it appears that the major differences between deoxy HbA and Lb may result from conformational changes in the vinyl groups. No evidence for ruffling in deoxy Lb was found. The spectra of carbonmonoxy Lb and HbA were also found to be very different. As in the deoxy case some of these frequency differences could be attributed to vinyl group conformational differences. However, from the large difference in the π-electron density sensitive line, it appears that the vinyl π-conjugation into the porphyrin in Lb(CO) may be different than it is in HbA(CO). The vinyl conformational differences may be a consequence of the looser heme pocket in Lb than in HbA. The difference in π-conjugation could make a significant contribution to the difference in ligand binding affinity for these two globins. (Portion of work done at U. of Calif. under NIH Grants HL-16087-HL-22252.)

W-AM-Pos44 SOLVENT EFFECTS ON PICOSECOND RELAXATION OF Cu(II) PROTOPORPHYRIN K.D. Straub and P.M. Rentzepis, VA Med. Ctr., Little Rock, AR and Bell Laboratories, Murray Hill,NJ

Cu(II) Protoporphyrin IX and its dimethyl ester have been studied by picosecond relaxation of the excited electronic states in solvents with varying polarity and ligand ability. The absorption spectrum of Cu(II) Protoporphyrin IX dimethyl ester in benzene is indicative of a square planar configuration of the central metal atom. The picosecond relaxation exhibits two decay times (400 psec and >1 nsec). In pyridine Cu(II) Protoporphyrin IX dimethyl ester and Cu(II) Protoporphyrin IX (free carboxy) exhibit an absorption spectrum of an octahedral complex of Cu(II) with a dramatically reduced excited state lifetime of approximately 45 psec. With water as solvent, the very fast relaxation is also observed while in acetic acid, the slow relaxation is seen. Thus, it appears that the more polar solvents give rise to a 6 ligand Cu(II) Protoporphyrin IX which allows a much faster relaxation than the 4 ligand complex in low polarity solvents. Since the 5 ligand Cu(II) Cytochrome c also has a slow relaxation, we conclude that only the octahedral Cu(II) complex demonstrates this rapid decay of the excited state.

W-AM-Pos45 SYSTEMATIC ELECTROSTATIC MODIFICATION OF AMINO GROUPS FOR THE STUDY OF HEMOGLOBIN SOLUTION PROPERTIES Scott Saunders and Bo Hedlund, Univ. of Minnesota, Minneapolis, MN 55455

Reductive carboxylation of proteins with glyoxalic acid has been employed for alteration of charge distribution of hemoglobin. At low levels of modifier, the four α-amino groups are the primary sites of modification (Acharya et al., Fed. Proc. 41, 1174 (1982)). Studies of labeling patterns by isoelectric focusing indicate differential labeling of oxy- and deoxyhemoglobin, suggesting different accessibility of the four α-amino groups in the two forms. Oxygen binding studies of hemoglobin labeled in the liganded form indicate substantial right shift of the oxygen binding curve. At higher degrees of labeling, by which up to 90% of lysine ε-amino groups can be converted to zwitterionic sidechains, hemoglobin oxygen binding curves become left shifted and cooperativity decreased. Under these conditions, the isoelectric point of hemoglobin is near pH 4.0 and each dimer carries up to twenty additional negative charges at neutral pH which leads to considerable electrostatic repulsion between dimers (Flanagan et al., Biochemistry 20, 7439 (1981)). This type of modification, by which any intermediate degree of lysine modification can be obtained, represents a powerful tool for the study of electrostatic forces in hemoglobin chemistry and any system where protein charge is an experimental variable. It also allows for experimental testing of theoretical calculations which have been used to estimate the role of such forces in stabilizing the hemoglobin tetramer. We have also utilized modified hemoglobin in studying hemoglobin solubility, both as a function of degree of modification and the effect of addition of small quantities of highly modified hemoglobin to solutions of unmodified hemoglobin. (Supported by NIH grant AM 28124).

W-AM-Pos46 **FLUORESCENT HEINZ BODIES AND CYTOPLASM OF ERYTHROCYTES CONTAINING HEMOGLOBIN KÖLN**

J. Eisinger, J. Flores, *Bell Laboratories, Murray Hill, NJ 07974, and* S. B. Shohet, *University of Cal. Med. Center, San Francisco, CA 94143*

Erythrocytes from two splenectomized patients with hemoglobin Köln disease (β98 Val→Met) were examined by fluorescence microscopy. When excited by 320-380 nm light, the cells were found to emit a strong green fluorescence, which bleached only minimally under epi-illumination. Most red cells contained a single prominent Heinz body, which fluoresced with twice the intensity as that of the cytoplasm. Front face fluorometry of Köln hemolysates and of Köln membranes mixed with hemolysate from normal cells showed that 80-90 percent of the total fluorescence yield of Köln cells originate in the cytoplasm with the remainder coming from the Heinz bodies in the membrane fraction. The same yellow pigment (YP) appears to be responsible for the fluorescence observed in both fractions. YP absorbs maximally at 409 nm and in the presence of LDAO, a non-ionic detergent, its emission spectrum has a maximum at 515 nm when excited at 450 nm. Under similar conditions bilirubin, in contrast, emits at 545 nm. The YP fluorescence yield is 10 times greater than that of bilirubin samples with the same absorbance at the excitation wavelength.

A fluorophore with an emission spectrum similar to that of the YP is also produced in normal erythrocytes following treatment with acetyl phenylhydrazine.

Hb Köln and similar hemoglobin variants in erythrocytes are considered to be oxidized to (non-fluorescent) hemichromes which precipitate as Heinz bodies. The spectral and other characteristics of the YP suggest that it is a dipyrrole, but chromatographic identification of the YP has not been achieved yet. The YP may be the product of a previously unknown heme breakdown mechanism which is operative in erythrocytes containing unstable hemoglobin.

W-AM-Pos47 SMALLANGLE NEUTRON SCATTERING STUDY OF MOLECULAR SUBUNIT STRUCTURE OF EARTHWORM HEMOGLOBIN: EFFECTS OF ALKALINE pH AND HEATING.

P. Martel and B.M. Powell, Atomic Energy of Canada Limited, Chalk River, Ontario, KOJ 1JO, Canada and O.H. Kapp and S.N. Vinogradov, Department of Biochemistry, Wayne State University School of Medicine, Detroit, Michigan 48201, U.S.A.

A small angle neutron scattering study of Lumbricus terrestris hemoglobin in solution at neutral pH was carried out. The results were interpreted in terms of several models for the subunit structure. The best fit is consistent with a hexagonal bilayer model made up of twelve spherical subunits, ≈ 48 Å in radius, each represented by an aggregate of nineteen small spheres ≈ 16.7 Å in radius. The scattering of hemoglobin subjected to a brief exposure to alkaline pH or to heating was also measured in order to determine whether any alterations in dimensions accompanied a decrease in the cooperativity of oxygen binding. It was found that an exposure of 20 minutes to 0.1 M sodium borate buffer, pH 9, resulted in no change in the elution volume in Sepharose Cℓ-6B gel filtration, and only minor changes in the observed neutron scattering at high angles; however, the exposure led to an irreversible decrease in the Hill constant from about 3.5 to 2.2. Heating produced irreversible and marked alteration in both the scattering from the hemoglobin and in its oxygen binding. The heat-induced changes in the scattering were interpreted in terms of partial aggregation and denaturation.

W-AM-Pos48 A PROTON NUCLEAR MAGNETIC RESONANCE INVESTIGATION OF HUMAN HEMOGLOBIN A_2: IMPLICATIONS ON THE STRUCTURAL BASIS OF THE ANTISICKLING EFFECT. Irina M. Russu, Allison K.-L. C. Lin, Susan Ferro-Dosch, and Chien Ho. Department of Biological Sciences, Carnegie-Mellon University, Pittsburgh, PA 15213.

Hemoglobin A_2 ($\alpha_2\delta_2$), a minor component of human erythrocytes, has been shown to have a marked inhibitory effect on the polymerization of sickle hemoglobin (Hb S) [Nagel et al., PNAS 76, 670 (1979)]. We have used proton nuclear magnetic resonance (NMR) spectroscopy at 300 and 600 MHz to investigate the conformation of the Hb A_2 molecule in solution. We find that (i) the replacement of the β chains by the δ chains in Hb A_2 conserves the $\alpha_1\delta_2$ interface but perturbs the $\alpha_1\delta_1$ interface of the molecule, and (ii) at least one surface histidyl residue in the deoxy form and one in the ligated form of Hb A_2 have pK values which are different from the corresponding ones of Hb A. A comparison between the present ^{1}H NMR data on Hb A_2 and those previously obtained in our laboratory on Hb S indicates that the amino terminal region of the δ chains in Hb A_2 has a conformation similar to that of the β chains in Hb S. Thus, our results suggest that the antisickling property of Hb A_2 does not originate from the alteration of the intermolecular contact site at the β6 position, but involves additional amino acid residues which are different in β and δ chains. We find that the substitution of the β116 and β117 histidyl residues in the δ chains does not play a significant role in the antisickling effect of Hb A_2 and thus, these amino acid residues do not participate in the intermolecular interactions responsible for the polymerization of Hb S. The implications of our ^{1}H NMR results to the molecular basis for the inhibitory effect of Hb A_2 on the polymerization of Hb S will be discussed. (Supported by a research grant from the National Institutes of Health).

W-AM-Pos49 NUCLEAR MAGNETIC RESONANCE INVESTIGATION OF THE INTERACTION BETWEEN NORMAL HUMAN ADULT HEMOGLOBIN AND ORGANIC PHOSPHATES. Keith A. Bupp, Irina M. Russu, and Chien Ho, Department of Biological Sciences, Carnegie-Mellon University, Pittsburgh, PA 15213.

The interaction between 2,3-diphosphoglycerate (2,3-DPG) and the normal human adult hemoglobin (Hb A) molecule has been investigated by high-resolution proton nuclear magnetic resonance (NMR) spectroscopy at 300 MHz. The chemical shifts and the longitudinal relaxation rates (T_1^{-1}) of twenty-two surface histidyl residues of Hb A have been measured as a function of pH and of 2,3-DPG concentration, at 27°C, in both deoxy and ligated forms. The results indicate that, in the presence of 2,3-DPG, the local conformations and/or the electrostatic environments of at least six histidyl residues of deoxy Hb A and three histidyl residues of ligated Hb A are altered. For example, the pK values of the β2 histidyl residues are found to be raised by ∿0.5 pH unit in the deoxy form and by ∿0.25 pH unit in the ligated form, in the presence of a 1:1 molar ratio of 2,3-DPG:Hb A. Under the same experimental conditions, the pK value of the β146 histidyl residues of deoxy Hb A is raised by ∿0.2 pH unit. We have also found that, in the ligated form, 2,3-DPG greatly affects the conformation of the heme pockets and its pH dependence. The implications of these results for the allosteric effect of 2,3-DPG on Hb A and for the molecular mechanism of the Bohr effect will be discussed. (Supported by a research grant from the National Institutes of Health).

W-AM-Pos50 FORMAL CHARGE OF THE IRON IN OXYHEMOGLOBIN. Alain Michalowicz, Serge Pin and Bernard Alpert (Intr. by E. Gratton), Lure, Universite Paris Sud, CNRS Bat. 209, 91405 Orsay, France.

Quantitative analysis of the formal charge of iron in hemoglobin and its isolated subunits was explored by X-ray Absorption Near Edge Structures (XANES) spectroscopy in the neighborhood of the K_α absorption edge of iron.

The X-ray absorption measurements were performed with the storage ring of L.U.R.E. in Orsay (France). No radiation damage of the irradiated sample was detected by visible absorption measurements made before and after X-ray exposition. Iron fluorescence was collected by an hyperpure germanium Ortex detector placed at 90° to the incident beam. Shift energy of the K-absorption edge was measured by the position of the peaks from the derivative of the fluorescence intensities versus the energies of the incident X-ray.

K-edge position of the iron in a fixed oxydation state with a change in the state of spin was examined. Reorganization of the electronic cloud that accompany a low-spin to high-spin transition displace the K-edge position of the iron never more than 0.5 eV. Unligated proteins (Fe^{2+}) and oxidized forms (Fe^{3+}) exhibit the expected ferrous to ferric energy K-edge shift of 5.5 eV. Comparative analysis of K-absorption edge positions for the oxidized and oxygenated hemoproteins show clearly that the iron in the $Fe\text{-}O_2$ complexe carries a formal charge of +3.

This fact poses serious questions about the model proposed by Perutz on a supposed low-spin to high-spin transition of a ferrous iron inducing the conformational change between HbO_2 and Hb. Therefore the K-edge X-ray experiments seem to be in qualitative good agreement with the previous theory of Weiss.

W-AM-Pos51 EQUILIBRIUM FOLDING-UNFOLDING PATHWAYS OF MODEL PROTEINS: EFFECTS OF MYOGLOBIN-HEME CONTACTS. S. Miyazawa and R. L. Jernigan (Intr. by M. Kanehisa) LTB, NCI, NIH, Bethesda, MD 20205

Protein folding-unfolding equilibrium has been investigated with a "Non-Interacting Globule-Coil Model"; each residue is assumed to take either the native or random coil state and no interresidue interactions are considered other than those within each native globule. A partition function is formulated to include all numbers, sizes and positions of native globules. Statistical weights of protein conformations are taken to consist of two parts: 1) intraresidue contributions evaluated from the empirical frequency in (ϕ,ψ) and 2) interresidue energies proportional to the numbers of contacts in the native globules. To describe relatively rare intermediates on folding pathways, the number of native residues is employed as a folding coordinate and the most probable conformations are calculated at each point along this coordinate. Then, equilibrium folding-unfolding pathways have been constructed by connecting most probable conformations by assuming simple growth. Previous applications to lysozyme, apomyoglobin, ribonuclease A and trypsin inhibitor indicated that 1) most probable conformations are insensitive to the values of the contact energy and the critical distance for contact residue pair definition, although the free energies depend strongly on them, and 2) pathways for trypsin inhibitor are similar to those obtained in a more detailed Monte Carlo simulation. However, even though native heme-protein contacts represent less than 6% of the total number of native contact residue pairs, their inclusion appears to change the folding pathway of apomyoglobin from growth and merging of two native domains to the growth of a single domain including the heme. This indicates that pathways derived with this method may be critically sensitive to the details of the contact map (inter-residue interactions) or physical constraints.

W-AM-Pos52 NEW STUDIES OF THE MAGNETISM OF OXY- AND CARBONMONOXY-HEMOGLOBIN. John S. Philo, U. Dreyer and T. M. Schuster, Biological Sciences Group, Biochemistry & Biophysics Section, The University of Connecticut, Storrs, CT 06268

We have measured the magnetic susceptibility of human HbO_2 and HbCO solutions at 20°C under various solvent conditions using a new superconducting susceptometer we have recently constructed. Measurements of apo-hemoglobin solutions have been used to establish a true diamagnetic reference state. We are unable to reproduce the data of Cerdonio et al.[1,2] who have reported paramagnetism of the heme in human HbO_2 and (at low ionic strength) also for HbCO. The precision of our data is at least an order of magnitude better than that of previous studies. Our data to date is not inconsistent with full diamagnetism for both HbO_2 and HbCO--the problem is to be certain that the samples are entirely free of methemoglobin. We are presently trying to establish firm upper limits for the paramagnetism (if any) of HbO_2 and HbCO.

[1] M. Cerdonio, A. Congiu-Castellano, L. Calabrese, S. Morante, B. Pispisa and S. Vitale, Proc. Natl. Acad. Sci. U.S.A. 75, 4916 (1978).
[2] M. Cerdonio, S. Morante, S. Vitale, G. Giacometti and M. Brunori in Interaction Between Iron and Proteins in Oxygen and Electron Transport, C. Ho, Ed. (Elsevier, New York, in press).

(Supported by NSF grants PCM 79-03964 and PCM 81-11320 and NIH grant HL-24644)

W-AM-Pos53 TEMPERATURE JUMP RELAXATION KINETICS OF DEOXY HB KEMPSEY +/- DPG. William T. Windsor, Biological Sciences Group, University of Connecticut, Storrs, Ct. 06268.

Experimental studies on mutant hemoglobins have been important in providing valuable information about the coopertivity of Hb A. Hb Kempsey, a high affinity mutant hemoglobin (β99 Asp→Asn), has been shown by various spectroscopic methods to have a number of interesting equilibrium properties. Its kinetic properties, however, are less well characterized. We have performed temperature jump relaxation measurements on deoxy Hb Kempsey. Preliminary experiments under conditions where deoxy Kempsey is partially dissociated (pH 7.0, 0.1M Hepes,0.1M NaCl, 1mM EDTA) show the presence of multiple phases which are not seen in deoxy Human Hb A. For deoxy Kempsey at least two phases are observed with relaxation times less than 150 μsec. A third but slower phase has a relaxation time of about 300 msec. In the absence of phosphates Kempsey is believed to be in the R quatenary state (1,2). The presence of DPG is known to shift the $R \rightleftharpoons T$ equilibrium toward the T state. When temperature jump experiments are performed with less than saturating amounts of DPG the amplitude and rates of the relaxation events are altered. The dependence of the relaxation phases on the concentration of protein and DPG will be presented.

1. M.F. Perutz, J.E. Ladner, S.R. Simon, C. Ho, (1974) Biochemistry 13 , 2163-2173.
2. K. Nagai, G.N. La Mar, T. Jue, H.F. Bunn, (1982) Biochemisty 21 , 842-847.

(Supported by NIH grant HL-24644)

W-AM-Pos54 PREFERENCIAL OF α and β OXYGENATION SUBUNITS OF HEMOGLOBIN: RESULTS OF MULTIDIMENSIONAL SPECTROSCOPIC OBSERVATION. A. Nasuda-Kouyama, H. Tachibana and A. Wada, Dept. of Physics, University of Tokyo, Tokyo 117, Japan (Intr. by D. Eden).

The preferencial oxygenation of the subunits of hemoglobin was studied spectrophtometically. The difficulty in discriminating the spectral changes upon oxygen binding to the α or β subunits can be surmounted by means of multidimensional spectroscopic observations and a correlation analysis of the data. As a control against normal hemoglobin, M-type abnormal hemoglobins are also used to know the oxygenation-sensitive bands of α and β subunits in the tetrameric state because one type of subunits can bind oxygen.

A multidimensional spectroscopic measuring system, which has been developed in our laboratory, makes it possible to carry out simultaneous and continuous acquisition of a set of spectroscopic data at several wavelengths on one sample solution during the course of increasing or decreasing partial pressure of oxygen. Data storage on floppy disc provides enough precision for a rigorous investigation of the correlation of oxygen equilibrium curves measured at several wavelengths. No chemical modification to enhance the spectral difference between subunits is necessary.

Detection of the difference of oxygen equilibrium curves between the oxygenation-sensitive bands of α and β subunits indicates that the β subunits have a higher affinity for oxygen than the α subunits. It's oxygen-binding equilibrium constant at T state is estimated to be about 5 times higher than that of α subunits from an analysis using the generalized concerted-transition model in which the effect of the quaternary-structure formation on the absorbance spectra is also taken into account.

W-AM-Pos55 PROBING THE PATHWAY OF REGULATORY ENERGY TRANSDUCTION IN HUMAN HEMOGLOBIN F. R. Smith and G. K. Ackers, Department of Biology, The Johns Hopkins University, Baltimore, MD 21218.

Identification of the sites and pathway of regulatory energy change within the hemoglobin tetramer is essential in understanding the cooperative mechanism of oxygen binding. For 22 mutant and chemically modified hemoglobins we have determined the total free energy used by the tetrameric molecule for alteration of oxygen affinity at the four binding steps [Pettigrew et al (1982) Proc. Natl. Acad. Sci. USA 79, 1849]. The results imply that the regulation of oxygen binding affinity is due to energy changes which are mostly localized at the $\alpha^1\beta^2$ interface (including the intersubunit contacts $\alpha^1\alpha^2$, $\alpha^1\beta^2$ and $\alpha^2\beta^1$). They also indicate that the structural perturbations at individual residue sites are energetically coupled. We are investigating the extent of this coupling at each of the three pairwise contacts, as a function of oxygenation state, by forming hybrids of these different hemoglobin molecules. Results are presented for the dissociation rate constants of several deoxy hybrid molecules involving $\alpha^1\beta^2$ and $\alpha^2\beta^1$ intersubunit contacts. For a mixture of two hemoglobins (e.g. HbA_o and Hb Kempsey) both parent and hybrid molecules coexist in equilibrium. We have been able to resolve and quantitatively analyze three separate kinetic phases corresponding to subunit dissociation of the parent and hybrid molecules. The observation of distinct kinetic phases is incompatible with 1) the existence of only two quaternary states for hemoglobin tetramers and 2) the hypothesis that mutant hemoglobins exist as an equilibrium population of these two states. These results argue strongly against simple two-state models as the mechanism of cooperative oxygen binding in human hemoglobin. Supported by grants from the NSF and NIH.

W-AM-Pos56 EFFECTS OF PROTONS ON THE OXYGENATION-LINKED SUBUNIT ASSEMBLY IN HUMAN HEMOGLOBIN. B. W. Turner, A. H. Chu, and G. K. Ackers, Biology Dept., The Johns Hopkins University, Baltimore MD 21218.

The linkage between oxygen binding and dimer-tetramer assembly in human hemoglobin has been studied over the range pH 7.4 - pH 9.5 at 21.5°C. At each pH, the oxygen binding isotherms were measured at a series of protein concentrations. The resulting data sets were analyzed simultaneously by least squares methods according to a model-independent thermodynamic treatment. Dimer-tetramer association constants for both unliganded and fully oxygenated species were incorporated in the analysis. From the pH dependencies of the derived oxygen binding constants for dimers and tetramers and of the subunit assembly constants, we have calculated the contributions of proton binding to these reactions. The principal results are as follows: (a) Release of Bohr protons by the tetramer is essentially complete after the first three oxygens are bound. 20% - 25% of these protons are released upon binding the first oxygen. (b) Detailed analysis of the composite data confirms the existence and magnitude of the dimer Bohr effect reported previously. The data are consistent with noncooperativity in oxygen binding by dimers at all pH's. (c) Oxygen binding affinities of triply-liganded tetramers are significantly higher at all pH's than the mean affinity per heme of the dimers. This effect--quaternary enhancement--which is now seen over a wide range of conditions, has significance for models of the cooperative mechanism in hemoglobin. (d) Oxygenation linked differences in the inter-subunit contact energies occur between at least four stages: unliganded, singly, triply, and fully oxygenated. (e) A correlation is found between proton release and enthalpic changes at the sequential oxygenation steps. Reactions linked to proton release are sufficient to account for all of the enthalpy of cooperativity in tetramer oxygen binding. Supported by grants from the NSF and NIH.

W-AM-Pos57 EXPONENTIAL PROGRESS CURVES IN THE GELATION OF DEOXYHEMOGLOBIN S. GW Christoph & RW Briehl, Albert Einstein College of Medicine, Bronx NY 10461

The basic model for the kinetics of hemoglobin S gelation (Hofrichter et al, PNAS 71:4864,1974), consisting of 3 stages (nucleation, fiber growth, and fiber alignment), predicts properties of the delay time but fails to predict the correct time dependence of growth progress. Employing cone-plate viscometry and light scattering (173° back scattering in a Chromatix KMX-6), we have observed growth progress curves (after the delay time) in 13.6mM(heme) deoxy HbS in 0.1M potassium phosphate, pH 7.0. Gelation was initiated by a temperature jump, usually to 20°. Excess viscosity ($\Delta\eta$) progressed with two exponential phases. The rate, $d(\ln\Delta\eta)/dt$, of the second, dominant, phase was $0.013sec^{-1}$ at a shear rate of $3.8sec^{-1}$, 0.13 at 38, and 0.27 at 192. At zero shear the estimated (extrapolated) rate was $0.01sec^{-1}$. In control light scattering experiments with high optical density solutions of deoxy HbA, scattering, I_s/I_o, was proportional, as predicted, to M_a/ε (M_a is apparent molecular weight; ε is extinction coefficient). M_a extrapolated to zero concentration was 63,000. Gelling preparations of deoxy HbS showed exponential growth in excess scattering (ΔI_s) with $d(\ln\Delta I_s)/dt=0.015sec^{-1}$ for the first 5% of the reaction, reproducible on cooling and rewarming. The rate remained the same up to about 40% fractional reaction.

Fieschko et al. (J Lab Clin Med 92:1019,1978) have observed exponential growth at low but non-uniform shear rates. Our present data extend this to uniform shear rates, and our light scattering results show that exponentiality exists even in the absence of the putative effects of shear in breaking fibers. This basic result, that polymer formation is proportional to the amount of polymer present, is consistent with a heterogeneous process on polymer surfaces, as proposed by Ferrone et al. (Biophys J 32:361,1980). Supported by NIH grants HL 07451 and HL 28203.

W-AM-Pos58 PHOTOLYSIS/RECOMBINATION OF CARBOXYMYOGLOBIN AT HELIUM TEMPERATURES: ANALYSIS OF THE EXAFS DATA. Chance, B., Johnson Res.Fdn.,Univ.of Penna., Phila., PA, Korszun, R., Inst. for Struc. & Func.Studies, 3401 Market St., Phila.,PA; Fischetti, R.,Univ. of Penna., Phila.,PA, and Powers,L. Bell Labs., Murray Hill, NJ

A structural "indicator signal" of X-ray absorption spectroscopy at 7173 eV indicates the formation of the geminate state (Mb*CO) in the low temperature photolysis and is correlated with changes of the EXAFS signals obtained in the reaction at 4°-10°K:

$$MbCO \leftrightarrow Mb^*CO \leftrightarrow Mb + CO$$

Three separate contributions to the first shell of each state are possible, heme nitrogen (Fe-Np), proximal nitrogen (Fe-N_ε) and Fe-CO, all of which may change under photolysis. These changes can only be interpreted by a small displacement of CO (<0.05 Å) coupled with a heme core expansion that is less than that of the chemical deoxy state. None of the changes is fitted by a summation of the data for Mb*CO and Mb. Core expansion (Fe-Np change) is supported by a shift of the absorption edge of 2 eV to lower energy on photolysis, similar to that observed in model compounds and other heme proteins. Changes in the Fe-CO geometry is supported by the disappearance of the Fe-CO absorption and the appearance of the Mb*CO 780 nm optical absorption band, differing from the Mb 760 nm band. Thus, Mb*CO formation involves a complex of structural changes, anyone of which may be rate limiting in the nuclear tunneling process involved in reformation of MbCO. Supported by NIH GM 27308, 37475, and 38385 and SSRL Project 623B(DOE,BES,NFS,DMR & NIH,BRP,DDR).

W-AM-Pos59 Hydrogen Exchange Studies by NMR As A Probe for the Dynamics of Hemoglobin

Kyou Hoon Han, Gerd N. La Mar, Thomas Jue and Yasuhiko Yamamoto
Chemistry Department, University of California, Davis

Changes in the ligation states and in the quarternary structures of HbA are well depicted in the exchange behavior of allosterically responsive hydrogens. Tritium labelling studies have provided substantial evidences in this regard where several sets of responsive hydrogens were found in regions other than the active sites of hemoglobin.

By using nuclear magnetic resonance spectroscopy (NMR), we were able to assign the $N_\delta H$ residues of the proximal histidines in both the α and β heme pockets and measure the exchange rates of these protons in D_2O.

The rate constant for oxy-Hb is almost 100 times greater than that of deoxy-Hb, showing that these protons are allosterically responsive. Also the α proton always exchanges faster than the β proton. However, the ratio of two rate constants critically depends on the pH. For deoxy-Hb, the half life is about 1.5 hours for the α and 36 hours for the β at pH 7.0.

Our results are consistent with the breathing hypothesis in which exchange rates are affected by transient local unfolding. However, our results show a set of allosterically sensitive protons in the heme cavities. Different exchange rates in the α and β cavities imply a non-uniform distribution of the allosteric effect, suggesting the limited applicability of some cooperativity models.

W-AM-Pos61 STUDIES ON A CHAIN MODEL OF POLYELECTROLYTE DNA MOLECULES IN IONIC SOLUTIONS

Yi-der Chen Laboratory of Molecular Biology, NIADDK, NIH, Bethesda, MD 20205

We propose a chain model for polyelectrolyte DNA molecules in solution based on Schellman's discrete version of a wormlike model[1] by including the electrostatic interaction in the formulation. That is, a DNA molecule is modeled as a string of rigid segments each having a fixed length ℓ and a finite number of negative charges. The value of ℓ is much less than the persistance length of the molecule. The average cosine of the complimentary bond angle, $<\cos\theta>$, is determined by both electrostatic and nonelectrostatic energy factors. As a preliminary study, only nearest and next-nearest neighbor interactions are considered. Both the radius of gyration and the persistence length of the polymer can be calculated easily. By adjusting the values of ℓ and the nonelectrolectrostatic persistence length, we are able to reproduce the radii of gyration of Col E_1 DNA at various Na^+ concentrations as obtained recently by Borochov *et al*[2].

1. J.A. Schellman, Biopolymers *13*, 231, (1974)
2. N. Borochov, H. Eisenberg, Z. Kam, Biopolymers *20*, 231 (1981).

W-AM-Pos62 APPLICATION OF THE POISSON-BOLTZMANN EQUATION TO DNA-DIVALENT METAL ION INTERACTIONS; EFFECTS OF FINITE IONIC SIZE. Joseph Granot, Physics Department, Purdue University School of Science at Indianapolis, IUPUI, Indianapolis, Indiana 46223.

The interactions between DNA and metal ions, which play a major role in conformational and dynamic properties of DNA, are dominated by the polyelectrolyte character of the highly charged DNA molecule. The Poisson-Boltzmann equation has been applied to DNA-ion interactions in many studies, usually with the DNA being modelled as a uniformly charged cylindrical rod, and the ions taken as point-charges. In the present study the finite size of the ions is introduced via distances of closest approach, and a general solution of the nonlinearized PB equation is derived for a system that contains a rod-like polyelectrolyte and mixed-valence counterions with different sizes. The choice of the distances of closest approach between the ions and the polyelectrolyte is based on the physico-chemical properties of the polyelectrolyte and ions in solution. The effects of the finite ionic size on the local ion concentration and the integrated charge fraction of counterions in the vicinity of the polyelectrolyte are discussed. The theoretical predictions regarding the overall extent of binding and the extent of inner-sphere binding of divalent counterions to rod-like polyions are compared with the results of NMR studies of the binding of divalent metal ions to DNA.

W-AM-Pos63 THE POISSON-BOLTZMANN EQUATION PREDICTS "CONDENSATION" OF THE COUNTER-IONS AROUND DNA. M. Le Bret and Bruno H. Zimm, Department of Chemistry B-017, University of California (San Diego), La Jolla, CA 92093.

We show that the distribution of counter-ions around a DNA molecule (modeled as a uniformly charged cylinder of 10 Å radius) can be predicted from the Poisson-Boltzmann equation, and that this distribution is in accord with the condensation idea introduced by Gerald Manning. The most remarkable thing about this distribution is the existence of a cloud of counter-ions that remains within a finite radius of the DNA cylinder no matter how much the system is diluted: this cloud may appropriately be called "condensed". The number of ions in this cloud is given by Manning's formula, $(1-1/\xi)N$, where N is the number of charges on the DNA and ξ for univalent counter-ions is given by $\xi=e^2/DbkT$, e the electronic charge, D the dielectric constant, b the axial charge spacing on the DNA, and kT as usual. For DNA $\xi\sim4$, so the whole condensed charge cloud contains approximately 75% as much charge as the DNA itself. At infinite dilution any given radius contains a definite fraction of the condensed cloud. For example, 50 Å contains 83% of it, 20 Å contains 68%, and 11 Å (only 1 Å outside the DNA surface) contains 22%.

These results come from solving the Poisson-Boltzmann equation exactly for the case where the DNA is surrounded only by its own counter-ions, using the solution given in 1951 by Alfrey, Berg, and Morawetz. By numerical solution we can show that the results are not much changed even when added salt is present.

W-AM-Pos64 DISCRETE CHARGE CALCULATIONS ON A-,B- AND Z-DNA James B. Matthew and Frederic M.Richards Dept. of Biochemistry, Univ of New Hampshire, Durham, NH 03824 and Molecular Biophysics and Biochemistry Dept., Yale University, New Haven, CT 06511

Recently, the static accessibility modified Tanford-Kirkwood algorithm for discrete charge calculations has been extended to account for the phenomemia of specific ion binding in the context of a general electrostatic effect (Matthew and Richards,(1982)Biochem 21, 4989). The effective dielectric value between surface charge sites depends predominately on the solvent ionic strength and the charge sites solvent accessibilities. Specific ion sites are determined by locating areas of high electrostatic potential at the solvent interface. At a given ionic strength the potential at a site is taken to describe the binding constant and therefore the ion site occupancy. For a two turn helix of B-DNA (20bp) the predicted bound sodium ($\bar{z}$) is the sum over sixteen sites. The $\bar{z}$ for B-DNA only increases from 3 to 8 as the ionic strength is increased from 0.01 to 0.50. Over the same range of ionic strength the free energy of the charge array increased from +0.6 kcal/bp to -0.05 kcal/bp. Parellel behavior is predicted for A- and Z-DNA with $\bar{z}_Z > \bar{z}_A > \bar{z}_B$. The most stable configuration, based on electrostatic criteria, for a two turn helix at high ionic strength (I=0.2 to 0.5) is that of Z-DNA. In this range the ratio of bound sodium to phosphate is predicted to approach 0.4. Many of the properties of linear polyelectrolytes which have been attributed to "Condensed counterions" (i.e. local bound ions which do not follow mass action; Manning (1978) Quart Rev of Biophysics II, 179) are now interpretable as the result of ionic equilibria. For example, the predicted insensitivity of bound sodium,$\bar{z}$, to increasing ionic strength is due to a see-saw effect between the calculated binding constant and the ion concentration.

W-AM-Pos65 HYDRATION FORCES BETWEEN PARALLEL DNA DOUBLE HELICES. D.R. Rau, B.-K. Lee, and V.A. Parsegian, N.I.H., Bethesda, MD 20205.

Using osmotic stress and x-ray diffraction, we have measured the repulsive force between parallel DNA double helices in condensed arrays. We find exponential repulsions, of decay distance 2 to 3 Ångstroms, first detectable at interaxial spacings of about 35 Å corresponding to some 15 Å separations between molecules. DNA repulsion behaves much like the "hydration force" between neutral or electrically charged bilayer membranes (e.g., Rand (1981) Ann. Rev. Biophys. Bioeng. 10:277-314) and bears little resemblence to the predictions of electrostatic double layer theory. Near molecular contact, DNA repulsion is only weakly affected by the ionic strength of the medium; at all separations it is virtually the same for native DNA as for poly A-T or poly G-C. The magnitude, but not the slope, of the repulsion curve is affected by the species of counterion in the medium. We conclude that this force represents the work of removing water from the vicinity of the macromolecule. Our application of the Marcelja and Radic formalism (1976, Chem. Phys. Letts. 42:129-130) shows that an exponential force can occur from the spatially varying perturbation of water near a polarizing surface. We suggest that the hydration force is a major factor in the interaction between particles undergoing molecular assembly. In particular, the packing of DNA in cells and in viruses must be accomplished in a way that overcomes or circumvents the effects of the hydrated water in the vicinity of the approaching particles.

W-AM-Pos66 ANISOTROPIC MACROMOLECULAR ROTATIONAL MOTION FROM NANOSECONDS TO MILLISECONDS B.H.ROBINSON, Chemistry, University of Washington, Seattle, Wa.; A.H.BETH, Physiology, Vanderbilt, Nashville, Tn; C.MAILER, Physics, UNB, Fredericton, N.B.; H.L.FRISCH, Chemistry, SUNY Albany, Albany N.Y.; L.R.DALTON, U.S.C., Los Angeles, Ca.

Electron Paramagnetic Resonance (EPR) is a powerful technique for observation of rotational motional processes for many biomolecules which tumble in the time range from a nanosecond to milliseconds. The "Delta S" method, using linear EPR spectra, and "ratio parameters", using Saturation Transfer (ST) EPR spectra, are the standard methods of data analysis which give correlation times. Below we outline how correlation times obtained by these methods may be interpreted in terms of generalized anisotropic rigid body motion.

A general correlation time comes from the time integral of the motional decorrelation function with an experimentally obtained weighting factor. We have found that the correlation times so defined all fall on a similar curve. We have calculated the EPR spectral responses for the motion of a variety of models: isotropic, prolate and oblate spheroid, and a uni-axial, infinitely long continuously twistable cable. All types fit the same curve.

The conclusion is that both the "Delta S" parameter and the STEPR ratio parameters, when plotted against a generalized correlation time for isotropic motion, can serve as a basis for the calibration of a variety of (anisotropic) motional processes. We have shown that by further studies of the temperature and viscosity dependence of the EPR parameters one can use the correlation times to discriminate among the different motional models. The results of this study are applied to the dynamics of DNA as monitored by EPR and STEPR, using spin-labeled intercalators. A clear distinction among the motional processes is shown.

W-AM-Pos67 A CONFORMATIONAL NMR STUDY OF POLY(5-FLUOROURIDYLIC) ACID. Ronald E. Loomis and James L. Alderfer, Biophysics Dept., Roswell Park Memorial Institute, Buffalo, New York 14263.

The conformational preferences for poly(U) and poly(FU) are determined by H-1 NMR spectroscopy at pH 6.0&9.5, and 6.0&9.0, respectively. These values are compared to those of UpU at pH 7.4. The coupling constants of poly(U) and poly(FU) (underlined) at the aforementioned pH's, along with the -pU portion of UpU are: $^3J_{4',5'}$(2.8, 2.4, 2.6, 3.1, 2.4), $^3J_{4',5''}$(4.3, 4.4, 4.6, 4.6, 3.2), $^2J_{5',5''}$(-11.9, -11.9, -12.2, -12.3, -11.9), $^3J_{5',P5'}$(4.2, 4.2, 4.3, 4.5, 4.4), $^3J_{5'',P5'}$(4.6, 5.0, 5.1, 4.3, 4.5). The ϕ(C5'-O5') rotomer population is (same order as above): f_t(0.73, 0.71, 0.70, 0.73, 0.72), f_g-(0.15, 0.17, 0.17, 0.13, 0.14), f_g+(0.12, 0.12, 0.13, 0.14, 0.14). The ψ(C4'-C5') rotomer population is (same order as above): f_g+(0.69, 0.72, 0.68, 0.63, 0.84), f_t(0.23, 0.24, 0.26, 0.26, 0.12), f_g-(0.08, 0.04, 0.06, 0.11, 0.04). Additionally, titration curves are obtained (δ vs pH) for poly(FU) & FUrd at a variety of temperatures. The H6 of poly(FU) & FUrd moves upfield with increasing pH, whereas the H1' of FUrd is pH independent, and H1' of poly(FU) moves downfield with increasing pH. A derivative-free nonlinear regression program (to fit the Henderson-Hasselbach eq.) is used to calculate pK_a from these plots. At 30°C a representative set of pK_a values are: FUrd, 7.42±0.11, poly(FU), 8.23±0.07. These collective data indicate: (1) the pK_a (H6) of the monomer is less than the polymer's, (2) N3-H ionization of the FU base is not directly responsible for the upfield shift of H1', rather changes in χ(CN) may be responsible, (3) for ϕ(C5'-O5') the -pU portion of UpU is much more g^+ than poly(U) or poly(FU), and poly(U) is more g^+, especially at high pH, than poly(FU), (4) for ψ(C4'-C5') the t population in poly(U), poly(FU), and the -pU portion of UpU are very similar. Supported by NIH Grant CA-25438.

W-AM-Pos68 MOLECULAR DYNAMICS OF PHENYLALANINE TRANSFER RNA. Stephen C. Harvey[a], Boryeu Mao[b], and J. Andrew McCammon[b], (a) Department of Biochemistry, University of Alabama in Birmingham, Birmingham, AL 35294 and (b) Department of Chemistry, University of Houston, Houston, TX 77004.

The atomic motions of yeast phenylalanine transfer RNA have been simulated using the molecular dynamics algorithm. The usual empirical energy parameters were used to describe bond stretching, valence angle bending, torsional rotations about bonds, and hydrogen bonds, and partial electrostatic charges and a distance-dependent dielectric constant were used to approximate solvent effects. Two simulations were carried out, one with a normal van der Waals 6-12 potential and the other with a modified van der Waals potential. The structure was derived from the 2.5Å structure of Hingerty, Brown, and Jack (J. Mol. Biol. 124,523 (1978)), refined by 100 cycles of steepest descent minimization and then warmed to 300°K over a period of 16 ps. An additional 4 ps of equilibration at 300°K preceeded the simulation. The structure remains close to that observed crystallographically, and here we compare the time-averaged backbone dihedral angles, the sugar puckers, and the hydrogen bond lengths with those of the crystal structure. The root mean square deviations and some of the correlations in the dynamic changes in these parameters are also discussed. (Supported by grants from the National Science Foundation).

W-AM-Pos69 MG2+ AND THE SOLUTION CONFORMATION OF t-RNA. John C. Thomas, John H. Shibata and Denis Hare, Department of Chemistry, University of Washington, Seattle, WA 98195.

The solution conformation of yeast-phe and coli-val t-RNAs has been investigated using intercalated ethidium dye as a probe. Both the fluorescence lifetime and the decay of the fluorescence polarization anisotropy of the ethidium/t-RNA complexes were measured using a picosecond dye laser and time-correlated single photon counting detection.

The fluorescence of the ethidium/t-RNA complexes exhibited essentially biphasic decay under all conditions studied and the lifetimes were found to decrease with increasing temperature. For yeast-phe t-RNA at low temperatures the major decay component has a lifetime close to 22ns which is consistent with a fully intercalated ethidium cation. The shorter lifetime is around 8ns which is not characteristic of a truly intercalated ethidium. In the case of coli-val t-RNA the lifetimes are about 17ns and 8ns; both of these times are shorter than expected for fully intercalated ethidium.

Measurements of the ethidium/t-RNA rotational diffusion times from the decay of the fluorescence polarization anisotropy indicate that Mg2+ has a profound effect on the conformation of both t-RNAs. At zero Mg2+ concentration the rotational diffusion times are on the order of 10ns which is less than half the value measured in the presence of even small amounts of Mg2+. Evidently in the absence of Mg2+ the t-RNA adopts a remarkably compact solution structure. We find also that coli-val t-RNA is even more compact than is yeast-phe t-RNA. As the Mg2+ concentration is increased the rotational diffusion times also increase, suggesting a more extended t-RNA structure in both cases.

W-AM-Pos70 INCREASE IN STIFFNESS OF DNA IN THE B-Z TRANSITION. T.J. Thomas and Victor A. Bloomfield, Dept. of Biochemistry, University of Minnesota, St. Paul, Minnesota 55108.

We have studied ionic effects on the solution properties of synthetic DNAs undergoing the B to Z transition by circular dichroism and laser light scattering. CD measurements show that poly (dG-dC) . poly (dG-dC), poly (dG-^{me}dC) . poly (dG-^{me}dC) and poly (dA-dC), poly (dG-dT) undergo the B to Z transition under a variety of conditions. The transition has been induced by NaCl, Co $(NH_3)_6^{3+}$, and spermidine^{3+}. X-ray analysis of oligonucleotides shows that Z DNA is thinner and more extended than the B form (Dickerson et al. Science 216, 475 (1982)), but there has been no experimental study of the effect of the transition on DNA flexibility. Total intensity light scattering measurements of the radius of gyration show that the persistence length of poly (dG-dC) . poly (dG-dC) increases from about 80 nm to 200 nm in the B to Z transition in 3.0 M NaCl, compared with the persistence length of calf thymus DNA of 55 nm at 0.1 M NaCl. Quasielastic light scattering shows that the translational diffusion coefficient decreases by about 10-15% in the B to Z transition. The Rouse-Zimm parameters also indicate an increase in the stiffness of Z DNA compared to the B form. In contrast, increasing the salt concentration with native DNAs is accompanied by an increase in the flexibility as measured by persistence length, diffusion coefficients and Rouse-Zimm parameters.

W-AM-Pos71 THE STRUCTURE AND DYNAMICS OF PBR322: AN ELECTRIC DICHROISM STUDY
Mickols, Wm. ; Univ. of New Mexico

The plasmid PBR322 can be isolated from its bacterial host (HB101) in supercoiled or nicked form. Comparison of the saturation $\Delta E/E$ for nicked ($\Delta E/E=-.72$) or supercoiled ($\Delta E/E=-.98$) plasmid gives corresponding angles of the nitrogenous bases with the electrical orientation axis of 82° for supercoiled plasmid and 73° for relaxed plasmid. The supercoils were titrated with ethidium bromide and the resulting $\Delta E/E$ relaxation parameters for one and two exponentials were determined. The relaxation times τ and amplitudes of the relaxing components were measured for .5, 1.0, and 2.0 mM ionic strength solutions. In all cases, changes in the values of τ and amplitudes were observed for various degrees of supercoiling. At .5mM ionic strength the τ increase with a corresponding decrease in supercoiling. Above this ionic strength the reverse was seen. Below .5mM ionic strength ethidium bromide has no effect on DNA structure.

W-AM-Pos72 DETECTION OF METASTABLE CONFORMERS OF SUPERCOILED M13 DNA, John H. Shibata, Jess P. Wilcoxon, J. Michael Schurr, and John C. Thomas, Department of Chemistry, University of Washington, Seattle, WA 98195.

Tertiary and secondary structure probes of supercoiled, double stranded M13 DNA reveal the significant role supercoiling exerts on conformation. The extent of tertiary folding as measured by the electrophoretic mobility on a 0.3% agarose gel establishes three distinct forms, I, II, and IV, with relative mobilities in the ratio of 2:1.5:1, respectively. In addition, the form with the lowest mobility (IV) exhibits an anomalously low scattered light intensity at 90 degrees scattering angle. A novel secondary structure probe is the value and uniformity of the twisting rigidity. The rigidity is determined by fitting the decay of the fluorescence polarization anisotropy (FPA) data of ethidium-DNA complexes to the appropriate model over different time spans. Two well defined rigidities exist, designated as A and B, where A is nearly twice as large as B. The lower rigidity occurs discretely in each of the different tertiary forms of M13 DNA, while the higher rigidity also occurs in forms I and IV, but not in form II. In attempting to convert form IA to form IB, another form, IA-B, with the same mobility, but a nonuniform rigidity is produced. Surprisingly, form IA spontaneously converts to form II over a period of time depending on the solution conditions. Form II has only one twisting rigidity associated with it, and is our most stable conformer; it is our candidate for the equilibrium form of M13 DNA. The existence of the different secondary structures is confirmed by a corresponding difference in the variation of the apparent diffusion coefficient as a function of the scattering vector. Circular dichroism and susceptibility to restriction endonuclease digestion studies further support the existence of at least six distinct metastable conformers.

W-AM-Pos73 CONFORMATIONAL DEPENDENCE OF DISSOLVED SUPERHELICAL DNA ON IONIC STRENGTH. G. W. Brady, D. H. Foos and K. Pulaski, Rennselaer Polytechnic Institute, Troy, NY 12181, S.U.N.Y. Albany, Albany, NY 12201 and N.Y. State Department of Health, Albany, NY 12201.

Earler sedimentation velocity studies suggested a transition might occur from a non-interwound superhelical form at low ionic strengths to an interwound superhelix at high ionic strengths[1]. With updated small angle x-ray diffraction techniques, Brady has determined the superhelix parameters of dissolved cop608 plasmid DNA at .05 Molar.[2] The results are consistent with a non-interwound superhelical conformation. Our most recent experiments indicate that cop608 DNA can also exist in the interwound form in solutions of ionic strengths greater than .05 M. The experiments suggest that the conformation could depend on the history of the sample. (Supported by National Science Foundation Grant PCM-8041337).

[1]Gray, N.D. (1967) Biopolymers 5, 1009-1019.
[2]Brady, G.W., D.B. Fein, H. Lambertson, V. Grassian, D. Foos and C.J. Benham (In press) Proc. Natl. Acad. Sci.

W-AM-Pos74 ABERRANT ELECTROPHORETIC MOBILITY OF PBR322 RESTRICTION FRAGMENTS. Nancy C. Stellwagen, Dept. of Biochemistry, University of Iowa, Iowa City, Iowa 52242.

A systematic survey has been made of the electrophoretic mobility of restriction enzyme fragments of pBR322 as a function of molecular weight, gel type, gel concentration, temperature, applied voltage, and time of electrophoresis. The mobility of all fragments on agarose gels followed a sigmoidal curve when plotted against log molecular weight. To see how mobility scaled with molecular weight, log-log plots were prepared using the same data. The mobility of high molecular weight fragments ($\sim$800-6000 b.p.) was approximately proportional to M^{-2}. The apparent mobility of low molecular weight fragments ($\sim$50-250 b.p.) scaled as M^{-x}, with x ranging from $\sim$5 to 27 or greater, increasing with time of electrophoresis.

On polyacrylamide gels a plot of mobility versus log molecular weight showed that some fragments migrated faster or slower than expected on the basis of their known molecular weights. This behavior could be enhanced or suppressed by changing the polyacrylamide concentration and/or applied voltage. Small changes in size of the restriction fragments sometimes caused significant changes in electrophoretic behavior. The scaling of mobility with molecular weight at each end of the molecular weight spectrum was obtained from log-log plots. The mobility of high molecular weight fragments was approximately inversely proportional to molecular weight, possibly indicating a reptation mechanism for migration through the gel. The mobility of low molecular weight fragments was approximately proportional to M^{-3}, possibly indicating that the rate determining step was rotational diffusion of the fragments to enter the pores.

W-AM-Pos75 Hydrogen-Exchange Behavior of B- and Z-Poly(dGdC)-Poly(dGdC). H. Dalton King, Neville R. Kallenbach, and S. Walter Englander, Departments of Biology and Biochemistry/Biophysics, University of Pennsylvania, Philadelphia, Pennsylvania 19104 (Intr. by Manjusri Das).

The hydrogen exchange behavior of the right handed B-form and the left handed Z-form of poly(dGdC)-poly(dGdC) has been investigated as a function of pH, catalyst, and temperature. Previous results by Ramstein and Leng (Nature, 288, 413 (1980)) have shown slow biphasic exchange kinetics for the Z conformation at pH 7.5 and 0°C in contrast to relatively fast kinetics for the B conformation. If the B-form is considered to be in equilibrium with the Z-form, then they both must share some common, unique open state, X:

$$B \rightleftharpoons X \rightleftharpoons Z$$

We are characterizing this open state by hydrogen-deuterium exchange (detected by stopped-flow methods) and by hydrogen-tritium exchange. Our results agree in general with those of Ramstein and Leng and indicate that the exchange behavior of both B- and Z-poly(dGdC)-poly(dGdC) is sensitive to pH. For example, the exchange kinetics of the Z-form is slowest at pH 7.5 and increases as pH deviates from that point. On the other hand, at 0°C, the B-form demonstrates increasingly faster kinetics from pH 8.5 downward. We also see in the B-form at low temperature the presence of two distinguishable classes of exchanging hydrogens. At higher temperatures, these merge into a single class.

W-AM-Pos76 DEUTERIUM EXCHANGE OF PURINIC 8-CH GROUPS: COMPARATIVE RATES FOR RIBO AND DEOXYRIBONUCLEOTIDES J.M. Benevides, D. LeMeur and G.J. Thomas, Jr., Department of Chemistry, Southeastern Massachusetts University, North Dartmouth, MA 02747.

Pseudo-first-order rate constants governing deuterium exchange of 8-CH groups in purine 2'-deoxy-5'-monophosphates (dAMP, dIMP, dGMP) and in cyclic dAMP (c-dAMP) were determined by laser-Raman spectrophotometry of D_2O solutions of the deoxyribonucleotides in the temperature interval 40-80°C. The exchange rate constants ($k=Ae^{-E_a/RT}$) and derived Arrhenius parameters (E_a, A) are close to the values observed previously for corresponding ribonucleotides (J. Raman Spectrosc. 11, 508-514, 1981; Biochemistry 14, 5210-5218, 1975), with the exception of dGMP which exchanges more slowly than rGMP (Biochemistry 18, 3839-3846, 1979). The differential in 8-CH exchange of dGMP and rGMP may be attributed to their different molecular conformations. For c-dAMP E_a is significantly smaller than for dAMP, confirming the trend observed previously of more rapid exchange of cyclic nucleotides vis-a-vis 5'-nucleotides. Rapidity of purine 8-CH exchange is apparently favored in cyclic isomers, as in dinucleotide monophosphates, by the lesser negative charge of the diesterified phosphate group. Extension of these studies to polyribonucleotides and polydeoxyribonucleotides indicates that different helical structures are also distinguishable by their respective rates of purinic 8-CH exchange.

Supported by N.I.H. Grant AI18758.

W-AM-Pos77 SOLVATION EFFECTS ON THE PHOSPHORUS NMR AND INFRARED SPECTRA OF CYCLIC MONONUCLEOTIDES AND SYNTHETIC POLYNUCLEOTIDES. D.B. Lerner, W.J. Becktel, R. Everett, M. Goodman and D.R. Kearns. Department of Chemistry, University of California-San Diego, La Jolla, CA 92093

The effects of solvation on the ^{31}P NMR and infrared spectra of the cyclic mononucleotides 3',5'cAMP, 2',3'cAMP and 3',5'cUMP have been studied in water: organic mixed solvent systems. Addition of organic solvents to the aqueous solutions of these cyclic mononucleotides causes an upfield shift of the phosphorus resonances and an increase in frequency of the infrared transitions assigned to the OPO antisymmetric stretch. The magnitudes of the changes in ^{31}P chemical shift and in the IR frequency with solvent are similar for the three mononucleotides studied, and in each case the solvent induced change in the PO_2^- antisymmetric stretch frequency in the infrared is directly porportional to the change observed in the ^{31}P chemical shift. Both ^{31}P NMR and PO_2^- infrared studies on the polynucleotide systems poly(A)·poly(U), poly(U)·poly(A)·poly(U) and poly(G)·poly(C) indicate two chemically distinct phosphodiester groups in the double helices and three in the triple helix. ^{31}P NMR and infrared spectroscopy appear to be sensitive probes of solvation of nucleic acids as well as conformational changes and when both techniques are used it is possible to distinguish between solvent and conformational effects in ^{31}P chemical shifts.

W-AM-Pos78 P-31 NMR STUDIES OF POLY d(G-T).d(C-A) . Bruce G. Jenkins and James L. Alderfer Biophysics Dept. Roswell Park Memorial Institute , Buffalo, N.Y. 14263

P-31 NMR spectra have been obtained for poly d(G-T).d(C-A) at a variety of temperature and salt conditions. The polymers were synthesized using DNA Polymerase I and characterized by CD,UV and thermal denaturation. The polymer was sonicated to a length of 75-175 base pairs. The P-31 NMR spectrum of poly d(G-T).d(C-A) in buffer (.25M NaCl,30mM NaPhosphate,3mM EDTA, pH 7.5) at 30°C appears as a doublet with resonances occurring at -4.2 and -4.4ppm relative to TMP. At 90°C (above the T_m) the P-31 spectrum exhibits not one line but two sharp lines occurring at -3.7 and -3.8 ppm in a ratio of 1:3, indicating an alternating magnetic environment on one of the single strands. At 5.6M CsCl the CD spectrum for poly d(G-T).d(C-A) shows an inversion of the positive band at 275nm while the negative band at 241nm remains unchanged. Corresponding P-31 NMR spectra indicate a quadruplet with resonances at -4.0,-4.3,-4.4,-4.5ppm in buffer at 30°C. For poly d(G-C) at high salt a doublet is seen with resonances at -4.3 and -2.8ppm indicative of the dinucleotide repeat unit expected for Z DNA. It would appear under these conditions d(G-T).d(C-A) is not in the Z form but rather a form closer to the alternating B form postulated for poly d(A-T). In addition CD studies of poly d(G-T).d(C-A) with many salts including $[Co(NH)_6]Cl_3$ indicate no CD inversion as seen for poly d(G-C). Although a left-handed form for this polymer[3] has been seen by Wells et al (JBC 257 pp 10166-171 1982) upon binding of the carcinogen AAF it is more probable that under ordinary conditions this polymer exists in a right-handed form , and assumes the left-handed form only upon sufficient chemical modification of the DNA. Comparative P-31 NMR studies are underway on poly d(G-A).d(C-T) . (This work partially supported by NIH grant 2T32-ES07057)

W-AM-Pos79 ETHIDIUM BROMIDE AS A STRUCTURAL PROBE OF TRANSFER RNA. Barbara D. Wells, Chemistry Department, University of Wisconsin-Milwaukee, Milwaukee, WI 53201.

Most models for protein synthesis employ conformational changes in tRNA; this necessitates the description of different solution conformations for tRNA. Ethidium bromide intercalates into a single, specific, tight binding site on tRNA. This binding can be utilized to probe the nucleic acid structure under various solution conditions. Ethidium binding can be monitored by fluorescence as the intensity of the dye emission is enhanced upon intercalation. Yeast $tRNA^{Phe}$ has a fluorescent base, Y, and the emission of Y has a reasonable overlap with the excitation of ethidium thus permitting the measurement of Föster energy transfer. Laser light scattering has shown differences in tRNA structure in buffers with and without magnesium but the actual structures are unknown. Experiments will be reported which have measured the intercalation of ethidium into yeast $tRNA^{Phe}$ with and without magnesium in the buffer. The fluorescence intensity is used to quantitate the intercalation as well as measure the distance between Y and ethidium. Polarized excitation spectra are used to estimate the orientation of the fluorophores. Using these parameters a model for the structure of tRNA with and without magnesium will be presented and discussed.

Supported by NIH grant, GM 30700.

W-AM-Pos80 A FLUORESCENCE STUDY OF THE BINDING OF ETHIDIUM BROMIDE TO DNA IN INTACT BACTERIOPHAGE T7. Paul Horowitz and Philip Serwer, Department of Biochemistry, University of Texas Health Science Center at San Antonio, San Antonio, Texas 78284

Procedures for measuring the entry rate of fluorescent, DNA-reactive compounds into bacteriophages have been developed using ethidium bromide (EB) as a test compound. Measuring the fluorescence enhancement of EB as it binds to packaged bacteriophage T7 DNA, the temperature dependence of the entry rate has been determined. From an Arrhenius plot of the data, an activation energy of 17.5 K cal/mole was found. Equilibrium binding studies were performed at 45°. These studies gave a binding constant of $9.5 \times 10^{4} M^{-1}$ and a stoichiometry of 0.14 moles of EB bound per nucleotide pair. DNA was ejected from bacteriophage T7 by temperature shock. Binding of EB to this DNA was apparently instantaneous and gave equilibrium binding parameters which were very similar to those obtained with salmon sperm DNA. The equilibrium binding parameters for encapsulated DNA measured here for T7 are similar to those reported previously for the binding of proflavin to bacteriophage T4. This result suggests that the DNA packing density and accessibility is the same in these two phages and that differences in phage morphology and polyamine content do not affect these aspects of condensed DNA structure (Supported by NIH grants GM25177 and Welch grant AQ-723 to PH and NIH grants GM24365 and Al-16117 and Welch grant AQ-764 to PS).

W-AM-Pos81 ACCESSIBILITY OF INTERCALATION SITES IN NATIVE CHROMATIN by Kenneth S. Schmitz and Mei Lu Department of Chemistry, University of Missouri-Kansas City, Kansas City, Missouri 64110

The interaction of proflavine with core particles, chromatosomes devoid of the external histones H1 and H5, polynucleosomes with the full complement of histones, and mononucleosomal DNA was examined by UV-visible absorption methods and sedimentation velocity techniques. These studies suggest that for ligand/phosphate ratios below 0.004 very little, if any, proflavine associates with the core particle and that binding commences only when the core particle begins to unfold as inferred from sedimentation data. In contrast, the chromatosome and polynucleosome preparations do exhibit some degree of association with proflavine prior to unfolding of the core particle substructure. For a given ligand/phosphate ratio less than 0.02, the chromatosome appears to bind more proflavine than the polynucleosomes. These data support a model in which only a small fraction of the total number of intercalation sites (potential) are actually physically accessible in the native structure of chromatin (J. Theo. Biol.,98(1982) 29-43). The implications of this model are that any recognition step in transcription and replication that involves intercalation can only take place initially in the linker region of DNA or that the core particle substructure must first unfold, and also that intercalating ligands such as proflavine and ethidium bromide cannot be used to study the dynamics of DNA in the native core particle as would be the case in fluorescence depolarization studies.

This research was partially supported by grants from the American Cancer Society and NSF.

W-AM-Pos82 INTERACTION OF AROMATIC IMIDES WITH DEOXYRIBONUCLEIC ACID - KINETIC STUDIES
Shau-Fong Yen, W. David Wilson, J. C. Smith, and E. J. Gabbay, Dept. of Chemistry and LBMS, Georgia State University, Atlanta, Georgia 30303

Intercalating molecules such as adriamycin, daunorubicin, and mitoxantrone are important clinical agents. The relationships of their biological activity and association or dissociation with DNA are not clear. For the purpose of elucidating the nature of intercalator-DNA interactions and DNA dynamics, we have designed and synthesized a new class of intercalating agents, naphthylene imides (I) and diimides (II). On the basis of the size of the substituent groups attached to the aromatic ring, the diimides are further classified into three categories: Type A, B, and C compounds are those with a methylene, methyl, amide (or adamantylamide), respectively, on the carbon adjacent to the diimide ring. Our previous studies (Yen, et al, Biochemistry 21, 2070 (1982)) have shown that all of these molecules intercalate with DNA. The present work shows the order of the apparent first order SDS-induced dissociation rate constants is Type A > B > C. These dissociation rate constants are independent of the molar ratio of diimide to DNA base pairs. The dissociation studies illustrate that (1) the dissociation rate constant for each diimide increases as the temperature increases; (2) the order of dissociation rate constants of diimides is Type B > A > C; and (3) the activation energies of Type A and B diimides are similar while that of Type C is lower. Grant support: National Institutes of Health GM 30267, RR09201, and GM 30552.

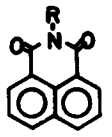
I

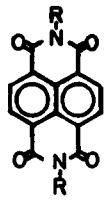
II

W-AM-Pos83 A THERMODYNAMIC INVESTIGATION OF THE BINDING OF ACTINOMYCIN D TO SALMON SPERM DNA AND SELECTED DEOXY-OLIGONUCLEOTIDES.
James Snyder. Department of Chemistry, Rutgers University, New Brunswick, New Jersey 08903.

Actinomycin D (Act-D) is a powerful antitumor drug which has been shown to bind to double-helical DNA in vitro. This binding capability is suspected to be the basis of the drug's anti-cancer activity. It is widely believed that the binding is intercalative and that the drug has a strong preference for GpC base pairs as a binding site. Using optical as well as microcalorimetric techniques, we have determined the complete thermodynamic profile for the binding of Act-D to sonicated Salmon Sperm DNA and specific oligonucleotides, including $(ATGCAT)_2$. The thermodynamic data will be presented and discussed in terms of several suggested binding models.

This work was supported by NIH Grant GM-23509.

W-AM-Pos84 NMR STUDIES OF UV PHOTOPRODUCTS OF UpU AND TpT.
Robert E. Rycyna, James L. Alderfer, Biophysics Department, Roswell Park Memorial Institute, Buffalo, N.Y. 14263.

NMR was used to examine structural changes induced by UV light in UpU and TpT. When UpU is irradiated at 254nm in aqueous solution, new P-31 resonances arise from photoproduct formation. Photodimers are identified by the small $\Delta\delta/d(\text{temperature})$ values expected from the more rigid phosphate backbone. Photohydrates revert to UpU upon heating and are assigned by their intensity reduction following temperature elevation. Photodimers, represented by U(p)U, are obtained in 90% yields without any indication of hydrates by irradiation at 300-330nm in the presence of a photosensitizer. The distribution of P-31 resonances after sensitized irradiation is: 14% U(p)U#2 at -3.0ppm, 9% U(p)U#3 at -3.24, 10% UpU at -3.91, 7% U(p)U#4 at -4.01, and 60% U(p)U#1 at -4.67 relative to TMP. Different proton coupled P-31 patterns are observed for photodimers suggesting various backbone conformations. The predominant photodimer, U(p)U#1, was isolated and analyzed by H-1 NMR. Extensive temperature and spin decoupling experiments at 200MHz suggest considerable structural alterations relative to UpU (e.g. one ribose H1' has a large J value(8.1Hz) while the other H1' is shifted far upfield). In order to facilitate resonance assignments, 2-D experiments such as δ-J resolved, scalar correlated/SECSY and modified-SECSY were done at 200MHz. When TpT is irradiated at 254nm in aqueous solution, formation of photoproducts also is observed by the appearance of new P-31 resonances. Evidence for hydrates was not found. Preliminary intensity distributions were found to be 15% T(p)T#2 at -3.46ppm, 5% T(p)T#3 at -3.98, 55% TpT at -4.01, and 25% T(p)T#1 at -4.53 relative to TMP. Proton coupled P-31 data indicate these photodimers also have a variety of backbone conformations. (Supported by ACS IN-54U and N.I.H. 2T32-ES07057).

W-AM-Pos85 FLOURESCENCE, OPTICAL MELTING AND RELATED INVESTIGATIONS ON THE EFFECTS OF CO-60 GAMMA RADIATIONS ON SALMON SPERM DNA.

S.Srinivasan and T.P.Ramachandran, Department of Biophysics, Institute of Medical Sciences, Banaras Hindu University, Varanasi 221005, U.P., India.

Salmon sperm DNA solutions were irradiated by Co-60 gamma radiations, doses ranging from 200 to 600 krads. From dye-induced fluorescence intensity measurements the number of ethidium bromide binding "sites" were found to decrease from a value of 0.195/nucleotide for the native DNA to 0.106/nucleotide for the DNA irradiated to 600 krads, with values falling in between for the intermediate doses. Similar reduction in hyperchromicity values were observed due to irradiation of the DNA. Circular dichroic measurements revealed that irradiation led to a decrease in the positive Cotton peak height and a red shift of the first cross-over wavelength. Optical melting studies showed that, concomitant with irradiation of the DNA, the melting temperature shifted to lower values from 71°C for the native DNA to 57°C for the DNA irradiated to 600 krads. Estimation of vant Hoff enthalpies showed a decrease in the energy "status" for the DNA. It is concluded that irradiation of the DNA leads to debasepairing and debasestacking along with a reduction in the energy status of the nucleic acid. Since at the molecular level the effects due to ionizing radiations and those due to intercalating drugs are the same, the results in the present studies are examined from the point of the effects of the anticancer drugs on the structure of the DNA.

W-AM-Pos86 SOLUTION STRUCTURE AND DYNAMICS OF THE LAMBDA REPRESSOR-OPERATOR COMPLEX. Michael A. Weiss, Committee in Biophysics, Harvard University, Cambridge, Mass.

Specific recognition of operator DNA by lambda repressor plays a central role in the differential control of gene expression in the phage. The physical basis of this recognition is not understood. I am using high-resolution proton magnetic resonance in order to define the solution structure and dynamics of the repressor-operator complex. This project has three parts: (a) study of the operator alone, (b) study of the repressor alone, and (c) study of both together. The DNA under investigation is a synthetic 17 base-pair oligonucleotide whose sequence is that of O_L1, the strongest repressor-binding site in the phage. Its 17 imino protons, which participate in Watson-Crick base pairing, and its 8 adenine C_2H protons, which lie in the minor groove of the double helix, have been assigned on the basis of Nuclear Overhauser Effects. The protein under investigation is the operator-binding domain of the lambda repressor, which consists of the first 92 residues. The crystal structure of this domain has recently been determined to 3.2A by Pabo and Lewis. Assignments of the aromatic amino acids have been made two-dimensional NMR methods, comparison with the crystal structure, and biosynthetic incorporation of deuterium labels. I have cloned and purified mutant repressors containing single amino-acid substitutions in order to confirm key assignments. Chemical shifts in these DNA and protein resonances occur in the complex.

W-AM-Pos87 KINETIC STUDIES OF SITE SPECIFIC PROTEIN-DNA INTERACTIONS. J.-H. Roe, S. Mazur, R. R. Burgess and M. T. Record, Jr., Departments of Chemistry, Biochemistry and Oncology, University of Wisconsin, Madison, Wisconsin 53706.

The nitrocellulose membrane filter assay has been used to investigate aspects of the kinetics of the interactions of E. coli RNA polymerase with the λP_R promoter, and of the interaction of E. coli lac repressor with the lac operator region of λ p^Rlac DNA. In the investigation of the kinetics of the interaction of RNA polymerase with the λP_R promoter, various filter assay methods (heparin-competition, initiation-stabilization) were employed to ensure that specific functional complexes were being observed. Under conditions of RNA polymerase excess, pseudo first order kinetics (binding-limited) were observed under all solution conditions. No evidence was obtained for a rate-limiting isomerization step involving a polymerase-DNA complex (as proposed by McClure (1980) from kinetic studies obtained with the abortive initiation assay). The forward rate constant was found to be a strong function of both temperature and salt concentration; more than half of the salt-dependence of the equilibrium constant was found in the forward rate constant. Both the magnitude of the forward rate constant ($\sim 10^6$ M^{-1} sec^{-1} under approximately physiological conditions) and its temperature and salt-dependences are inconsistent with a simple diffusion-limited reaction, and may indicate the existence of a conformational or binding pre-equilibrium in the reaction mechanism.

W-AM-Pos88 AB INITIO CALCULATION FOR THE EFFECT OF H-BONDING INTERACTION OF PROTEINS ON THE STABILITY OF ADENINE-URACILE PAIR. A. Sarai and M. Saito, Department of Physics, Nagoya University, Nagoya, Japan, and Department of Biophysics, University of Illinois, Urbana, IL. The H-bonding interaction of proteins with adenine-uracil base pair was investigated by the ab initio MO method (STO-3G level). We found that the stability of base pair was greatly affected by the H-bonding interaction of several residues of protein in different ways, depending on whether the interacting species is charged or neutral, whether the interaction is made from major groove or minor groove, and which of adenine or uracil is H bonded. The base pair was destabilized when the H bond O....H-N in the major groove side was interacted by several residues examined; in particular, residues with acidic side chains such as aspartate decreased the binding energy of the base pair by up to 38% when coordinated at the nitrogen site. On the other hand, it was stabilized when the oxygen of uracil in the minor groove side was H bonded by residues with basic side chains such as lysine, and when the ring nitrogens of adenine were interacted by the same residues (stabilization was up to 28%). These results indicate a possibility that the stability of base pair is controlled by the specific interaction of proteins. Such control may be relevant to the local melting process of double helix by RNA polymerase and other processes with repressor and catabolite gene activator proteins, which interact with nucleic acids and regulate transcription. The change of stability of base pair might also be relevant to the local conformation change of double helix.

W-AM-Pos89 THE ROLE OF THE FOLDING DOMAIN OF HISTONE H5 IN CHROMATIN STRUCTURE. Daniel C.F. Chan, Lawrence H. Piette, and Jean-Jacques Lawrence+. Cancer Center of Hawaii, Honolulu, Hawaii, 96813 and +Centre d'Etude Nucleaires de Grenoble, France.

Histone H5 contains three tyrosines in its central apolar region of the molecule. All three tyrosines can be labeled by an imidazole spin label in low ionic strengths but only one tyrosine becomes accessible to the spin label when the central globular domain of the molecule is folded in high ionic strengths. Spin labeling the buried tyrosines prevents the folding of the globular structure, which, in turn, affects the proper binding of the H5 molecule to the stripped chromatin. Chromatin reconstituted from such an extensively modified H5 molecule has a weaker protection of the 168-base-pair chromatosome during nuclease digestion and it forms irregular large aggregates in conditions when native chromatin normally condenses into a higher-order structure. However, when only the surface tyrosine is labeled, such a molecule can still bind correctly to the stripped chromatin, yielding a complex very similar to that of native chromatin. This complex is still capable of condensing into a regular higher-order chromatin structure. Our data supports the idea that not just the presence of the linker histone H5, but the presence of an intact H5 molecule with a folded central domain is essential in the recognition of its specific binding sites on the nucleosome. Our data also shows that, during the chromatin condensation process, the tumbling environment of the spin label attached to the surface tyrosine is not hindered but remains as mobile as it is when the reconstituted complex is subjected to lower ionic strengths. This suggests that either the labeled domain of the H5 molecule is not directly involved in the condensation process, or the formation of the higher-order chromatin structure does not result in a more viscous or tighter environment around this labeled surface tyrosine.

W-AM-Pos90 TIME LAG IN ATP HYDROLYSIS BY REC A PROTEIN: KINETIC MECHANISM IMPLICATIONS, Arne Strand, Department of Biochemistry, University of Arizona, Tucson, AZ 85721.

Single-stranded DNA (ssDNA) increases the rate of ATP hydrolysis by the E. coli RecA protein over five hundred-fold. Several steps of the kinetic mechanism of this ssDNA-activated ATPase have been observed by monitoring fluorescence or light-scattering changes in a stopped-flow fluorometer (White and Strand, Bioph. J. 37, 377a, 1982). An initial fast step, in which addition of ATP produces a rapid decrease in scattering signal, is followed by a second step in which the observed scattering signal increases slowly. This suggests that the initial fast step is dissociation of RecA and ssDNA by ATP, followed by a slower second step in which RecA and ssDNA reassociate. At 25-30°C the rate constant for the second step is approximately equal to the steady-state rate of ATP hydrolysis under the same conditions. Further examination of the reassociation has shown that at temperatures less than 25°C the rate constant for this step is several-fold smaller than the steady-state rate of ATP hydrolysis. At $T < 25°C$ the time course of ATP hydrolysis shows a lag in phosphate production. The length of the lag is predicted by the rate constant of the reassociation step. This is consistent with a model, in which, following rapid dissociation of RecA and ssDNA by ATP, slower reassociation of RecA and ssDNA occurs to form a catalytically productive complex designated ATP·RecA*.ssDNA. Following the time lag corresponding to formation of this complex, phosphate is produced by ATP hydrolysis at a rate faster than reassociation, and thus cannot proceed via the initial dissociation and reassociation steps. (Supported by research grant from the American Cancer Society).

W-AM-Pos91 ROLE OF ZINC IN ESCHERICHIA COLI RNA POLYMERASE. Daniel Solaiman and Felicia Y.-H. Wu, Department of Pharmacological Sciences, State University of New York at Stony Brook, Stony Brook, New York 11794.

E. coli RNA polymerase(RPase) is a Zn-metalloenzyme containing two Zn ions. To study the role of Zn in this enzyme, we have developed method to remove Zn and to reconstitute apoenzyme into active enzyme. The two Zn ions were removed by sequential dialysis against Tris buffer containing 8 M urea-10 mM EDTA(pH 8.0) followed by solution containing 0.05 M KCl-10 mM EDTA (pH 2.2). The enzyme activity of denatured RPase could be partially(40-60%) recovered by dialysis against reconstitution Tris buffer I (8 M urea, 10^{-5}~10^{-4} M $ZnCl_2$, pH 8.0) and then Tris buffer II (20% glycerol, 10^{-5}~10^{-4} M $ZnCl_2$, pH 8.0). If $ZnCl_2$ was omitted from the reconstitution buffers, the activity recovered was less than 20%. The RPases reconstituted in the absence and presence of Zn contain 0.2 and 1.0 ± 0.2 Zn ion, respectively, as determined by atomic absorption spectrometry. Studies with ^{65}Zn indicated that Zn is incorporated during dialysis against buffer II. Further incubation of the apoenzyme with excess Zn at 37°C for one hr. did not result in increased enzyme activity. Native Zn_2-RPase, Zn_1-RPase, and apoenzyme showed similar patterns in sucrose density gradient sedimentation suggesting that Zn ion does not affect the gross structure of enzyme. In addition, Zn_1-RPase shows reduced abilities in DNA binding and the formation of the DNA-enzyme-RNA ternary complex as compared to the Zn_2-enzyme, while the rates of the abortive initiation for both Zn_1- and Zn_2-enzymes are comparable.

(Supported by NIH GM 28057-02 and NSF PCM8119326)

W-AM-Pos92 NMR STUDIES ON ESCHERICHIA COLI RNA POLYMERASE-ATP COMPLEX IN THE PRESENCE OF DNA TEMPLATE. Dipankar Chatterji, Cheng-Wen Wu, and Felicia Y.-H. Wu, Department of Pharmacological Sciences, State University of New York at Stony Brook, Stony Brook, New York 11794.

E. coli RNA polymerase(RPase,$\alpha_2\beta\beta'\sigma$) is a Zn-metalloenzyme which contains two Zn ions in the β and β' subunits of the enzyme. Recently, we have selectively substituted one Zn located in the β subunit with various divalent paramagnetic metals, e.g. Co(II), Mn(II), Ni(II) or Cu(II), and studied the proximity relationships between the substrate ATP and the intrinsic metal of the enzyme by ^1H and ^{31}P NMR spectroscopy (Chatterji and Wu, Biochemistry, 21, 4651, 4657 (1982)). We now report similar NMR studies in the presence of DNA template, which provide more meaningful information concerning the role of intrinsic metal in gene transcription. A fragment of poly(dA·dT) having ca. 60 base pairs was used as the template in these studies. The distances from bound ATP to the paramagnetic metal center of the Mn-Zn and Co-Zn RPases were determined in the presence of equimolar amounts of enzyme and DNA fragment. The correlation times(τ_c) for the Co-^1H and the Mn-^1H interactions were found to be 6.3×10^{-12} and 2×10^{-9} sec, respectively, whereas that for the Mn-^{31}P interaction was 1.4×10^{-9} sec. The distances from the intrinsic metal to H_2,H_8, and H_1' were calculated to be 4.1±0.6, 6.7±0.7 and 6.0±0.7 Å, and those to the α-, β-, and γ-phosphorus atoms were 7.5±0.8, 9.4±1.0 and 9.8±1.0 Å, respectively. While the distances from metal to the base and sugar moieties did not alter significantly, the phosphate moieties of ATP moved closer to the metal center by the addition of DNA. Such a movement may contribute to the higher affinity of ATP to the enzyme in the presence of DNA(K_d=0.09 mM) than in its absence(K_d=0.15 mM). The implication of these results in relation to our earlier study will be discussed.

(Supported by NIH GM28057-02 and NSF PCM8119326)

W-AM-Pos93 MECHANISM OF RNA POLYMERASE OPEN COMPLEX FORMATION AT THE E. COLI GALACTOSE OPERON. Stephanie H. Shanblatt and Arnold Revzin, Department of Biochemistry, Michigan State University, E. Lansing, MI 48824.

Initiation of transcription at the gal operon can occur from either of two overlapping promoters. In the presence of the catabolite activator protein (CAP) transcription from the P1 promoter begins at nucleotide +1. The P2 promoter, active only in the absence of CAP, initiates 5 bp upstream (at -5) of the P1 start site. We have shown previously that when RNA polymerase binds to CAP/cAMP-gal promoter DNA complexes a second CAP molecule binds as well. The two CAP molecules, bound contiguously on the DNA just upstream of RNA polymerase, are necessary for efficient CAP-dependent transcription from the P1 promoter.

The addition of RNA polymerase to gal promoter DNA in the presence of subsaturating amounts of CAP (less than 2 CAPs/promoter) leads to a rapid redistribution of the CAP molecules such that all CAP-RNA polymerase-gal promoter complexes contain 2 CAP molecules; the remaining RNA polymerase-promoter complexes have no bound CAP. The effect of this second CAP molecule on RNA polymerase open complex formation has been examined by kinetic studies using restriction fragments containing either one ("-60 fragment") or both ("-90 fragment") CAP binding sites. The dissociation rate of heparin-resistant open complexes formed on the -60 fragment in the presence of CAP is much faster than that observed for similar complexes on the -90 fragment. We also found that the binding of the second CAP enhances the rate of formation of open complexes. These data suggest that the mechanism of open complex formation is ordered: the first CAP binds at -35, followed by RNA polymerase, and then the second CAP binds upstream of the first. It is this second CAP molecule which permits RNA polymerase to rapidly form a stable open complex competent to initiate transcription. (Supported in part by NIH).

W-AM-Pos94 DYNAMIC LIGHT SCATTERING (DLS) STUDIES OF VIRUSES. J.M. Schurr and J.P. Wilcoxon, Department of Chemistry, University of Washington, Seattle, WA 98195.

An exact theoretical expression for the apparent diffusion coefficient D_{app} (K) of a thin rigid rod with arbitrary anisotropy of its translational diffusion coefficient D_o is derived from the first cumulant of its dynamic structure factor. D_{app} (K) is predicted to reach a limiting plateau value at extremely large values of KL, where K is the scattering vector and L the rod length. However, that limiting plateau value is approached only very slowly along a quasi-plateau with a very gradual slope.

DLS studies have been performed on Tobacco Mosaic (TMV) and M-13 virus from $K^2=(0.2\text{-}20)\times10^{10}\,cm^{-2}$ using 632.8, 363.8 and 305.1 nm laser radiation. For TMV, the present data yield $D_o=(4.19\pm0.10)\times10^{-8}$ cm^2/sec (T=20 °C), and with the literature data of L=2980Å and the rotational diffusion coefficient $D_R=318\ sec^{-1}$ yield $\Delta=D_{\parallel}-D_{\perp}=(1.79\pm0.38)\times10^{-8}$ cm^2/sec. The experimental data closely follow the curve of $D_{app}(K)$ vs. K^2 calculated for these parameters over the entire K^2 range.

The behavior of M-13 virus is in distinct contrast to the results of TMV. Although the experimental data for small values of K^2, ($K^2<1.2\times10^{10}\ cm^{-2}$) yielded $D^o=(2.4\pm05)\times10^{-8}$ cm^2/sec and $\Delta=1.24\pm3\times10^{-8}$ cm^2/sec (T=21 °C), in excellent agreement with the theory of Tirado et al. and the measured D_R value, the experimental $D_{app}(K)$ values exceeded those of the theoretical curve by increasing amounts at large values of K^2. This behavior is likely due to the additional flexibility of M-13 which allows additional faster contributions to the relaxation of the rod. Interestingly, the value of K^2 at which the curves begin to deviate from one another corresponds to a fluctuation wavelength of ∿4800Å, approximately half the rod length.

W-AM-Pos95 AN *E. COLI* REGULATORY MUTANT OF THE *dnaA* REGION. H. Eberle, C. Stillman, N. Forrest and D. Sporn

A mutant of *E. coli*, PR1, has been isolated which appears to overproduce certain proteins with molecular weights similar to those of products of genes in the *dnaA* region. The PR1 mutation was found map in the *dnaA* region. Further characterization of this mutant by comparative two-dimensional gel analysis indicates that these proteins co-migrate with proteins coded for by λ*tnaA* transducing phages which carry the *dnaA* region. Attempts are underway to determine more precisely the location of the mutation within the *dnaA* region, and to characterize the transcription of genes in the *dnaA* region of this mutant.

This work is supported by NIH Grant GM28430 and by Contract No. DE-AC02-76EV03490 with the U.S. Department of Energy at the University of Rochester Department of Radiation Biology and Biophysics.

W-AM-Pos96 DYNAMICS OF GENE REGULATION IN THE BACTERIOPHAGE λ LYSOGENIC-TO-LYTIC GROWTH SWITCH Madeline A. Shea and Gary K. Ackers, The Johns Hopkins University, Baltimore, MD 21218

We have developed a quantitative model for the dynamic network of processes in bacteriophage λ which maintain stable lysogenic growth and drive the irreversible switchover to viral replication and cell lysis. The model has two major components: (a) A statistical thermodynamic theory incorporates known protein-DNA interaction energies into expressions for the probability of the various configurations of proteins bound to the three-site regulatory regions, O_R and O_L, and their overlapping promoters; (b) A kinetic model couples these probabilities to the net production of transcriptional control proteins. The model correctly predicts the lysogenic synthesis of cI repressor and the repression of the *cro* and *N* genes. During induction of lysis, it predicts a burst of cro and N protein synthesis followed by a turnoff of early genes by cro; this is one of several features not explicitly programmed into the model but which arise as a direct consequence of the differences in binding energies and the variations in concentrations of the regulatory proteins during induction of lysis. Our calculations demonstrate how the equilibrium between ligands vying for the same genomic sites with varied affinity precisely synchronizes physiological behavior. We have investigated alterations in the balance of binding affinities, cooperative and catalytic interactions, and have shown how their presence stabilizes the prophage, while their absence contributes to virulence. This model and the results obtained through its use demonstrate a powerful approach to understanding how complex dynamic properties in genomic regulatory systems may arise from fundamental interactions among their molecular constituents. The success of the model to predict physiological characteristics for mutant and wild-type phage provides support for the underlying physico-chemical assumptions used in its formulation.

W-AM-Pos97 BINDING PARAMETERS AND GENERAL QUANTITATIVE MODELS FOR LAC REPRESSOR-OPERATOR INTERACTION: Paul W. Chun and Joo H. Kim. Dept. of Biochem. and Mol. Bio., Univ. of Fla. 32610.

The binding parameters for lac repressor-operator interaction are evaluated using a series of general, statistical thermodynamic models based on polyacrylamide gel electrophoretic patterns for the protein-DNA ladders reported by Fried and Crothers [Nucleic Acid Research (1981) 9, 6505-6525]. These models, derived based on the statistical weights of the probability generating function, consider theoretical cases involving single or multiple independent operator sites, the interaction between multiple operators, nearest-neighbor exclusion operator sites, and overlapping site interaction with repressor.

Of those models tested, that for a system having one specific operator site with n non-specific operator sites best fit the experimental data, with values for $K_\alpha = 2.52 \times 10^8 M^{-1}$ and $K = 2.40 \times 10^7 M^{-1}$. An equilibrium competition binding assay with poly d(A-T) gave a non-specific binding constant of $K_D' = 2.48 \times 10^8 M^{-1}$.

A Scatchard plot [Ann. N.Y. Acad. Sci. (1949) 51, 660-674] of $\bar{\nu}/[R]$ versus $\bar{\nu}$, the average number of repressors bound, generated from the integrated intensities of the protein-DNA ladders, where $\bar{\nu} = \sum_i i I_i$, suggests that there is a single binding site, with any further binding of repressor at non-specific sites being independent and non-cooperative.

This work was supported by NSF Grant PCM 79-25683.